National Library of Canada

Acquisitions and Bibliographic Services Branch

395 Wellington Street
Ottawa, Ontario
K1A 0N4

Bibliothèque nationale du Canada

Direction des acquisitions et des services bibliographiques

395, rue Wellington
Ottawa (Ontario)
K1A 0N4

Your file Votre référence

Our file Notre référence

NOTICE

The quality of this microform is heavily dependent upon the quality of the original thesis submitted for microfilming. Every effort has been made to ensure the highest quality of reproduction possible.

If pages are missing, contact the university which granted the degree.

Some pages may have indistinct print especially if the original pages were typed with a poor typewriter ribbon or if the university sent us an inferior photocopy.

Reproduction in full or in part of this microform is governed by the Canadian Copyright Act, R.S.C. 1970, c. C-30, and subsequent amendments.

AVIS

La qualité de cette microforme dépend grandement de la qualité de la thèse soumise au microfilmage. Nous avons tout fait pour assurer une qualité supérieure de reproduction.

S'il manque des pages, veuillez communiquer avec l'université qui a conféré le grade.

La qualité d'impression de certaines pages peut laisser à désirer, surtout si les pages originales ont été dactylographiées à l'aide d'un ruban usé ou si l'université nous a fait parvenir une photocopie de qualité inférieure.

La reproduction, même partielle, de cette microforme est soumise à la Loi canadienne sur le droit d'auteur, SRC 1970, c. C-30, et ses amendements subséquents.

Canada

OPTIMIZATION AND EVALUATION OF AN ELECTRO-MECHANICAL BATTERY/CHEMICAL BATTERY SERIES HYBRID ELECTRIC DRIVETRAIN FOR VEHICULAR APPLICATIONS

Thesis Presented
by

Michel B. Keating

in partial fulfilment of the degree of
M.A.Sc. (Mechanical Engineering)

Department of Mechanical Engineering
University of Ottawa
Ottawa, Canada

April, 1995

ISBN 0-612-07882-5

Canada

UNIVERSITÉ D'OTTAWA
UNIVERSITY OF OTTAWA

ACKNOWLEDGEMENTS

The author wishes to express grateful appreciation to Dr. R. C. Flanagan for his encouragement and advice during the course of this work. Thanks are also due to Mr. Luc Ménard for his help with the computing facilities, to Unique Mobility Inc. for their data on electric motors and controllers and to the Natural Sciences and Engineering Research Council for their financial support.

ABSTRACT

The objective of this thesis is to present the results of an optimization study which was conducted in order to come up with preliminary design objectives for a hybrid electric vehicle. The vehicle type is a Chrysler mini-van equipped with an energy source, a buffer and an electric motor/generator capable of propelling as well as decelerating the vehicle. The energy source is a lead-acid battery pack which is load levelled using an electro-mechanical battery. Because of its high power charge/discharge capability, the electro-mechanical battery is ideally suited to be used as a buffer. It is composed of a high speed fibre composite rotor or flywheel directly coupled to an electric motor/generator. Thus, the drivetrain is all electric and the vehicle can be classified as a zero emission vehicle.

The energy efficiency of the drivetrain is affected by both the sizing of components (battery pack, electro-mechanical battery, drive motor) and the way in which power and energy are managed between the battery pack and electro-mechanical battery. Thus, in order to maximize vehicle range, a control strategy or power split between the battery pack and electro-mechanical battery was devised such that a constant continuous low power output from the battery pack would result. Furthermore, appropriate analytical models were developed for each component of the drivetrain and computer simulations of the vehicle operating over the Federal Urban Drive Schedule were performed.

Using the analytical models along with computational methods, an optimization search was then performed to define certain drivetrain parameters which would allow the hybrid mini-van to have the greatest possible range. The drivetrain parameters to be defined through optimization are:

- the size of the lead-acid battery pack,
- the size of the flywheel used in the electro-mechanical battery,
- the size of the electric motor/generator which is coupled to the flywheel,
- the size of the electric motor/generator used to propel the vehicle and,
- the amount of energy to be stored in the flywheel before the vehicle begins its drive schedule.

Thus, optimization yielded a set of drivetrain parameters which would allow the battery pack to keep the maximum fraction of its rated capacity (amp-hours) after the vehicle has completed the Federal Urban Drive Schedule. The optimization search was constrained by a minimal vehicle performance which is imposed by the drive schedule, a minimum battery voltage, a maximum overrating of the electric motor/generators and, a control on the amount of energy stored in the flywheel in order to avoid over or under charging.

The optimized hybrid electric drivetrain parameters were determined as:

- battery pack size = 620 kg,
- flywheel size = 0.58 kW·h maximum energy storage capability,
- flywheel motor size = 30 kW rated continuous power output,
- drive motor size = 62 kW rated continuous power output,
- amount of energy initially stored in the flywheel = 0.50 kW·h.

The mini-van equipped with this optimized hybrid electric drivetrain would have a curb weight of 2070 kg and a payload capacity of 600 kg. In order to complete the Federal Urban Drive Schedule, the battery power output would be constant and set at 7.72 kW except during regenerative braking when the battery would be shut-off. Power peaks of up to 52 kW would be provided by the electro-mechanical battery with the flywheel speed remaining between 20 000 rpm and 40 000 rpm throughout the drive schedule. Total energy losses in the electro-mechanical battery incurred throughout the drive schedule result in a turnaround efficiency of 77.7 %. The total amount of energy required from the battery pack in order for the vehicle to complete the 12 km long drive schedule is 2.31 kW·h. The hybrid vehicle can repeat the drive schedule and travel a distance of 68 km using 80% of the battery's rated capacity. Thus, with a total mass of 858 kg, the hybrid drivetrain achieves an energy density of 13.6 W·h/kg. The performance of the hybrid electric drivetrain was compared to that of an all electric drivetrain. When equipped with the battery only drivetrain, vehicle range is limited to 25 km because the battery can no longer meet the performance requirements of the drive schedule. Thus, without the electro-mechanical battery to absorb the power peaks, energy density falls to 4.93 W·h/kg for the electric drivetrain equipped with lead-acid batteries only.

TABLE OF CONTENTS

LIST OF FIGURES

LIST OF FIGURES (cont.)

LIST OF TABLES

ABBREVIATIONS and GLOSSARY

AC: **Alternating current.**

A: **Ampere.**

Amps. or Amp.: **Amperes.**

BPM: **Battery pack mass.**
Size of the chemical battery pack expressed in terms of its total mass in kilograms.

BPT: **Battery power at terminals.**
Power measured at the terminals of the battery pack.

BSOC: **Battery state of charge.**
Defines the charge condition of a battery as the fraction of the battery's rated capacity which has not been supplied by the battery.

BSOC @ FUDS END: **Battery state of charge at the end of the Federal Urban Drive Schedule.**
The charge condition of the battery after the vehicle has completed a single pass over the FUDS.

Compound hybrid.
Defines a vehicle whose tractive effort is supplied by two different energy sources through either or both of their respective actuators.

CVT: **Continuously variable transmission.**

Control strategy.
Management of energy or power split between the two energy sources of a hybrid vehicle in order to meet the tractive effort required to propel the vehicle.

Coulombic efficiency.
Percentage of charge returned to a battery which is used effectively to produce lead and sulphuric acid. The rest of the charge produces hydrogen and oxygen gasses.

Curb weight.
Mass of a vehicle excluding all variable masses such as: payload, driver, passenger and fuel.

Cut-off voltage.
Used as an indicator of a battery's complete discharge, this voltage is measured at the terminals of a battery which is supplying current to a load.

DOE: **United States Department of Energy.**

DOD: **Depth of discharge.**
Defines the charge condition of a battery as the fraction of the battery's rated capacity which has been supplied by the battery.

ABBREVIATIONS and GLOSSARY (cont.)

Design variable.
Drivetrain component specification which is to be set so as to maximize the objective function.

DC: **Direct current.**

DMPS: **Drive motor power measured at shaft.**
Also defined as P_r.

DMPT: **Drive motor power at terminals.**
Power flowing into the drive motor controller to propel the vehicle or, power flowing out of the drive motor controller during regenerative braking.

DMS: **Drive motor size.**
Size of the electric motor/generator used to propel the vehicle; expressed in terms of its maximum continuous rated shaft power output in watts. Also defined as P_m.

Drivetrain.
All components necessary to produce a tractive effort to the drive wheels of a vehicle. Does not include wheels, suspension, steering or braking components.

Electric drivetrain.
Vehicle propulsion system utilizing a lead-acid battery as an energy source and an electric motor/generator to meet the tractive effort necessary to propel the vehicle.

EMB: **Electro-mechanical battery.**
Energy storage unit utilizing a flywheel to store energy in the form of kinetic energy, and an electric motor/generator to transfer this energy into electrical energy and vice versa.

Energy density.
Total useable energy output of a component or system, related to the mass of the component or system.

EPA: **United States Environmental Protection Agency.**

FUDS: **Federal Urban Drive Schedule.**
Duty cycle expressed in terms of vehicle velocity used to simulate a typical drive through the streets of a large city.

Flywheel.
Mechanical energy storage device which uses the rotational inertia of a rapidly rotating disk to store energy.

ABBREVIATIONS and GLOSSARY (cont.)

FWMPT: **Flywheel motor power at terminals.**
Power flowing into the flywheel motor controller to recharge the electro-mechanical battery or, power flowing out of the flywheel motor controller during discharge of the electro-mechanical battery.

FWMS: **Flywheel motor size.**
Size of the electric motor/generator used in the electro-mechanical battery; expressed in terms of its maximum continuous rated shaft power output in watts. Also defined as P_f.

FWS: **Flywheel size.**
Size of the energy storage rotor used in the electro-mechanical battery expressed in terms of the energy stored (joule) at its maximum speed. Also defined as E_f.

FWSOC: **Flywheel state of charge.**
The amount of energy stored in the EMB expressed as a fraction of the energy stored at the EMB's maximum speed.

FWSOC @ FUDS START & END: **Flywheel state of charge at the beginning and end of the Federal Urban Drive Schedule.**
The amount of energy stored in the EMB at the end of the FUDS is compared to the amount of energy that the EMB started off with.

Glider mass.
Mass of vehicle which has no payload or driver and is stripped of all its drivetrain components. Glider mass includes wheels, suspension, steering and braking components.

GVWR: **Gross vehicle weight rating.**
Maximum total mass which can be supported by a vehicle's suspension system.

h: **Hour.**

Hybrid electric drivetrain.
Vehicle propulsion system utilizing a lead-acid battery as an energy source, an electro-mechanical battery to load level the energy source (buffer) and an electric motor/generator to meet the tractive effort necessary to propel the vehicle.

ICE or IC engine: **Internal combustion engine.**

IECEC: **Intersociety Energy Conversion Engineering Conference.**

JPL: **Jet Propulsion Laboratory.**

Objective function.
In optimization, it is the quantity which is to be maximized with the correct choice of design variables. Also defined as BSOC @ FUDS END.

ABBREVIATIONS and GLOSSARY (cont.)

Open circuit voltage.
Voltage measured at battery terminals when zero electric current is delivered by battery. Also defined as E_{oc}.

Parallel hybrid.
Defines a vehicle equipped with two different energy sources supplying independent tractive efforts through their respective actuators.

Power density.
Power handling or output capability of a component or system, related to the mass of this component or system.

Range.
Total distance that a vehicle can travel until vehicle performance is limited by the battery's charge condition.

Rated capacity.
Amount of charge, expressed in ampere-hours, which can be delivered at a specified current by a fully charged battery before reaching its cut-off voltage.

Regenerative braking.
Action by which the kinetic energy of a moving vehicle is recuperated during its deceleration.

rpm: **Revolutions per minute.**

Rotor. See Flywheel.

Series hybrid.
Defines a vehicle equipped with two different energy sources which supply, through a common actuator, the tractive effort necessary to propel the vehicle.

SAE: **Society of Automotive Engineers.**

Terminal voltage.
Voltage which is measured at the terminal lugs of a battery or battery pack.

Turnaround efficiency.
Efficiency with which an energy storage device can accept, store and discharge energy.

VTM: **Vehicle test mass.**
Curb weight plus driver (100 kg).

LIST OF SYMBOLS

A= Net energy supplied by battery pack to complete the FUDS with the hybrid electric drivetrain, (joule)

B= Net energy supplied by battery pack to complete the FUDS with the electric drivetrain equipped with regenerative braking, (joule)

C= Net energy supplied by battery pack to complete the FUDS with the electric drivetrain without regenerative braking, (joule)

CA= During the charging of the battery; fraction of charge returned to the battery which does not go into the production of hydrogen and oxygen gasses

Cd= Coefficient of aerodynamic drag

e= Natural exponential (2.7183)

E_b= Sum of all energies supplied by battery pack during the FUDS, (joule)

E_c= Sum of all energies supplied by the drive motor controller during regenerative braking on the FUDS, (joule)

E_d= Sum of all energies supplied to the drive motor controller in order to propel the vehicle over the FUDS, (joule)

E_f= Flywheel maximum energy storage capability; energy stored at top speed, (joule). Also defined as FWS.

E_i= Sum of all energies supplied to the flywheel motor controller to recharge the EMB for the duration of the FUDS, (joule)

E_n= Net energy supplied by battery pack to complete the FUDS, (joule)

E_o= Sum of all energies supplied by the flywheel motor controller during the discharge of the EMB for the duration of the FUDS, (joule)

E_{oc}= Open circuit voltage; voltage measured at battery terminals with zero electric current, (volt)

E_r= Sum of all energies available from the drive wheels of the vehicle during regenerative braking on the FUDS, (joule)

E_s= Sum of all energies supplied to the drive wheels of the vehicle in order to complete the FUDS, (joule)

LIST OF SYMBOLS (cont.)

E_t= Terminal voltage; voltage measured at battery terminals, (volt)

f(i)= Function of electric current

i= Electric current, (ampere)

I_b= Electric current supplied by battery, (ampere)

I_f= Electric current flowing through flywheel motor, (ampere)

I_m= Electric current flowing through drive motor, (ampere)

P_{cf}= Power loss in the flywheel motor controller, (watt)

P_{cm}= Power loss in the drive motor controller, (watt)

P_f= Flywheel motor maximum continuous rated shaft power output, (watt). Also defined as FWMS.

P_m= Drive motor maximum continuous rated shaft power output, (watt). Also defined as DMS.

P_r= Drive motor power at shaft, (watt). Also defined as DMPS.

P_s= Flywheel motor power at shaft, (watt)

R_b= Battery internal resistance, (ohm)

t= Time, (second or hour)

U= Electromotive force, voltage, (volt)

V= Vehicle velocity, (m/s)

♦= Location in the drivetrain layout where energy summation is performed

CHAPTER 1: INTRODUCTION

1.1 Motivation

The horse drawn carriage was being replaced at the turn of the century by both the internal combustion engine and the battery powered vehicle. In fact, because it was easier to use, battery power was, at one time, more popular than the internal combustion engine. With the invention of the electric starter in the 1920's, the electric vehicle lost its only real advantage and it wasn't until the 1970's that the electric vehicle reappeared as one of the solutions to the energy crisis. Lately, environmental concerns have given the electric vehicle a net advantage over the fossil fuelled vehicle. Indeed, much research has given concrete results in order to mass produce a vehicle which will meet market demands. California set the pace by requesting that 2% of the new cars being sold in 1998 have zero emission of pollutants.

For the manufacturers, the objective is to produce an electric vehicle which, in terms of performance, competes well with the gasoline powered vehicle. Therefore, much work has gone into increasing both the power density (W/kg) and energy density (J/kg) of the electric drivetrain. One indirect way of achieving these objectives it to split the energy requirements of the vehicle between two different sources of power; one source which is capable of accepting as well as delivering energy and is

characterized by a high power density and another source which simply delivers energy and is characterized by a high energy density. An increase in both energy and power density of the electric drivetrain is therefore possible by controlling the interaction of the energy source with the power source so as to maximize the benefits of each. A drivetrain operating in this fashion is defined as a hybrid drivetrain.

With the objective being load levelling of the energy source while the power source is cycled to meet the power peak, one can think of many possible drivetrain designs which could be qualified as hybrid [10, 12, 14, 17, 22, 31, 32]. In this study, a design using an electro-mechanical battery (EMB) as a power source and a chemical battery pack as an energy source has been retained. Thus, an increase in the energy and power density of the drivetrain can be achieved because the EMB is characterized by a high power density while load levelling of the battery pack results in an increase of the battery pack's energy density [11, 14, 35, 40].

The EMB is a device or system which can store energy mechanically and uses an electrical transducer to convert electric power into mechanical work and vice versa. A high performance fibre composite rotor (flywheel) uses rotational inertia to store mechanical energy in the form of kinetic energy and is directly coupled to an electric motor-generator which acts as an electrical/mechanical energy converter. Developed at the

University of Ottawa, the fibre composite rotor or flywheel is a proven technology [38, 41, 42] and the development by Unique Mobility Inc. of a high speed brushless permanent magnet motor/alternator [44, 38] provides an efficient path for the transformation of mechanical energy into electrical energy and vice versa.

Thus, both the chemical battery pack and the EMB use electricity as the mode of power transmission and the drivetrain can therefore use a single traction system which is electric. Indeed, a single electric machine transfers all power to/from the drive wheels and interacts with both the EMB and battery. A hybrid drivetrain configured in this fashion; where both energy sources meet the road load through the same traction device, is said to be a series hybrid drivetrain.

The concept of the electro-mechanical battery/chemical battery series hybrid electric drivetrain has been presented and now its analysis can be addressed.

1.2 Thesis Objective, Scope and Structure

This thesis provides a preliminary analysis for the design of a mini-van powered by an electro-mechanical battery/chemical battery series hybrid electric drivetrain whose performance is expected to equal that of a fossil fuelled vehicle operating on an urban drive schedule. The objective is to circumscribe

certain design specifications necessary to the development of a hybrid electric vehicle. This thesis therefore presents the method used to find the drivetrain component sizes, ratings and operational controls to be used as target specifications for the development of the EMB/battery electric drivetrain and its components. Maximization of vehicle range is used as the main criteria in choosing the component ratings and control strategy of the hybrid electric drivetrain. Thus, an optimization technique is used and the performance of the drivetrain, in terms of energy consumption and efficiency, is evaluated using mathematical models describing the energy transfer through each component as a function of size and operating point.

Although these models were derived using test and design data, this thesis is purely analytical. Furthermore, because this work is part of the preliminary steps in the design of a hybrid electric vehicle and, that, no actual prototype vehicle has yet been built, the results of the simulations carried out in this study are not compared to any test results. Simulations of a conventional battery powered electric vehicle have however been conducted. This therefore allows a direct comparison to be made between the electric vehicle and the hybrid electric vehicle in terms of their expected performance and energy consumption.

The main body of the thesis is divided into five chapters and is structured as follows. Chapter 2 presents an overview of the pertinent operating characteristics of the conventional

electric drivetrain as well as the EMB/battery hybrid electric drivetrain. The benefits of load levelling the chemical battery and how this can be achieved with the electro-mechanical battery is explained. Constraints and design objectives for the hybrid electric vehicle are presented in Chapter 3 with an explanation of how the optimal sizing and control of the drivetrain components results in the maximization of vehicle range. Thus, boundaries and constraints to the optimization problem are set up and a justification for the choice of objective function is put forward. Also presented are: the method used to calculate the value of the objective function as well as the technique used to compare the different values of the objective function so as to find the optimal hybrid drivetrain configuration. In order to calculate the value of the objective function, the performance of individual drivetrain components has been mathematically modeled as a function of component size and operating point. These models are presented in Chapter 4.

The results of the optimization are presented in Chapter 5 along with an analysis which shows the sensitivity of the objective function to changes in the drivetrain component sizing. Thus, the final proposed design specifications for the hybrid electric vehicle are presented. The operation of the optimized hybrid electric vehicle is then simulated and a complete analysis of energy consumption and efficiency is effected. Finally, in Chapter 6, an overview is made of other aspects of the hybrid electric vehicle design which should be addressed prior to the

further development of the EMB/battery hybrid electric vehicle.

1.3 Previous Work in the Field of Hybrid Vehicle Simulation and Optimization

Active research in the field of electric vehicles has increased steadily over the last three decades. Although a considerable amount of testing was and is being done on electric vehicles and their components, modelling and simulation is a simple and cost effective method of predicting the performance, energy consumption and emissions of vehicles when basic changes are made to the components of the drivetrain. For internal combustion engine powered vehicles or conventional battery powered electric vehicles, simulations, in most cases, merely confirm and quantify the predictable changes in vehicle performance brought about by modifications of the drivetrain components. For the hybrid vehicle, however, simple predictions of vehicle performance cannot be done without the use of simulations. Indeed, the increased number of components in the drivetrain (a hybrid drivetrain has two or more energy sources along with the components necessary to transfer this energy), the configuration of the drivetrain (parallel hybrid, series hybrid or compound hybrid), the control of the drivetrain (power split between energy sources) and the different types of components available for hybrid drivetrains (batteries, fuel cells, diesel engines, gas turbines, generator sets, continuously variable transmissions, flywheels, hydraulic pumps, electric motors, etc.)

makes it very difficult to intuitively assess how changes in the hybrid drivetrain will affect the performance of the vehicle.

Thus, modelling and simulation of hybrid vehicles was done initially to verify the reductions in fuel consumption of internal combustion engines which were load levelled with a buffer energy storage device such as a battery pack. Indeed, Gelb et al. [1] modeled a hybrid drivetrain incorporating a spark ignition engine coupled to a generator with a lead-acid battery pack acting as a load leveller. The simulation was done with components of fixed size and the generator was used to supplement the battery pack whenever the power requirements of the LA-4 route (non-freeway portion of the federal urban drive schedule) became excessive. Frank et al. [2,3,4] did a similar study in 1973 using the 1972 Federal Test Procedure schedule and was able to compare the results with test data from a prototype. Later, the design was modified such that the battery was replaced with a flywheel linked through a C.V.T. to a conventional I.C. engine drivetrain. Using a lighter flywheel instead of a battery proved beneficial in terms of fuel consumption. The operation of the flywheel/I.C.E. vehicle over the FUDS was simulated in order to optimize the power or duty split between I.C.E. and flywheel so as to achieve maximum fuel economy. Component sizes were however not optimized. Schilke et al. [5,6] had a project which was very similar to the flywheel/I.C.E. vehicle developed by Frank, the only difference being the drivetrain layout and the function of the C.V.T.. Again, components of the drivetrain were sized in

order to meet minimum performance requirements or constrained by design limitations.

Liddle [7] simulated the operation of a gas turbine/battery hybrid vehicle in order to compare the performance of the series vs. parallel hybrid drivetrain in terms of fuel consumption and pollutant emissions. The United States Department of Energy in conjunction with Jet Propulsion Laboratory and General Electric sponsored a hybrid vehicle development program in which Liddle participated [8]. Simulation was required in order to find a suitable design for a I.C.E./Battery hybrid which could be commercially viable. The development of the ELVEC and HYVEC computer programs was hence made possible. Although no optimization was done with HYVEC, it allowed the analysis and comparison of several different drivetrain configurations in terms of energy consumption, pollution and operating/life cycle costs. Liddle increased the versatility of HYVEC in order to analyze other I.C.E. based hybrid drivetrains [9,10].

Burke et al. [11, 12, 13] has used another simulation program (SIMPLEV) to present the load levelling characteristics of ultracapacitors and bipolar lead-acid pulse batteries. These energy storage devices were used in conjunction with I.C.E.s or a battery pack. Component sizing was not optimized but was chosen to meet the peak requirements of the FUDS. Initially developed for battery testing by E.G. & G. Idaho Inc., SIMPLEV is a commercially available software which is quite complete; its

output includes component performance, energy consumption, fuel consumption, pollutant emissions and estimates of engine wear. However, according to Adams et al. [14], some manipulation of the SIMPLEV software is necessary in order to simulate hybrid vehicles. Adams et al. has used SIMPLEV to investigate the performance of several battery/fuel cell hybrid drivetrains. Laboratory testing of several fuel cells and batteries was done in order to formulate adequate models for these energy sources. Using the simulation, effective improvements in the drivetrain's energy and power density was verified and compared to the test results of a dual battery equipped van operating over the FUDS. Dual battery hybrids have also been simulated by Murray et al. [15]. This study showed that impendence matching is very important in determining the size of the fuel cell and battery. Energy as well as operating/life cycle costs are also presented in this Los Alamos National Laboratory report.

Other hybrid drivetrain configurations have been studied such as the diesel/hydraulic drive urban bus presented by Buchwald et al. [16]. Here, the diesel engine is of fixed size and operates in on-off mode. The hydraulic system is used as an energy storage and power transfer device. Simulation was used to investigate different control strategies and to optimize the hydraulic pump size. The stirling engine based hybrid is yet another configuration which is being proposed by Schreiber et al. [17]. In this study, the stirling engine is used as a prime mover and simulations were done, using flywheels and batteries as

buffers. Optimization was not performed but was recognized to be helpful in increasing the overall system efficiency.

Marr et al. [18] has used optimization to minimize the life cycle cost of a diesel-generator/lead-acid battery hybrid bus. The objective here was to find the control strategy which would put the least amount of wear on the diesel engine and battery pack. Work on diesel/battery buses was also performed by ORTECH International [19]. Simulations lead to the conclusion that optimization of the diesel generator size and control strategy was necessary in order to achieve maximum efficiency. This was addressed in a subsequent paper published by the authors; Triger et al. [20]. Flanagan [21] used optimization to size the major components of a diesel/flywheel drivetrain used in a minibus. Simulation of the minibus operating over an actual bus route yielded the engine size and operating point as well as flywheel size and C.V.T. ratings based on the minimization of fuel consumption.

Other hybrid buses such as the Fiat hybrid bus [22, 23] and the University of Florida hybrid bus [24, 25] have used simulations in the development stage of the program in order to evaluate the energy savings potential of using lead-acid batteries to load level a diesel generator. Although the simulation was used to compare different control strategies for the power split between the battery pack and diesel engine, drivetrain component sizes were not optimized.

Bumby et al. [26, 27], however, have recognized optimization to be a necessary step in the design of a hybrid drivetrain. In this study, an I.C.E./battery parallel hybrid vehicle was simulated over the SAE J227a(D) schedule. The analysis included the efficiency with which electric power is generated and the efficiency of the petroleum production process. The objective was to minimize the overall energy consumption of the vehicle by correctly sizing the components of the drivetrain and finding the optimal power split between the I.C.E. and electric traction system. Donoghue et al. [28] did a study which is, in many respects, similar to the one presented by Bumby et al. [26, 27]. Optimization was used to size the battery and I.C.E. of a parallel hybrid vehicle with the objective function being the minimization of acquisition cost, life cycle cost and petroleum consumption. An analysis on the choice of constraints and their influence on the results of the optimization is also presented. Optimization was also considered by Kramer et al. [29] in the design and control of a solar/battery hybrid vehicle. Indeed, optimization was used in both the sizing of drivetrain components and control of power to maximize speed during a predetermined race course.

A more general approach to the simulation of hybrid vehicles has been presented by Willis et al. [30, 31]. In this study, the load levelling component of the I.C.E. based hybrid drivetrain has been modelled as a simple spring having a specified charge/discharge efficiency. By using sequential optimization, a

control strategy was presented which, while adjusting itself to an undetermined duty cycle, remained optimal in terms of minimizing fuel consumption. Similarly, Spiekhout et al. [32] presents an I.C.E. based hybrid vehicle simulation program. All other components of the drivetrain can be interchanged and the drivetrain layout as well as control strategy can be modified. Direct optimization cannot be performed but several outputs such as energy consumption, efficiencies, pollution and wear can be used to compare various drivetrain configurations.

Studies have also been made of hybrid drivetrains incorporating, as an energy storage unit or buffer, an electro-mechanical battery similar in design to the one presented in this thesis. Lustenader et al. [33, 34] developed, built and tested a prototype electro-mechanical battery (EMB) under the auspices of General Electric. The prototype, utilizing a steel flywheel coupled to an AC motor, was used to imitate the operation of a more advanced composite flywheel concept. Thus, simulations of a 3500 pound battery/flywheel electric vehicle operating on the SAE J227a(D) schedule were conducted in the laboratory using the appropriate load and power sources. The vehicle and drivetrain components were modeled mathematically and a computer was used to control the operation of the flywheel module. The objective was to evaluate different modes of operation or control strategies and estimate range and energy consumption. The staff at Garrett AiResearch have also worked on a hybrid vehicle incorporating a load levelling high speed fibre composite flywheel [35]. In this

case, however, the flywheel is not directly coupled to an electric machine. Instead, the flywheel is connected to a differential planetary gearset which splits power between an electric motor/generator and the drive wheels of the vehicle. This flywheel/lead-acid battery hybrid vehicle project included some preliminary systems analysis which were performed by Chang [36]. Although no optimization was performed, the operation of the vehicle over the FUDS was computer simulated to demonstrate the load levelling capability of the flywheel and to estimate system losses and component efficiencies. Later, a prototype vehicle was built and laboratory tested on the FUDS [35]. Testing was also done on an EMB/diesel-generator hybrid bus. Results of these tests were reported by Heidelberg et al. [37]. Measurements were performed on an actual bus route to document the mechanical and electrical energies/power and, thus, present the actual operating efficiency of the drivetrain components.

Finally, the design of an EMB for hybrid electric vehicle drives has been presented by Flanagan et al. [38] and this thesis is an extension to the analysis of an EMB equipped vehicle presented by Flanagan and Keating [39]. Thus, the modelling of a high speed fibre composite rotor coupled to a permanent magnet D.C. machine and the complete modelling and optimization of all other components in the EMB/lead-acid battery series hybrid electric drivetrain give this thesis its particularity. Moreover, this thesis presents a complete justification and explanation of the optimal control strategy along with computer simulations

which give the performance of all components in the drivetrain as the vehicle completes the FUDS.

CHAPTER 2: THE EMB/BATTERY HYBRID ELECTRIC DRIVETRAIN

2.1 The Electric Drivetrain

Conventional electric vehicles use batteries as an energy source. This battery pack can be compared to the fuel tank of a gasoline powered vehicle; and the tractive effort required to propel the vehicle is supplied by an electric motor. The batteries are discharged, the motor is driven; hence the vehicle moves. In order to bring the vehicle to a stop or to simply reduce its velocity, the electric motor could be converted to operate as an electric generator. The kinetic energy of the vehicle is therefore recuperated and used to recharge the battery pack [45, 46, 47]. This operational characteristic is called regenerative braking or regenerative energy. Figure 2-1 shows a conceptual layout of the main components used in the drivetrain of the conventional electric vehicle.

This set of components will be referred to as the electric drive or drivetrain and also the electric only drivetrain. The arrows indicate the flow of power or energy. Note that in order to assure a safe deceleration under a panic stop and as back up, the electric generator would be assisted by friction brakes which dissipate the kinetic energy as heat.

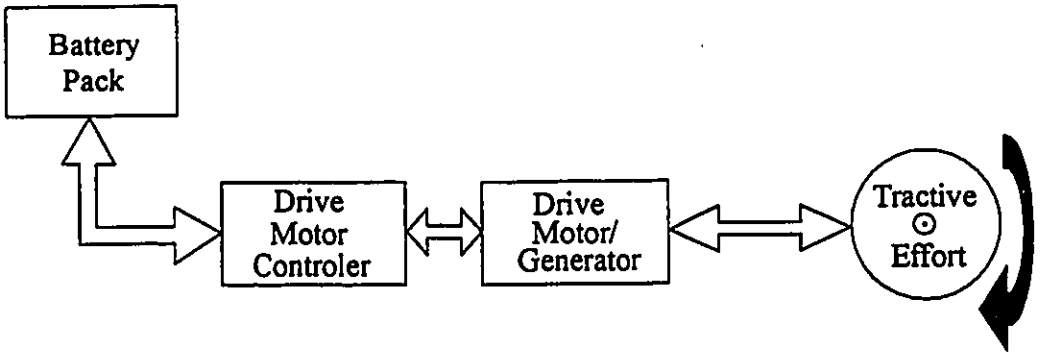

Figure 2-1: Schematic of the Electric Drivetrain.

2.2 The Hybrid Electric Drivetrain

2.2.1 Battery Performance and Design Characteristics

It is obvious that under normal driving conditions, the electric drivetrain must be equipped with a battery pack capable of being discharged at a rate high enough to provide the required amount of power to accelerate the vehicle. Similarly, during deceleration, the battery pack must accept charge at high rate in order to recover the maximum amount of kinetic energy. The battery pack must therefore deal with frequent and relatively high peaks of power. The maximum amount of power that a battery can provide is dependant on the chemical reaction rate of the reactants in the battery [48, 49]. In other words, the chemical reaction rate must meet the required current being drawn from the battery. If the reaction rate is not high enough, the voltage drops and the power is simply not available. In other words, the

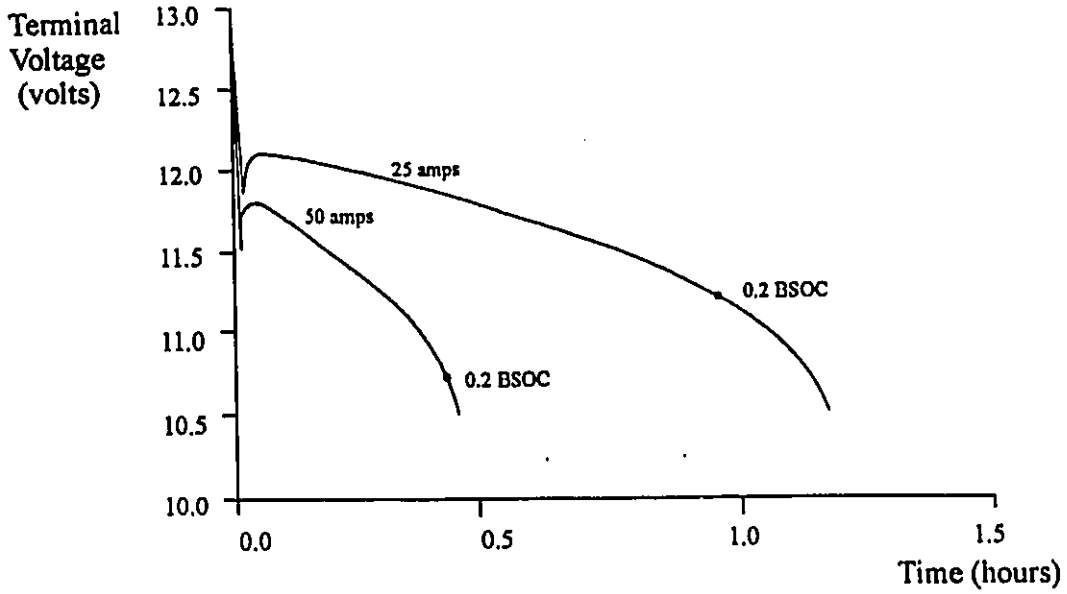

Figure 2-2: Terminal Voltage vs. Time for Constant Current Discharge of a Lead- Acid Battery. [48]

battery reaches its limiting chemical reaction rate which results in the short circuiting of the battery. Figure 2-2 shows the voltage drop of a typical lead-acid traction battery while the battery is being discharged at a constant current.

If left short circuited for prolonged or repeated periods, damage to the battery would result. Therefore, the battery at this point is considered to be completely discharged because it cannot meet the power requirements. Hence, the battery has a state of charge equal to zero. Ideally one would never allow a battery to be discharged to such a low level. However, if at this point, the power requirements were lowered, the reaction rate would now meet the current draw and the battery could be

discharged further. Thus, the limiting chemical reaction rate is dependent on the amount of reactants remaining in the battery. This fact explains why a battery which is being discharged at a high rate is considered to be completely discharged even though there is a substantial amount of reactants remaining in the battery. This amount of reactants remaining could be used up if the rate of discharge were reduced. For the battery being discharged at a high rate, this "unusable" amount of reactants adds mass to the battery; a mass which does not react and therefore does not increase the total amount of charge or electrons delivered by the battery. Thus, the rate at which the energy from the battery is removed (power) greatly influences the total amount of energy which can be extracted from the battery [47, 48, 50]. Figure 2-3 shows this relationship for a typical lead-acid battery. This plot was obtained using the battery model presented in Chapter 4.1 and simulating several constant power discharges to a cut-off voltage of 10.5 volts.

This trade-off between power and energy is augmented by the way in which batteries are designed. It is common practice to increase the surface area through which the chemical reaction takes place in order to increase the limiting chemical reaction rate [48]. This surface area can be increased by using non-reactive materials to which the reactants are attached or through which the reactants are allowed to flow. The use of these non-reactive materials increases the power capability or power density of the battery but also increases its size and mass. This

extra mass which is non-reactive does not increase the total amount of charge or electrons delivered by the battery. In other words, the energy density (W•h/kg) of the battery is lowered to meet the high power demands.

Because of this trade-off between power and energy, it is very difficult to design a battery pack which can be light and deliver high peaks of power while allowing the vehicle to travel a reasonable distance before the batteries are discharged. Also, the design must take into consideration the fact that the battery pack must be able to recharge at the high rates produced by regenerative braking. For the vehicle, the use of a battery pack

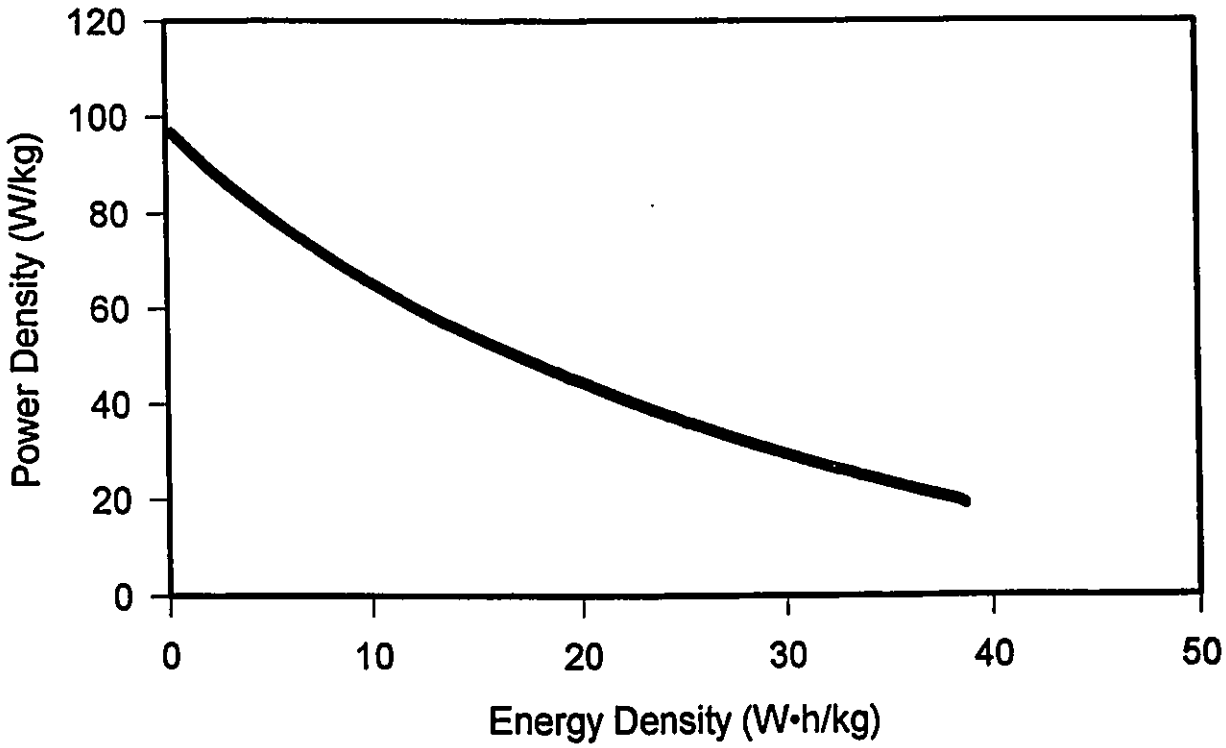

Figure 2-3: Power Density vs. Energy Density for a Lead-Acid Battery.

translates into a trade-off between performance and range.

2.2.2 Load Levelling

This trade-off could be reduced if not eliminated on a vehicle equipped with two different energy sources. One source of energy would operate at a relatively low power level, hence giving the vehicle the required range. The other source of energy would kick in to enhance the performance of the vehicle and, in a sense, be considered a power source instead of an energy source. A vehicle of this type is said to be equipped with a hybrid drivetrain or hybrid drive. It makes of course no sense to have a very large power source capable of supplying repeated surges of power without ever being recharged during the time it takes to discharge the energy source. This sort of utilization would bring us back to the original problem and the use of an energy source would be redundant. The situation is comparable to installing a large and a small engine on a gasoline powered vehicle; the large engine can easily do the job of the small engine and more. The objective here is to use the hybrid drive to load level the energy source which would otherwise have to meet the continuously varying power demands of most vehicles.

Indeed, the power requirements of a vehicle on an urban itinerary are often times very low (i.e.: deceleration and constant low velocity) and even fall to zero (i.e.: stand still and coasting) [51]. It is during these times that the energy

source could be used to recharge the power source, hence having the power source ready for the next peak of power (i.e. acceleration). The power source in fact would be more appropriately called a power accumulator and would be sized to provide just enough energy to meet the demands of one or two peaks of power.

2.2.3 The Energy Source

The choice of an energy source for a hybrid electric vehicle is very straight forward, with the objective being that it must store and deliver electrical energy with a minimum amount of loss. The power output can remain low but the energy density should be as high as possible. Ideally, the energy pack should be rechargeable or easily renewed. A battery pack is an obvious choice but fuel cells are also an excellent possibility. Owing to its low cost and high energy density, the aluminum-air cell is a serious candidate with research to prove its viability [52, 53]. However, the availability of data pertaining to the performance of the aluminum-air cell is not sufficient to allow its use in this study. Furthermore, it is of interest to compare the electric drivetrain with the hybrid electric drivetrain in so far as their efficiencies and battery pack performance requirements are concerned. In order to have a base from which a comparison can be made, both drivetrains will use the same type of battery pack. Because of regenerative braking, the type of battery used on the electric drivetrain must be of the type which can be

electrically recharged. Because of its existing popularity with electric vehicles, the lead-acid battery has been studied extensively, thus generating relevant data [40, 46, 54, 55, 56, 57, 58, 59]. The choice was therefore made to use the lead-acid battery in this study.

2.2.4 The Power Accumulator

The power accumulator on the other hand should be a lightweight and compact system or device capable of charging and discharging its energy at a high rate with minimum loss. In other words, a component having a high power density. The capability of storing energy with minimal loss is also an obvious advantage. Many devices can, to a greater or lesser extent, meet the requirements mentioned above. For example;

- A small battery pack designed to have a high power density [1, 2, 23],
- A set of high performance electrical condensers [11, 12],
- A compressor/turbine system in which the energy is stored in the compressed gases [31],
- A hydraulic system using a spring loaded piston to store energy [16, 61],
- A steel flywheel or inertia wheel [3, 6, 21, 60],
- A high performance fibre composite flywheel battery [35, 37, 38].

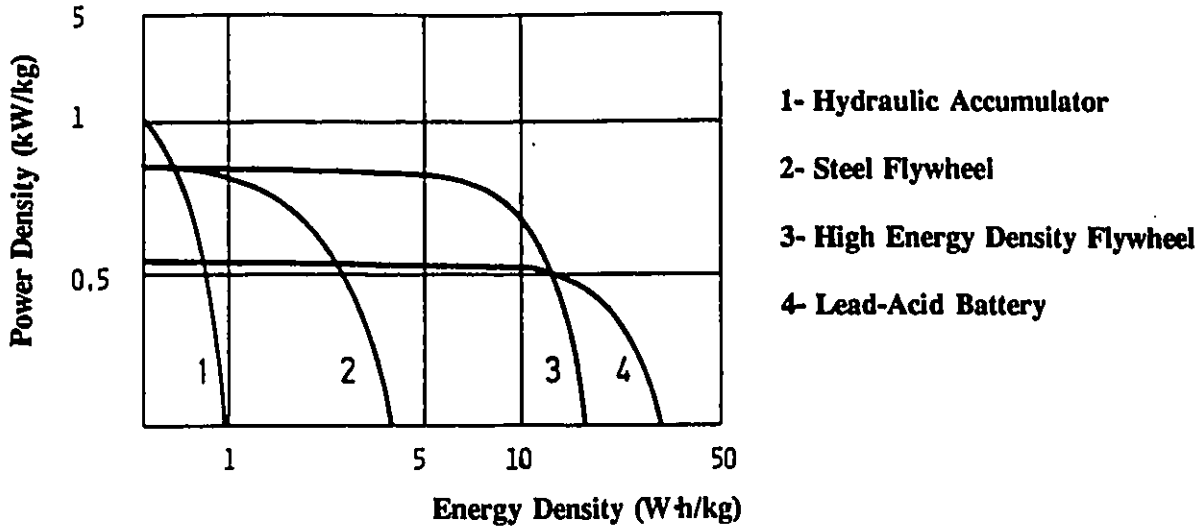

Figure 2-4: Power Density vs. Energy Density for Various Energy Storage and Conversion Units. [16]

The fibre composite flywheel battery offers the best performance in terms of power density and energy density and is therefore ideally suited to be used as a power accumulator. This high performance is due in part to the high yield stress and low density of the fibre composite. The high strength of the fibre composite allows it to withstand very high centrifugal forces, and hence, very high rotational velocities. With kinetic energy being proportional to the square of the velocity; the amount of energy stored is very high for a relatively low rotating mass. Indeed, rotors similar to the one shown in Figure 2-5 can store up to 80 W·h/kg for 100,000 energy or stress cycles. On a specific volume (kW/m³) or specific power (kW/kg) basis, no other component available (e.g.: IC engines, batteries, fuel cells) can match their performance. Energy storage rotors or flywheel

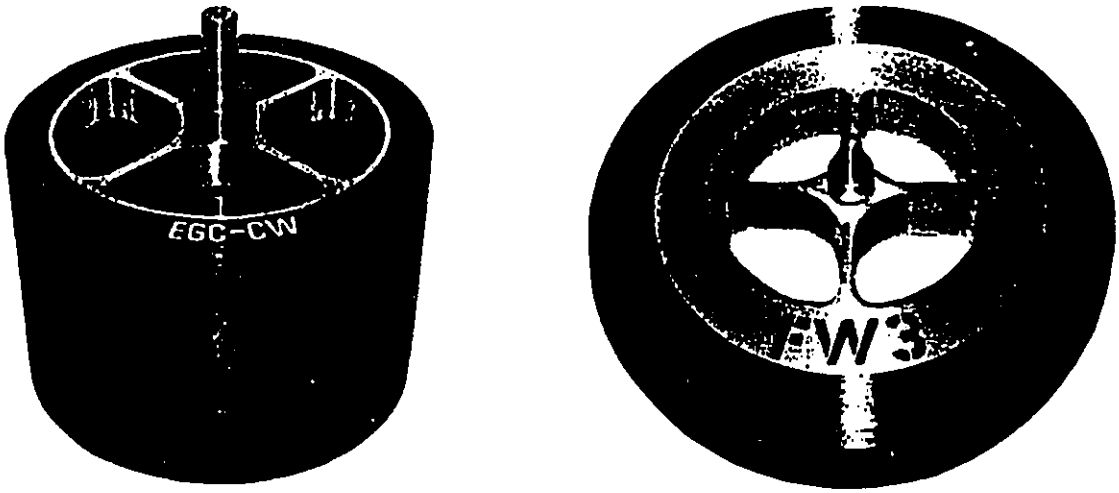

Figure 2-5: High Performance Fibre Composite Rotors. [38, 42]

batteries have attracted considerable attention, especially for road vehicles operating on urban duty cycles, due to their inherent high power and high charge/discharge rate characteristics. Research into rotor energy storage peaked during the late 1970's, and by the mid 1980's, practical high performance fibre-composite rotors became a proven technology [35, 37, 41, 42, 43].

2.2.5 The Electro-Mechanical Battery

The high performance rotor must now be interfaced with the rest of the drivetrain in order to extract or return energy so as to directly or indirectly provide a tractive effort for the vehicle. With its high operating efficiency and high power handling capability, this interface will qualify the flywheel

battery as a high power density unit. Many systems are available (i.e.: hydraulic drive, continuously variable transmission, clutch and electric motor/generator) but the electric motor/generator can most effectively meet the constraints of high rotational velocities (up to 50 000 rpm), high vacuum levels and low mass. Therefore, the power accumulator used in this analysis consists of a high performance fibre composite rotor or flywheel directly coupled to a high speed permanent magnet motor/alternator all fully enclosed in a vacuum container [38, 44]. What can more appropriately be called the electro-mechanical battery (EMB) or flywheel battery is shown in Figure 2-6. Note that the electric motor coupled to the fibre composite rotor or flywheel is converted to an electric generator when the EMB is being discharged.

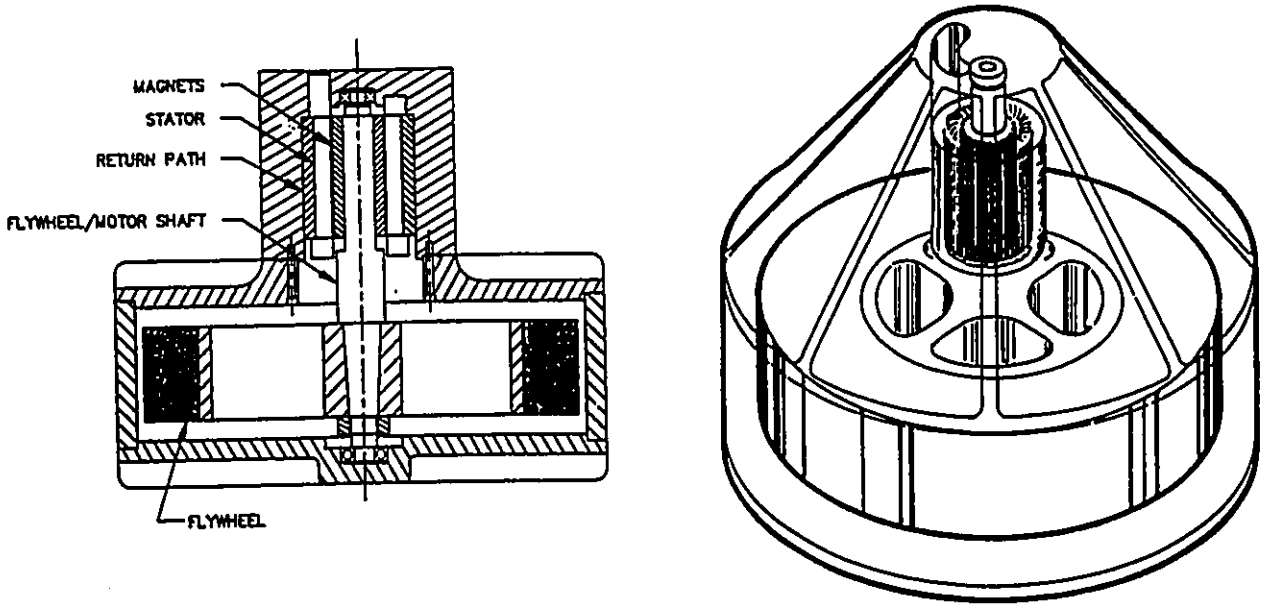

Figure 2-6: Electro-Mechanical Battery. [38, 44]

2.2.6 Operation of the Hybrid Electric Drivetrain

The hybrid electric drivetrain, or hybrid drive, is now complete; the lead-acid battery pack and the electro-mechanical battery discharge into a common bus supplying the electric drive motor which in turn provides the tractive effort necessary to propel the vehicle. The conceptual layout of the main components used in the hybrid electric drivetrain are shown in Figure 2-7. The arrows indicate the flow of power or energy.

Typically, the hybrid electric drivetrain operates as follows. During hard acceleration and high speed cruising the battery and EMB are discharged in order to supply the drive motor with sufficient power. For low speed cruising and low acceleration, the battery is discharged at a constant rate greater than that needed by the drive motor. The excess battery power is used to recharge the EMB. If the vehicle is coasting or at a standstill, no power is needed for the drive motor, all battery power is used to recharge the EMB. Finally, in order to slow down the vehicle, the drive motor is converted to a generator and the electricity being generated is used to recharge the EMB. The demands on the battery pack and EMB can vary depending on how the vehicle is driven; but the flow of power must be regulated and redirected in order to have a constant and predictable vehicle performance.

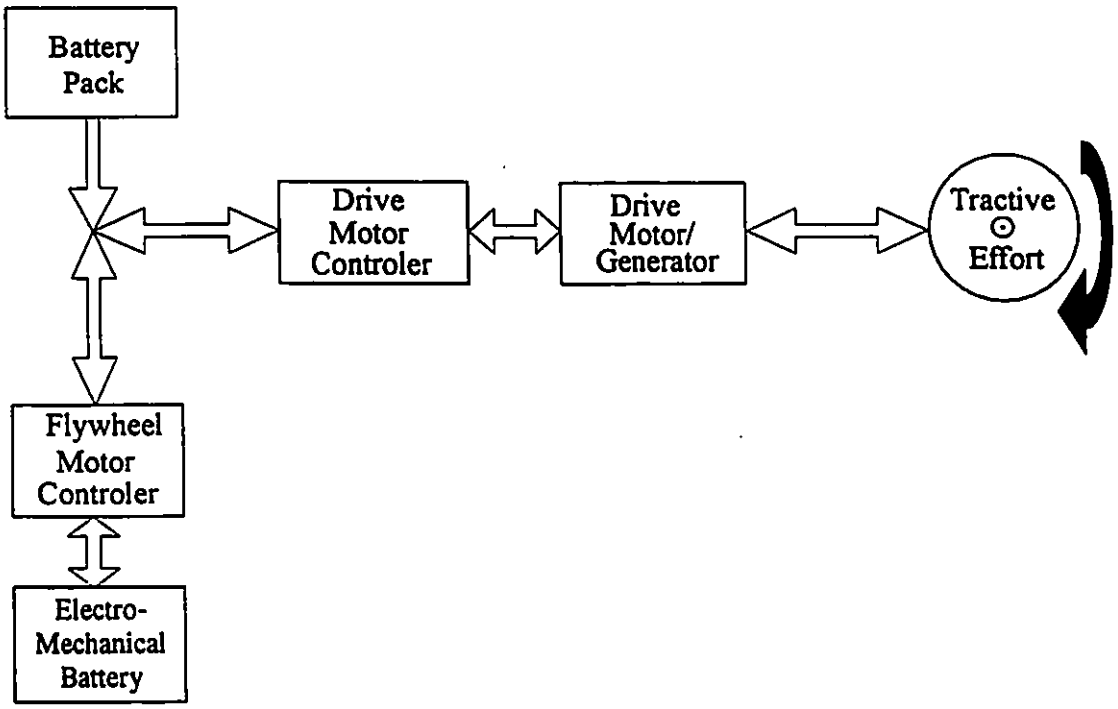

Figure 2-7: Schematic of the EMB/Battery Hybrid Electric Drivetrain.

CHAPTER 3: OPTIMIZATION PROCEDURE

3.1 Main Objective of the Optimization

With the operational characteristics of the hybrid electric drivetrain loosely established, it is the objective of this study to formulate and set the design characteristics or parameters (i.e., flywheel size, battery size, motor sizes, vehicle type and control strategy) of an EMB/battery hybrid electric drivetrain equipped vehicle so as to meet certain performance objectives.

3.1.1 Range Maximization and the Battery State of Charge (Objective Function)

The most sought after performance objective for an electric vehicle is range maximization. Indeed, the electric vehicle has the reputation of being a short distance runner necessitating more frequent battery charges than fuel fill-ups on a gasoline fuelled car [62]. With the battery pack being the energy source, it makes sense to minimize its output in order to maximize the vehicle's range. The battery pack output to be minimized is the amount of charge (A·h) being removed from the battery pack in order for the vehicle to meet a certain task. This is the basis on which a fair comparison can be made of the different options available for a given design characteristic (e.g., a small drive motor compared to a large drive motor).

Minimizing the amount of charge was chosen over the

minimization of the energy or power drawn from the battery pack because the voltage available at the terminals of a battery decreases as the current draw increases [49, 54, 63]. The following equations develop the explanation and the relationship between battery voltage f(i) and current is shown in Figure 3-1. (The plot of Figure 3-1 was obtained using the battery model presented in Chapter 4.1 with the BSOC set at 1.0).

$$\text{Energy} = \text{Power} \cdot t$$

$$\text{Energy} = U \cdot i \cdot t$$

$$\text{Energy} = f(i) \cdot i \cdot t \quad \text{where } i \cdot t = \text{amount of charge (A·h)}$$

$$\text{Energy} = f(i) \times (\text{amount of charge}) \qquad -(1)$$

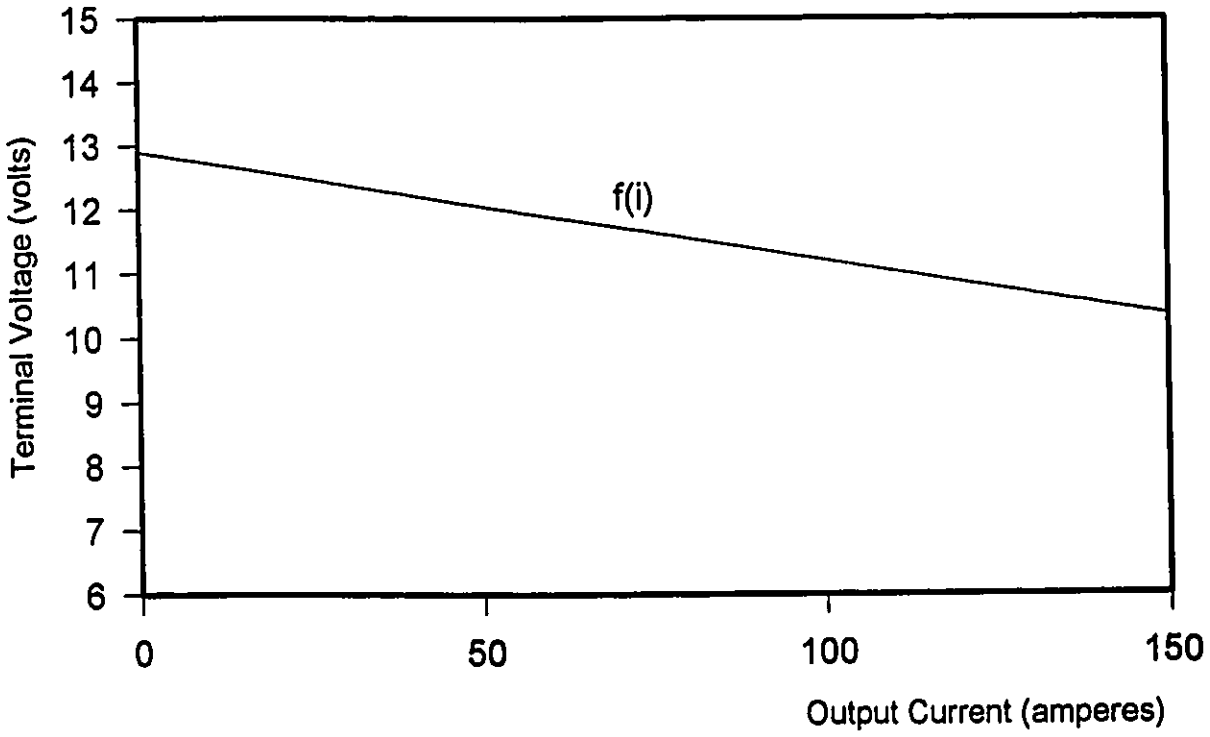

Figure 3-1: Terminal Voltage vs. Current for a Fully Charged Lead- Acid Battery.

Equation 1 shows that a battery being discharged at different rates (i) can supply equal amounts of energy but that the amount of charge removed must vary. This means that although the same amount of energy was drawn from the battery, the amount of charge remaining in the battery is not the same and it is this amount of charge remaining which determines how much more the battery can be discharged. Hence, this amount of charge remaining gives an indication of the expected range of the vehicle.

3.2 Constraints

3.2.1 Vehicle Driveability (performance) and the Duty Cycle

Another important performance objective for an electric vehicle is its driveability. In order to win public acceptance, the electric vehicle should be able to accelerate, stop and cruise like most vehicles on the road today. In other words, the design characteristics of the hybrid electric vehicle must be such that it can perform certain tasks or duties similar to those performed by a gasoline powered vehicle. Therefore, in this study, a vehicle equipped with the hybrid electric drivetrain is required to meet a specified duty cycle. This duty cycle will be the same for all permutations in the design characteristics of the components in the hybrid electric drivetrain. At the end of the duty cycle, the amount of charge remaining in the battery pack will be compared to the amount of charge needed to perform the cycle. Consequently, the objective function is the fraction

of charge remaining in the battery (battery state of charge) at the end of the duty cycle and the optimized hybrid electric drivetrain will have a set of design characteristics or parameters which allows the battery pack to keep the highest percentage of its initial charge at the end of the cycle. In other words, with the battery pack being fully charged at the beginning of the duty cycle, the objective is to operate the hybrid electric drivetrain and size its components so as to maximize the battery's state of charge at the end of the duty cycle.

The duty cycle chosen is the Federal Urban Drive Schedule (FUDS). This cycle is simply a velocity profile which the vehicle is required to follow and does not involve any driving into head winds, hills or curves. The FUDS was developed for the United States Environmental Protection Agency in order to assess the fuel consumption and pollutant emissions of fossil fuelled light duty passenger vehicles. A vehicle being tested for fuel consumption and emissions is simply required to meet the velocities which are given at intervals of one second. Figure 3-2 presents the FUDS as a velocity versus time plot. The maximum velocity is 90 km/hr and the cycle lasts 23 minutes during which time the vehicle will have travelled 12 km. Peak accelerations are in the order of 0 to 60 km/hr in 17 seconds and 30 to 75 km/hr in 15 seconds. Apart from the driver, the vehicle is driven over the FUDS unladen of any cargo.

The FUDS has been chosen for this study because it is used

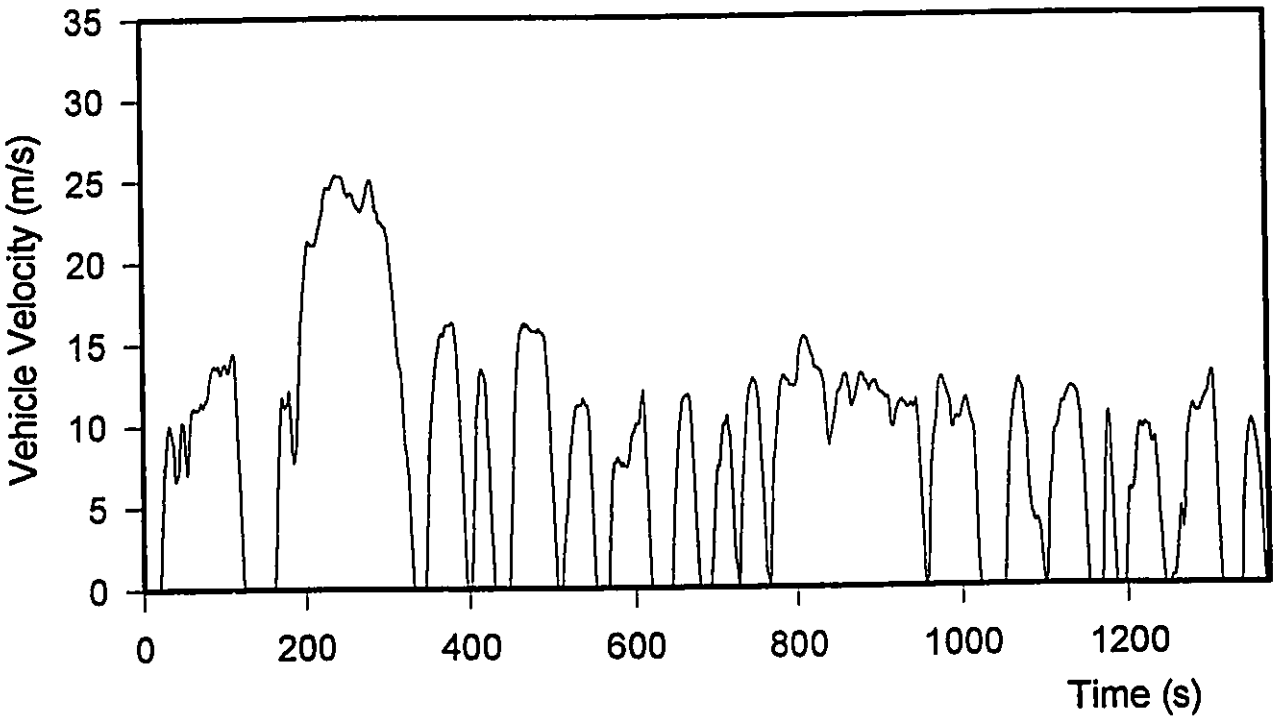

Figure 3-2: The Federal Urban Drive Schedule. [51]

to evaluate the fuel consumption of all passenger cars sold in North America, and as such, is representative of a typical drive through urban streets and freeways [51]. It is assumed that if the hybrid electric drivetrain can meet this schedule, its performance is sufficient to obtain a driveability comparable to vehicles equipped with internal combustion engines.

3.2.2 Control Strategy

Knowing that the objective of this study is to present a hybrid electric vehicle offering the greatest possible range,

some of the design parameters of the hybrid electric drivetrain can be set intuitively. This is the case for the control strategy; the manner and conditions in which the power flows from one component of the hybrid drivetrain to another.

From what has been demonstrated about battery performance, it makes sense to drain the battery at the lowest rate possible in order to get the most energy out of the battery. For the hybrid electric drivetrain, this objective is easy to meet because the total energy requirement of the vehicle can be averaged out over the duration of the FUDS. Indeed, the hybrid electric drivetrain makes it possible to load level the battery pack. Hence, if the battery is left on for the duration of the FUDS, its power output remains constant and is equal to the total energy required for the vehicle to complete the FUDS divided by the time it takes to complete the FUDS. This is the lowest possible rate at which the battery can be discharged in order to supply all the energy required to complete the FUDS.

There are, however, certain occurrences in the FUDS which require that the battery output be temporarily set to zero. This is the case during regenerative braking. For the hybrid electric drivetrain, regenerative braking energy is returned to the EMB. If the battery is left on during these instances, the EMB has to absorb both power from braking and from the battery. This means the EMB must absorb energy at a higher rate (power) which adversely affects the operating efficiency of the EMB. However,

if the battery is shut off during regenerative braking, it means a decrease in the amount of time that the battery can stay on during the FUDS, hence, a reduction in the amount of time over which the energy requirements of the FUDS can be averaged out. In order to meet the total energy requirement of the FUDS, the constant power output from the battery must therefore be increased slightly. This slight increase of power from the battery decreases the operating efficiency and energy density of the battery but the losses incurred here are smaller than those resulting from the inefficient high power operation of EMB. Hence, shutting-off the batteries during regenerative braking is the most efficient way of operating the hybrid electric drivetrain. However, it is understood that, if the vehicle is in actual use and not operating on a predetermined duty cycle such as the FUDS, leaving the battery on during regenerative braking is perhaps not efficient but may be desirable in order to rapidly recharge the EMB which is, for some reason, close to full discharge. This situation is avoided in the FUDS because the battery power output is sufficiently large to keep, at all times, an acceptable amount of charge in the EMB. (See section 3.2.3 for an explanation of how the amount of energy in the EMB determines the constant power output from the battery).

The battery power output must also be temporarily set to zero when the EMB is fully charged and the demand from the drive motor is lower than the constant power output of the battery. This is of course necessary in order to avoid overcharging the

EMB. The resultant reduction of on-time for the battery means an increase in the value of the constant power output from the battery, hence, a decrease in the available energy density of the battery. This situation is not conducive to the maximization of the vehicle range and it explains why a properly optimized hybrid electric drivetrain will have its components sized such that the EMB will never or rarely be fully charged. This restriction on battery power output is therefore not applicable to the optimized hybrid electric drivetrain but it has been retained in order to permit evaluations of non-optimal hybrid electric drivetrains which are required for the solution of any optimization problem.

High rate charging of batteries is generally inefficient and virtually impossible when the batteries are close to full charge [46, 48, 56, 58, 63]. The EMB on the other hand is designed for high rate charge and discharge of energy and as such is generally more efficient than the battery during high rate charging. The hybrid electric drivetrain's overall efficiency is therefore maximized if all the regenerative braking energy is used to recharge the EMB only. Also, the design of the hybrid electric drivetrain is such that the lead-acid battery pack could be replaced with other non-rechargeable energy sources such as fuel cells or an I.C. engine-generator module. For these reasons, the battery pack of the hybrid electric drivetrain will only supply energy and recharging will not be possible during the duty cycle.

If a condition occurs such that the EMB is fully charged

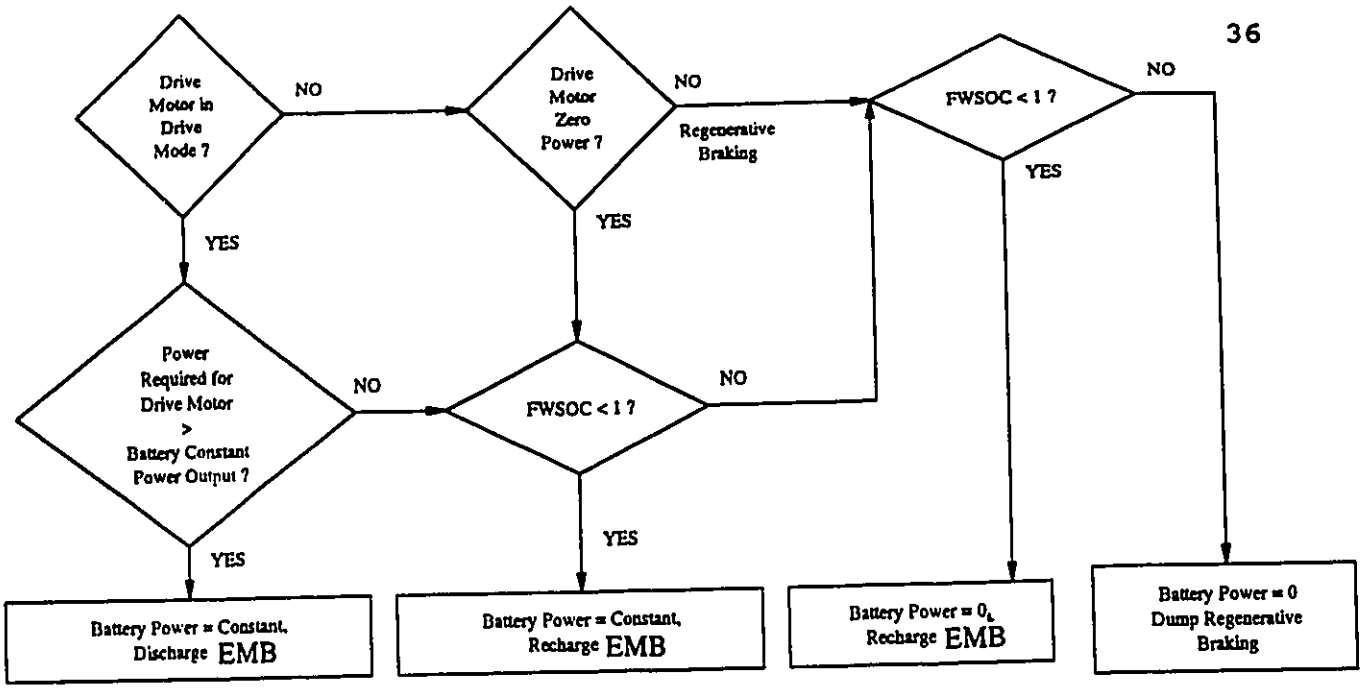

Figure 3-3: Control Strategy of the Hybrid Electric Drivetrain.

during regenerative braking, the regenerative braking energy is simply dumped (the battery pack of the hybrid electric drivetrain cannot be recharged). This method of operation is not the most efficient but, again, if the components of the hybrid electric drivetrain are optimally sized, this condition does not occur. The dumping of regenerative braking energy when the EMB is full is therefore a constraint which, when used in the optimization, naturally eliminates any combination of components that yields an inefficient operation of the hybrid electric drivetrain.

Thus, in this study of the hybrid electric drivetrain, the battery either comes on for limited periods of time at a predetermined power level (See section 3.2.3 for an

explanation of how the constant battery power output is determined) or is shut-off completely for limited periods of time. The EMB makes up or absorbs the difference of power which is either necessary to propel the vehicle or in excess of what is required to propel the vehicle. Note that for the electric only drivetrain, recharging of the battery pack during regenerative braking is possible. Indeed, the battery model used for this study predicts the losses and performance of the lead-acid battery pack during charge or discharge at any power level (See Chapter 4.1 for limitations of the model).

3.2.3 Battery Output and the Net Energy Output of the EMB

The question arises: What value should be assigned to the constant power output from the battery pack? Considering its direct influence on the outcome of the objective function, it is important that the battery's constant power level be set in such a way as to provide a fair basis on which all permutations/ combinations of the design parameters can be compared. Therefore, the power level will be set so as to meet the following constraints:

(i) In order to provide for the use of the hybrid drivetrain in real life situations, the minimum amount of charge in the EMB must be constrained. 25% of the maximum charge that the EMB can store is generally sufficient to provide the vehicle with a "safety net"

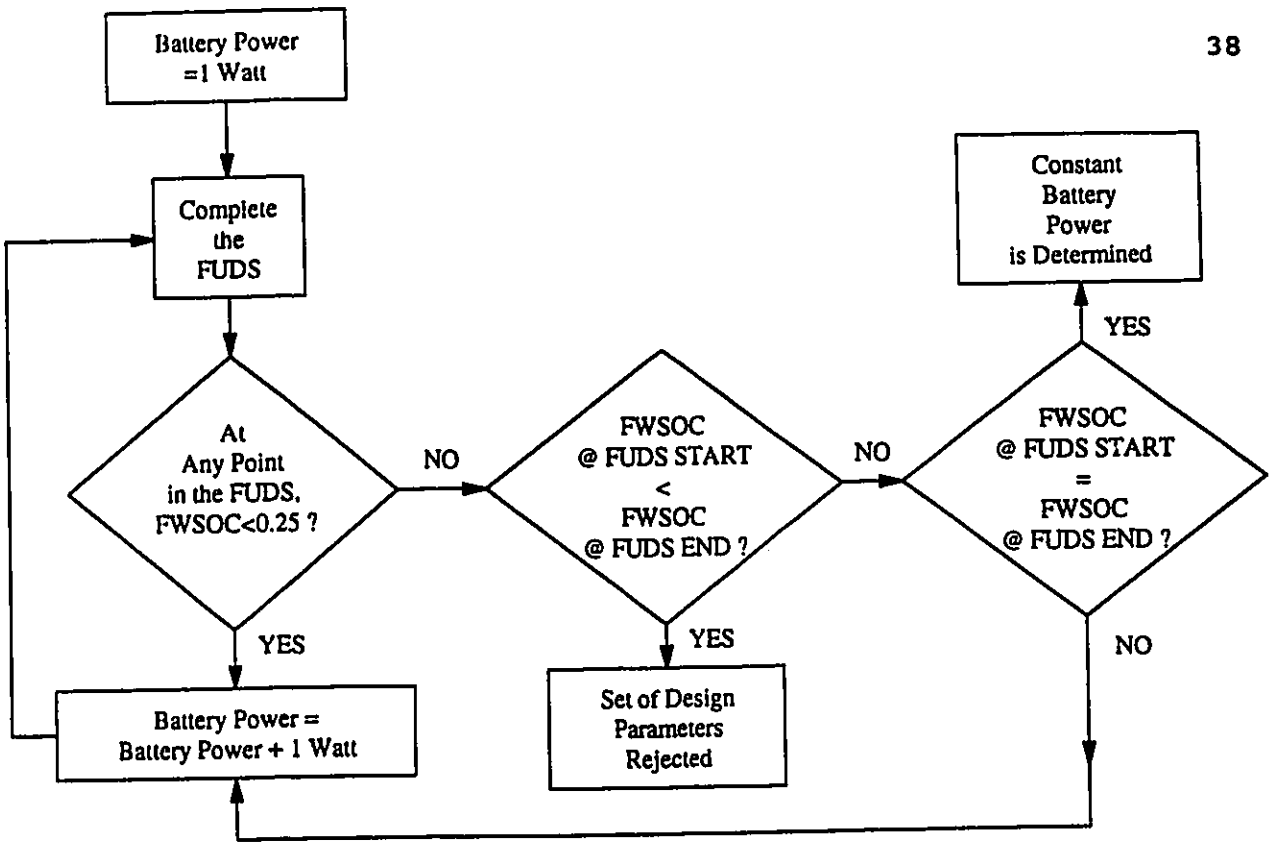

Figure 3-4: Determining Battery Pack Constant Power Output.

should the demand for more energy be requested [21, 34, 35, 37]. Therefore, during the duration of the duty cycle, the EMB will not be allowed to be discharged beyond this 25% limit nor will it be allowed to be overcharged (the battery power falls to zero and regenerative energy is dumped when the EMB is fully charged).

(ii) In order to avoid using the EMB as a source of energy, the state of charge of the EMB or flywheel state of charge (FWSOC) must be the same at the beginning and

end of the duty cycle.

If, for a set of design parameters, constraint (i) is met but constraint (ii) cannot be met, then the set is rejected and cannot be considered as the optimal solution.

3.2.4 Component Performance Limitations

Because the voltage at the terminals of the battery pack decreases with increasing power output, a minimum allowable voltage must be specified. Hence, if the constant power output from the battery is high enough to cause the voltage to drop below this minimum, the set of design parameters causing this situation will be rejected.

Similarly, the drive motor/generator and flywheel motor/generator cannot be operated at power levels so high as to cause overheating. This is why the sum of all losses in the electric motor/generator must always be below the rate at which heat can be dissipated from the motor casing. However, the motor/generators used in this study can handle up to two times their rated heat dissipation rate for short periods of time (less than 30 seconds). This constraint will be adhered to and any set of design parameters will be rejected if one or both motor/generators are overworked.

3.3 Preassigned Parameters

3.3.1 Vehicle Type

Other design parameters are set arbitrarily due to certain requirements and limitations. Hence, the objective of lowering energy consumption was not considered in the choice of a vehicle into which the hybrid electric drivetrain would be installed. Indeed, for the purposes of this study, the type of body or aerodynamic characteristics of the vehicle are those of a mini-van as shown in Figure 3-5 and Table 3-1.

The reason for this choice is that the mini-van is often used as a fleet vehicle and thus represents an excellent way of introducing the electric vehicle onto the market. Also, mini-vans and sedans on the road today often share the same internal combustion engine powertrain. Thus, the hybrid electric drivetrain designed for the mini-van could perhaps be used on other vehicle types (e.g., light truck, station wagon, sedan and sports). Lastly, because of space and payload limitations, the conversion to battery power is easier to accomplish in a van than any other light-duty passenger vehicle.

The mass of the vehicle however cannot be fixed because it is dependant on the size of the components used in the hybrid electric drivetrain (i.e., battery size, motor sizes, flywheel size). There is, of course, a baseline mass or glider mass to which the masses of the various components is added. The total vehicle mass is important because it affects both the power required to accelerate/decelerate and the rolling resistance.

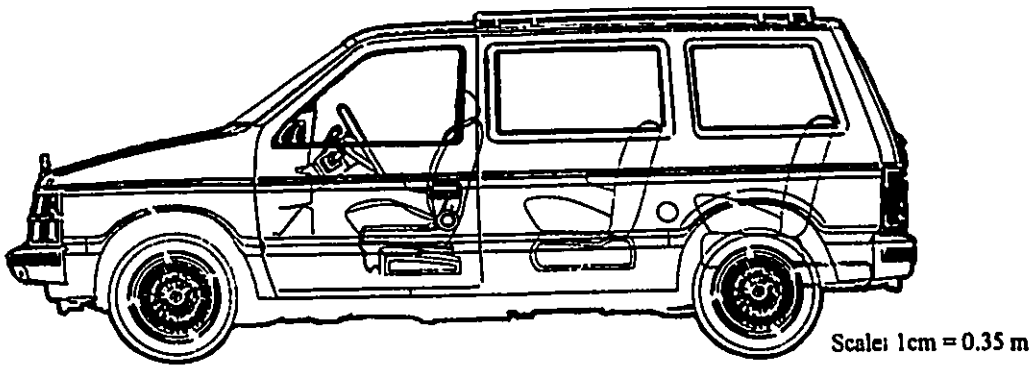

Figure 3-5: Chrysler Mini-Van

Table 3-1: Mini-Van Specifications.

Vehicle Test Mass (VTM,kg)	Glider Mass (production vehicle stripped of I.C. engine and ancillaries)		1212 kg
	Payload (driver)		100 kg
	Electric Drivetrain Ancillaries (motor mounts, wiring)	Drivetrain Mass	60 kg
	Drive Motor Controler		20 kg
	Drive Motor		variable
	EMB Motor Controller		20 kg
	EMB Containment		50 kg
	EMB Motor		variable
	EMB Flywheel		variable
	Battery Pack		variable
	Battery Box		45 kg

Equivalent Translating Mass of Rotating Members	60 kg
Rolling Resistance (newtons)	0.0931·(VTM)
Coefficient of Aerodynamic Drag	0.32
Vehicle Frontal Area	2.66 m^2
Air Density	1.2 kg/m^3

3.3.2 Temperature

Due to the unavailability of reliable data concerning the influence of temperature on the operation of the motor/generators and battery pack, the temperature of these components has been set to ambient or to a specified operating temperature and considered not to vary. Furthermore, the study of the effect of temperature variations on the performance of any or all components of the hybrid electric vehicle is not an objective.

3.3.3 Motor Controllers

The motor/generator controllers are available in only one model and size, which forces us to use the same ones throughout the analysis.

3.4 Design Variables

With certain design parameters being set (i.e.; duty cycle, vehicle type and control strategy) we now have a fair and constant basis on which other design variables can be evaluated and compared. An optimization technique will select the set of design variables which will give the hybrid electric vehicle its maximum range. Hence, with the objective being range maximization, optimization will result in the proper sizing of certain components. This task cannot be done intuitively or arbitrarily due to the various and conflicting effects that the

component's size has on the efficiency of the hybrid electric drivetrain. For example; if a very large flywheel is used in the hybrid electric drivetrain, the amount of energy stored in the flywheel is also very large. Thus, the flywheel could operate in a limited speed range and still be able to provide the necessary energy to accelerate the vehicle. Furthermore, this speed range could be kept low in order to keep the drag losses at a minimum and thus increase the overall drivetrain efficiency to meet the objective of minimizing the energy or charge drawn from the battery. However, a large flywheel is heavy and therefore increases the total vehicle mass. This of course increases energy consumption which is not in agreement with the objective of minimizing the charge drawn from the battery. Also, the large physical dimensions of an oversized flywheel produce higher drag losses which could off-set the advantage of low speed, limited speed range operation. Similarly, an undersized flywheel provides the advantage of reduced mass and reduced drag but the wider operating speed range means high drag losses at high speed and low flywheel motor efficiency at low speed.

Thus, it is obvious that the effects brought about by a simple increase or decrease in the size of the flywheel are not easy to assess when the objective of range maximization is considered. Table 3-2 lists the flywheel size along with the other design variables which need to be optimally sized and, through an intuitive analysis, the most obvious effects brought about by variations in the size of the components are put forward.

Table 3-2: The Design Variables.

Undersizing of the Design Variables brings about effects which are conducive in		Optimal sizing of the Design Variables yields a maximum BSOC @ FUDS END	Oversizing of the Design Variables brings about effects which are conducive in	
minimizing BSOC @ FUDS END	maximizing BSOC @ FUDS END		maximizing BSOC @ FUDS END	minimizing BSOC @ FUDS END
-low battery efficiency	-low vehicle test mass	**Battery Pack Mass (BPM)**	-high battery efficiency	-high vehicle test mass
-flywheel operates over large rpm range	-low vehicle test mass -low drag losses	**Flywheel Size (FWS)**	-flywheel operates over small rpm range -low speed and low drag losses	-high vehicle test mass -high drag losses
-high losses at high power	-low vehicle test mass -low losses at low power	**Flywheel Motor Size (FWMS)**	-low losses at high power	-high vehicle test mass -high losses at low power
-high losses at high power	-low vehicle test mass -low losses at low power	**Drive Motor Size (DMS)**	-low losses at high power	-high vehicle test mass -high losses at low power
-low flywheel motor efficiency	-low drag losses	**Flywheel State of Charge at Beginning and end of duty cycle (FWSOC @ FUDS START & END)**	-high flywheel motor efficiency	-high drag losses

3.5 Solution Technique

3.5.1 Evaluation of the Objective Function

The value of the objective function is calculated numerically using a computer algorithm which calculates the amount of charge removed from the battery pack for every second during the duty cycle. The amounts of charge removed for each second are then summed over the complete cycle to give the total amount of charge removed from the battery pack. The mass or size of the battery pack gives us the amount of charge available at the beginning of the cycle. Thus, the percentage of charge remaining in the battery pack at the end of the cycle can be deduced.

In order to calculate the amount of charge removed from the battery pack for each second in the duty cycle, the amount of power/energy required or available at the wheels of the mini-van is calculated using information about the physical characteristics of the vehicle (i.e., aerodynamic drag, mass and rolling resistance) and the velocity/acceleration characteristics of the duty cycle. This power and energy is either supplied by (drive) or returned to (regeneration) the vehicle drivetrain and, as shown in Figure 3-6, the models describing the losses in each drivetrain component, together with the control strategy and constraints allow an evaluation of the instantaneous power/energy flowing to/from/through each component. Thus, for each second in the duty cycle, an amount of charge removed from the battery pack can be evaluated.

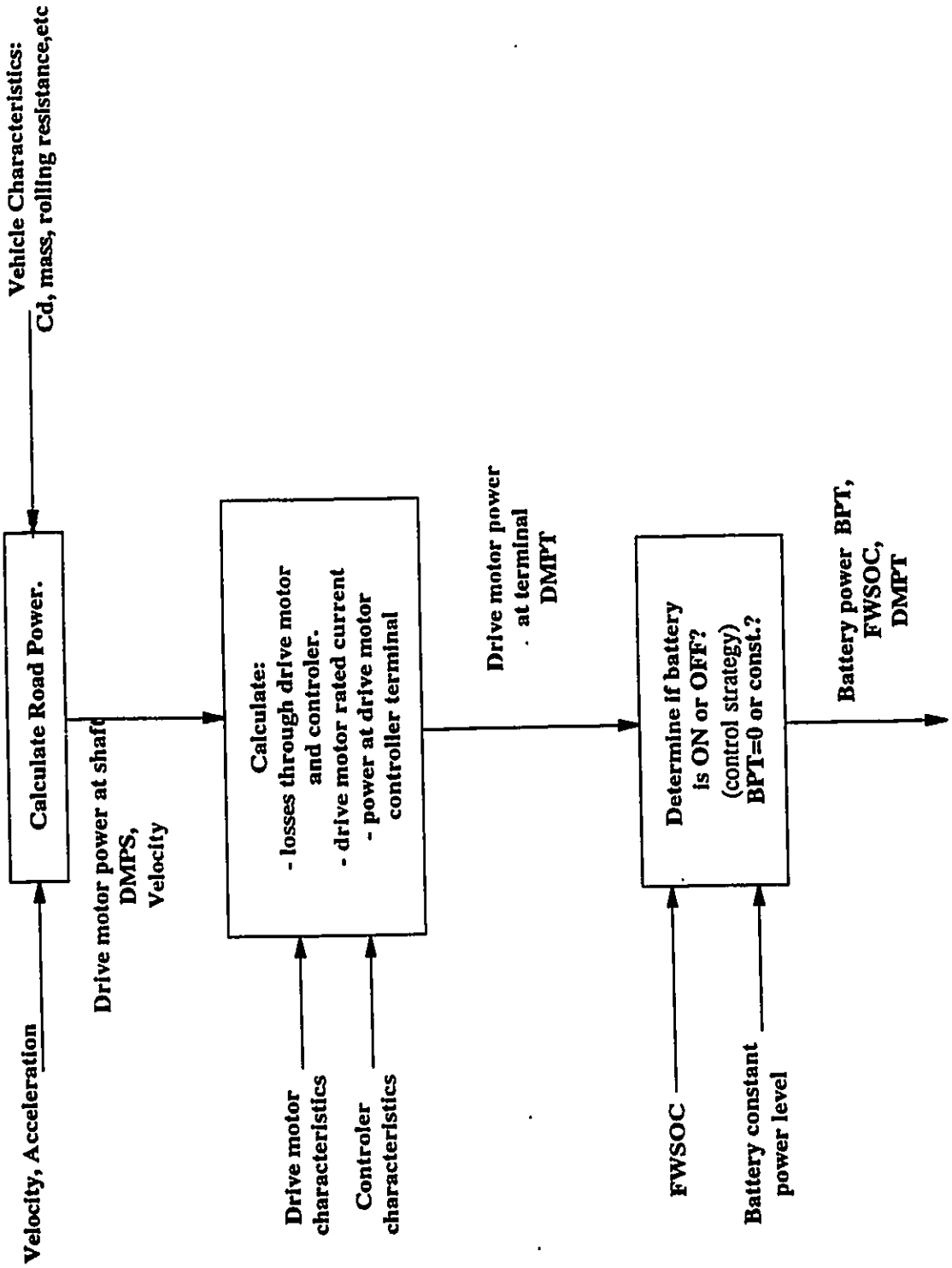

Figure 3-6A: Evaluation of Instantaneous Power and Energy Consumption in the Hybrid Electric Drivetrain.

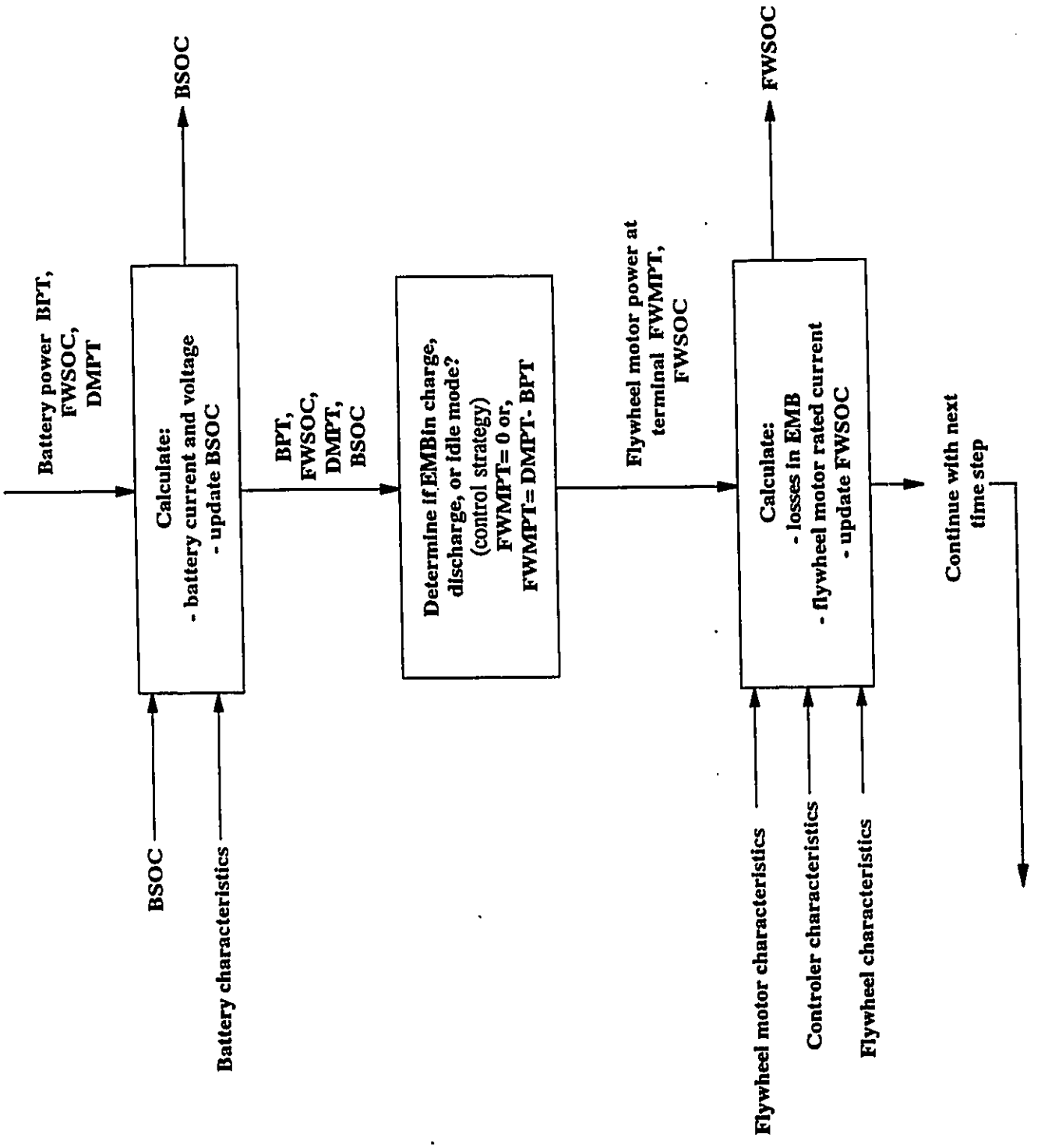

Figure 3-6B: Evaluation of Instantaneous Power and Energy Consumption in the Hybrid Electric Drivetrain.

3.5.2 Optimization Method

Because of the multi-dimensional nature of the problem (i.e., the design vector has five variables), it is necessary to use a multi-dimensional optimization method. The choice of technique to be used is further constrained due to the fact that the value of the objective function has to be calculated numerically. Therefore, any analytical method as well as any method requiring derivatives have to be ruled out. Furthermore, due to the complexity of the problem and the presence of several constraints, the existence of local maxima and the probable non-linear behaviour of the objective function cannot be ignored. Considering all of the above-mentioned arguments, along with the added convenience of being relatively easy to program, an exhaustive search technique was adopted for this study [28,64].

This technique requires the complete scanning of the design variable space. In other words, all combinations of the design variables are tried out in a search for the optimal combination. A coarse search is done by assigning different values to each design variable (e.g., { battery pack mass = 100 kg, 500 kg, 1000 kg, 1500 kg, 2000 kg}, { drive motor size = 10 kW, 50 kW, 100 kW, 150 kW, 200 kW}, {flywheel size = ...}, etc.). From this choice, optimum design variables are found (e.g., {1000 kg}, {100 kW}, etc.) and a second more refined search is done around the optimum (e.g., { battery pack mass = 500 kg, 750 kg, 1000 kg, 1250 kg, 1500 kg}, {drive motor size = 50 kW, 75 kW ...}, etc.).

The refinement of the search is continued until the variation in the value of the objective function (battery state of charge at the end of the duty cycle, BSOC @ FUDS END) becomes negligible from one search to the next. A tolerance of 0.05% is considered acceptable.

The exhaustive search technique and the use of an iterative procedure to calculate the objective function value requires large amounts of computation time. Fortunately, due to the theoretical nature of this study, evaluations in real time are not necessary and rapidity is therefore not of prime importance.

CHAPTER 4: MODELLING OF THE HYBRID ELECTRIC DRIVETRAIN COMPONENTS

In order to evaluate the instantaneous power/energy flowing to/from/through each component in the hybrid electric drivetrain, it is necessary to establish efficiency (or loss) equations or performance maps for each component in the hybrid electric drivetrain. Therefore, distinct models describing these losses have been developed for the battery pack, the EMB, the motor controllers and the drive motor.

4.1 Lead-Acid Battery Pack

Because battery mass or size is a variable, the model was normalized against a "gauge" battery. The "gauge" battery used is a Delco-Remy power unit with a mass of 15.2 kg [54]. A certain number of gauge batteries are therefore required to provide the necessary battery pack mass (BPM) and all gauge batteries in the battery pack provide an equal amount of power whose sum is equal to the power required from the battery pack. Furthermore, the gauge batteries are connected in series/parallel so as to obtain a nominal bus voltage of 216 volts which is the operating voltage of the motor controllers.

Although electric vehicle modelling and development have gone on for decades, battery models or experimental performance maps are not well developed. Further, batteries are affected by a number of parameters, including : (i) operating temperature;

(ii) battery age; (iii) number of charge/discharge cycles; (iv) battery size and geometry; (v) battery design; (vi) idle time; (vii) the charge/discharge rate; ;(viii) charge acceptance or charge efficiency and the (ix) battery state of charge [40, 46, 47, 48, 54, 57, 58, 63]. In short, a comprehensive battery model cannot be developed at the present time. This is particularly distressing in assessing the hybrid electric drivetrain because one of its principal advantages, that of load levelling the battery, cannot be properly accounted for.

For the model, a new or near new battery operating at ambient temperature is assumed. The battery equivalent Thevenin circuit shown in Figure 4-1 is used [59, 65] and the battery terminal voltage (E_t) can be expressed as:

$$E_t = E_{oc} - I_b \cdot R_b \qquad \text{——— (2)}$$

where E_{oc} is the open circuit battery voltage, I_b the instantaneous current and R_b the equivalent battery internal resistance.

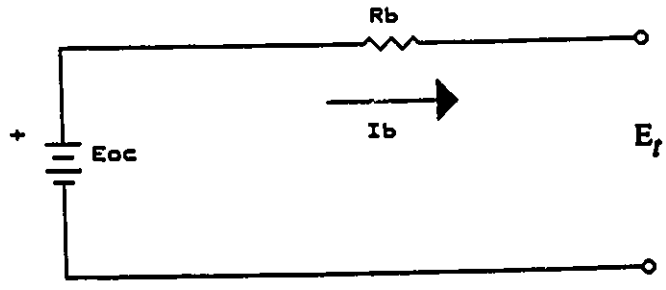

Figure 4-1: Battery Equivalent Thevenin Circuit. [65]

It is now necessary to develop expressions for the circuit terms as functions of the battery state of charge (BSOC) and for charge or discharge conditions.

Agruss [54] presented the results of charge and discharge tests that were done on a 15.2 kg Delco-Remy lead-acid power battery. By curve fitting these test results, the following relationships can be developed:

During Discharge:

$$E_{oc} = 12.9 - 1.0 \cdot (1-BSOC), \text{ Volts} \qquad (3)$$

$$R_b = 0.017 + 0.01 \cdot (1-BSOC), \text{ Ohms} \qquad (4)$$

During Charge:

$$E_{oc} = 12.9 - 1.0 \cdot (1-BSOC), \text{ Volts} \qquad (5)$$

$$R_b = 0.017 + 0.07 \cdot (BSOC), \text{ Ohms} \qquad (6)$$

Figure 4-2 shows the gauge battery performance map predicted by the model. A fully charged unit (BSOC = 1.0) corresponds to an open circuit voltage of 12.9 volts and a capacity of 34 amp-hours (A·h). For further clarification, a battery state of charge equal to 0.0 means that the battery has been discharged by an amount equal to its rated capacity.

Rated capacity is determined by measuring the amount of time it takes for the terminal voltage under load to drop to its cut-off voltage when the battery is discharged (starting from full charge) at a specified constant current. Unfortunately, no

standardization for battery rating has been established. Thus, it is clear that a battery's rated performance can be changed by specifying different values for: (i) cut off voltage, (ii) constant rate (current) discharge, and (iii) open circuit voltage which defines a fully charged battery. The scale for battery state of charge will also be affected by these values and this in turn would modify the values of E_{oc} and R_b. Nevertheless, this model assumes that the linear dependence of R_b and E_{oc} on battery

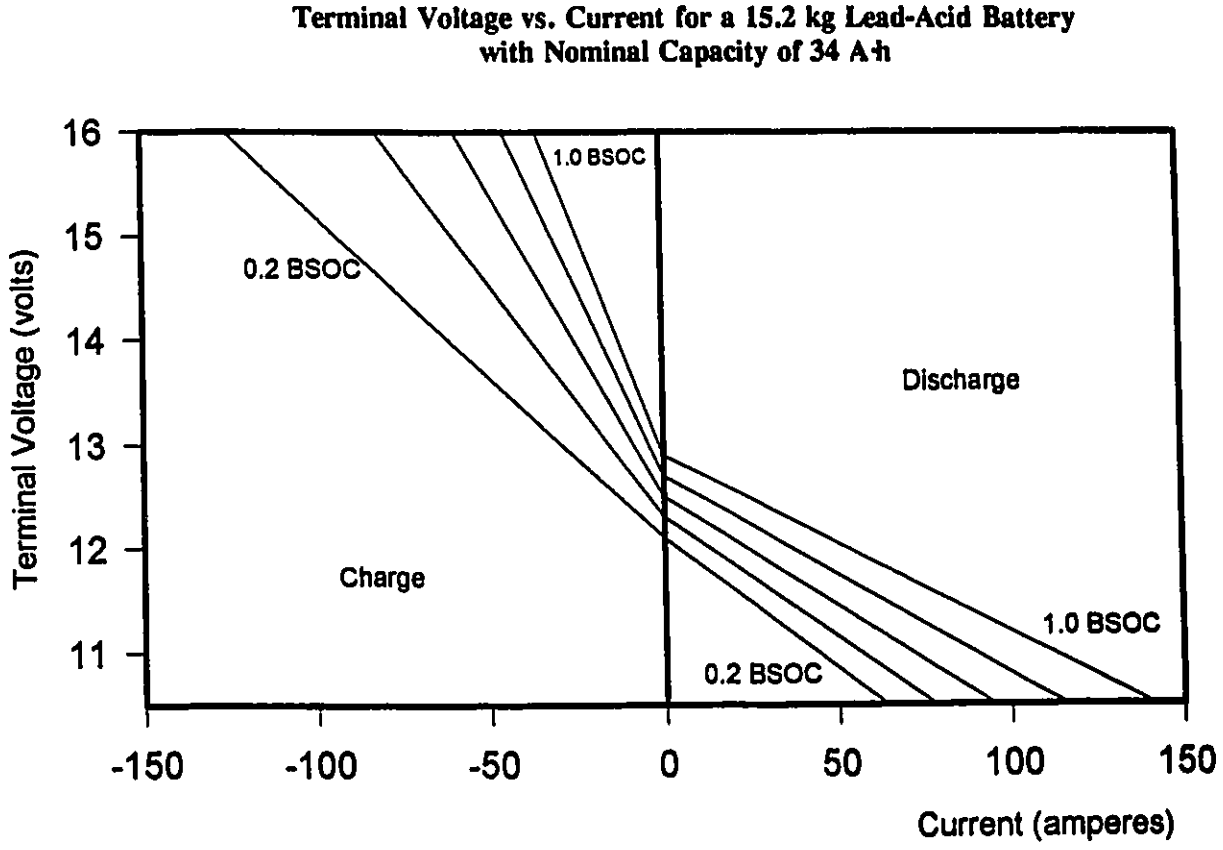

Figure 4-2: Battery Performance Map

state of charge would still remain [54, 57, 59, 65]. Furthermore, the principal of additivity (i.e., the charge removed is additive and independent of the current) is used to establish the battery state of charge.

For battery terminal voltages between 10.5 volts and 16 volts, and for battery state of charge (BSOC) between 0.2 and 1.0, the performance map of Figure 4-2 is in agreement with the test results presented by Agruss [54]. Outside of these boundaries however, the predictions of the battery model cannot be verified because accurate test results could not be obtained outside of these boundaries. Indeed, testing above 16 volts and below 10.5 volts did not give consistent results and the tests were never performed below BSOC of 0.2.

This means that full discharge of the battery pack cannot be predicted by the model and, therefore, evaluations of vehicle range are based on the battery reaching a cut-off voltage of 10.5 volts or a BSOC of 0.2, whichever comes first. This of course underestimates vehicle range because cut-off voltages down to 7 volts are sometimes specified for very high power discharges which are typical of vehicles equipped with electric only drivetrains. Similarly, the load levelling and resultant low power discharge of the battery pack in a hybrid electric vehicle means that the battery can be discharged further than the battery's rated Amp-hour capacity. Thus, in a hybrid electric drivetrain, a battery could, for example, reach a BSOC of minus

0.3 before being considered fully discharged.

For the electric only drivetrain, the use of regenerative braking results in high rate charging of the battery pack. Fortunately, only moderate power levels are obtained from regenerative braking on the FUDS. This means that, for the electric only drivetrain, the terminal voltage of the gauge battery never rises above 16 volts during regenerative braking. The battery model can therefore account for all of the regenerative braking energy. However, on a more demanding duty cycle the use of an electric only drivetrain would result in the dumping of some of the regenerative braking energy in order to prevent excessive out-gassing and damage to the battery.

Indeed, during any charging process, some out-gassing occurs. Thus, as shown in Figure 4-3, not all the charge supplied to a battery is converted to a "reactive state" [40, 45, 46, 48, 56, 58]. The fraction of charge accepted (CA) is dominated by the battery state of charge and is modeled as:

$$CA = 2 - e^{(0.92 \cdot BSOC)^{**}9.8} \qquad \text{(7)}$$

Equation 7 and the resultant curve of Figure 4-3 were derived to fit the test data presented by Nowak [56] and Rowlette [58]. Repeated discharge/charge tests were performed on lead-acid batteries and the difference between Amp-hours discharged and Amp-hours returned was recorded. These tests were done for full

and partial discharges of the battery. Thus a charging efficiency or coulombic efficiency could be plotted as a function of battery state of charge.

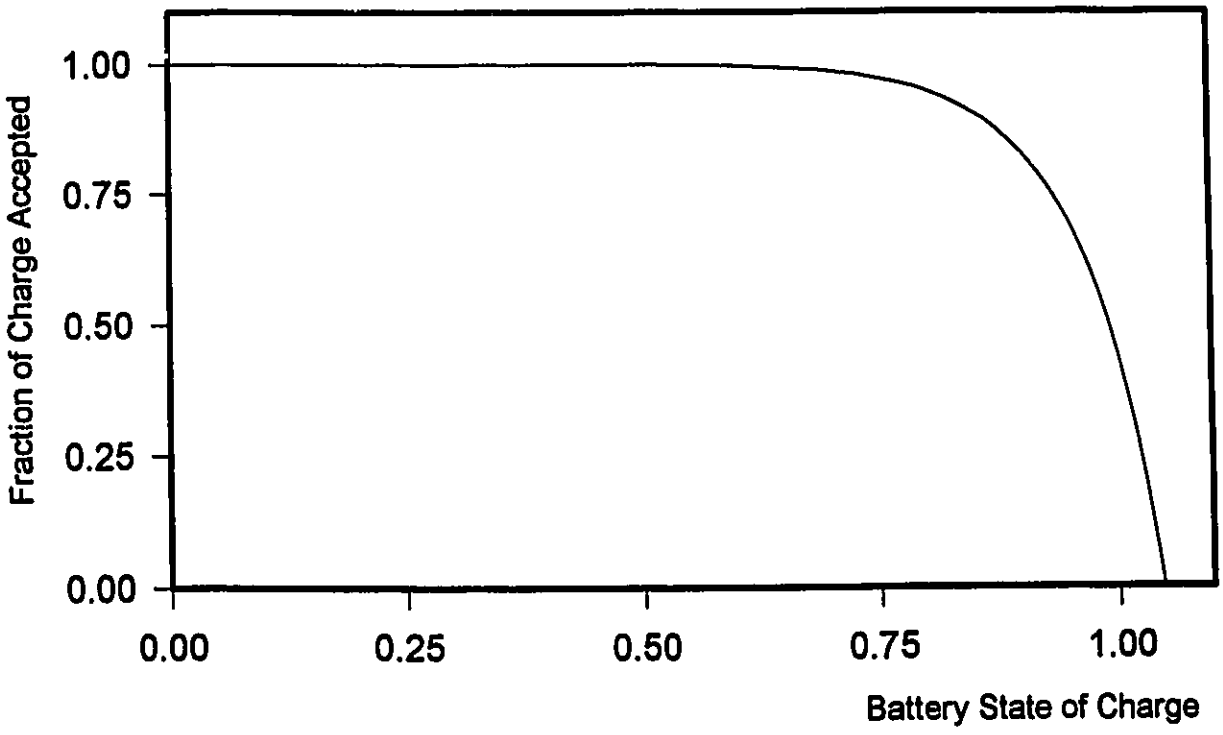

Figure 4-3: Battery Charge Acceptance Characteristics.

4.2 Drive Motor/Generator

An electric motor can be modeled by developing equations which represent the power loss in the unit, namely: copper, windage, hysteresis, eddy current and bearing losses. For this study, test and design data from a 50 kW rated DC brushless motor, built and tested by Unique Mobility Inc., was used. To allow analysis and component size evaluation, the loss equations are written in terms of maximum rated motor power (P_m, watts).

Rated motor power is the shaft power supplied by a motor running continuously at its maximum permissible operating temperature (120°C). For all DC motors, the rated motor power increases with speed to a point where mechanical losses (windage, bearing, hysteresis and eddy current) become so high as to significantly decrease the motor efficiency. Therefore, at a temperature of 120°C the maximum rated motor power is reached at a speed of 7500 rpm. However, the loss equations in this model are established for a constant operating temperature of 60°C. Based on these equations, the calculated maximum power output is higher than the maximum rated motor power (P_m). This discrepancy is of no consequence since the maximum rated motor power is used merely to identify the drive motor size.

Because the motor is directly coupled to the drive wheel of the vehicle, the loss equations can also be expressed in terms of vehicle speed (V, m/s). Here, a motor speed of 7500 rpm

corresponds to a vehicle speed of 120 km/h (33.3m/s) and, the instantaneous drive motor shaft power can be taken as the road power (P_r, watts) determined by the vehicle and duty cycle characteristics. Now, motor armature current (I_m) can be correlated with shaft power and speed as:

$$I_m = P_r / (8.226 \cdot V), \text{ amperes} \quad \text{——— (8)}$$

From data correlation, the empirical loss equations which are valid for both motor and generator can be written as:

$$\text{Copper Loss} = 834\ I_m^2 / P_m, \text{ watts} \quad \text{——— (9)}$$

$$\text{Windage Loss} = 1.81 \times 10^{-6} \cdot V^2 \cdot P_m, \text{ watts} \quad \text{—— (10)}$$

$$\text{Hysteresis Loss} = 2.875 \times 10^{-4} \cdot V \cdot P_m, \text{ watts} \quad \text{—— (11)}$$

$$\text{Eddy Current Loss} = 2.51 \times 10^{-6} \cdot V^2 \cdot P_m, \text{ watts} \quad \text{— (12)}$$

$$\text{Bearing Loss} = 1.343 \times 10^{-4} \cdot V \cdot P_m, \text{ watts} \quad \text{—— (13)}$$

Under continuous operation, the sum of these losses must not exceed the maximum heat dissipation rate of the motor, which is given by:

$$\text{Maximum Heat Dissipation} = 3.4 \times 10^{-2} \cdot P_m, \text{ watts} \quad (14)$$

From the maximum heat dissipation rate, a maximum permissible motor armature current can be expressed as a function of speed (V) and motor size (P_m):

$$\text{Maximum Current} = (P_m/28.9) \cdot (3.4 \times 10^{-2} - 4.218 \times 10^{-4} \cdot V - 4.32 \times 10^{-6} \cdot V^2)^{0.5}, \text{ Amperes} \quad \text{—— (15)}$$

The mass of the drive motor is given by:

$$\text{Drive Motor Mass} = 3.202 \times 10^{-4} \cdot P_m \text{ , kg} \qquad \text{——— (16)}$$

4.3 Motor Controllers

The solid state controllers, designed and tested by Unique Mobility, have resistive and switching power losses. For this analysis, both the drive motor and flywheel motor controllers are assumed to be the same and independent of motor size. From the design data, the power loss in drive motor controller (P_{cm}) can be expressed as a function of drive motor armature current (I_m).

$$P_{cm} = 0.06 \cdot I_m^2 + 1.296 \cdot I_m \text{ , watts} \qquad \text{——— (17)}$$

The mass of each controller is equal to 20 kg.

An efficiency map which takes into consideration the losses in both drive motor and controller is shown in Figure 4-4 for a 62 kW rated drive motor.

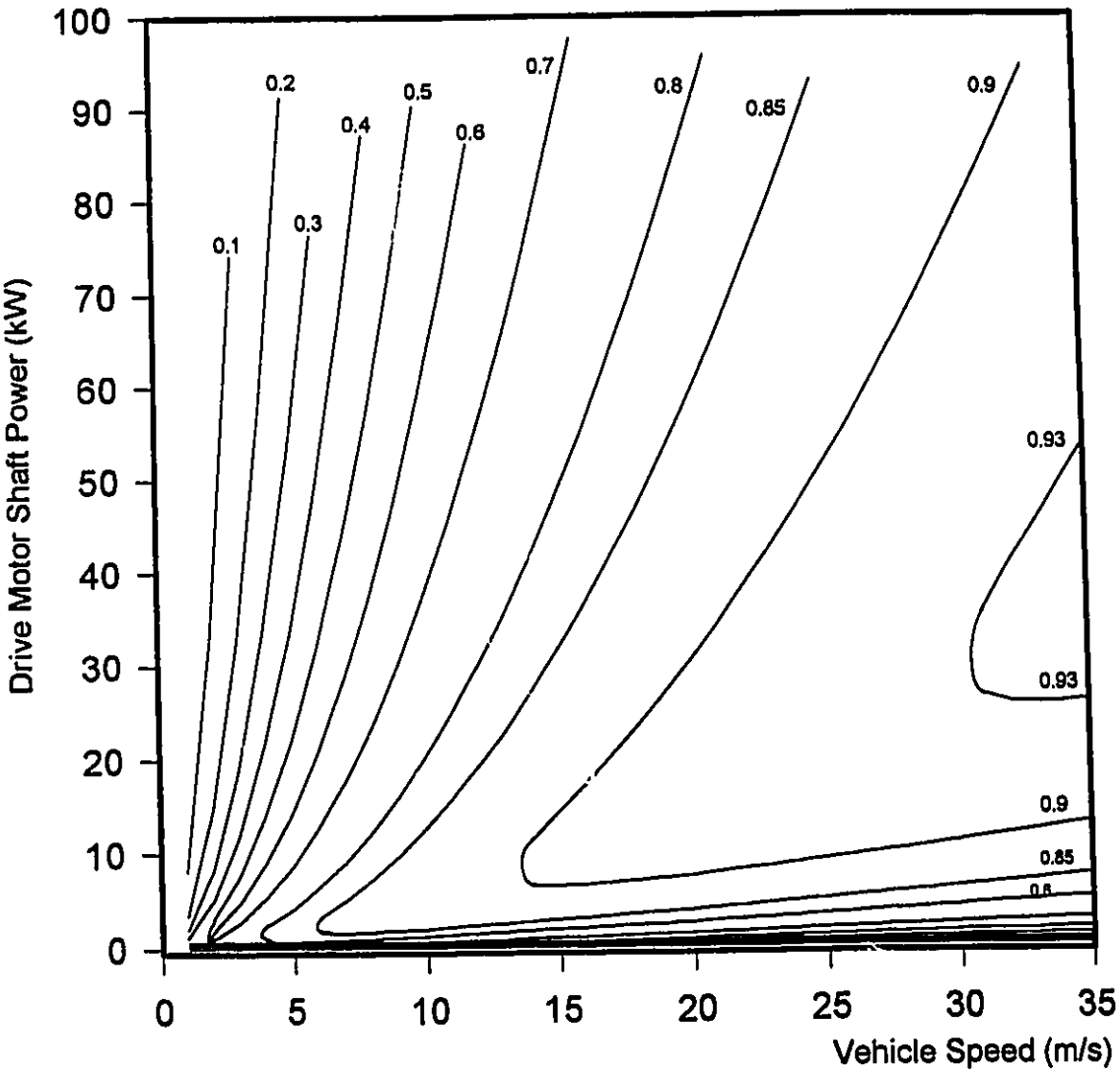

Figure 4-4: Efficiency Map for 62 kW Rated Drive Motor

4.4 Electro-Mechanical Battery

The EMB consists of a high performance fibre composite flywheel directly coupled to a high speed permanent magnet motor/alternator [38]. The unit is enclosed in a sealed vacuum container and is supported with a set of ceramic bearings. Thus, the type of losses that are associated with the flywheel motor/generator are the same as those associated with the drive motor. Here however, the mechanical losses (windage and bearings) are largely attributed to the flywheel [38, 66, 67, 68] although a small component of the bearing loss is attributed to the motor.

The loss equations were correlated with data from several flywheels designed and tested at the University of Ottawa [38, 42] and a 50 kW, 40 000 rpm motor designed by Unique Mobility. As with the drive motor, in order to facilitate analysis and component size evaluation, the loss equations are written in terms of maximum rated flywheel motor power (P_f,watts) and maximum rated flywheel energy storage (E_f, joules). The maximum rated flywheel motor power (P_f) is defined much the same way as the drive motor with a temperature of 120°C and a speed of 40 000 rpm. The maximum rated flywheel energy (E_f) or flywheel size is defined as the amount of kinetic energy stored in a flywheel spinning at its maximum design speed of 40 000 rpm.

Because the flywheel and motor are directly coupled, all rotational speeds can be expressed as the square root of flywheel

state of charge (FWSOC) which is defined as the ratio of instantaneous flywheel energy to maximum rated flywheel energy. For clarity; a FWSOC equal to 1.0 means the flywheel and motor are spinning at top speed (40 000 rpm), a FWSOC equal to zero means the flywheel's angular velocity is zero and a FWSOC equal to 0.25 describes the flywheel/motor spinning at half its maximum design speed.

Flywheel motor armature current (I_f) can be expressed in terms of the flywheel motor instantaneous shaft power (P_s,watts) and the motor speed as:

$$I_f = P_s/(210 \cdot (FWSOC)^{0.5}) \text{ , amperes} \qquad (18)$$

The loss equations which are valid in both charge and discharge modes at an operating temperature of 60°C and pressure of 10^{-2} Torr can be written as:

$$\text{Copper Loss} = 317 \cdot I_f^2/P_f \text{ , watts} \qquad (19)$$

$$\text{Hysteresis Loss} = 5.163 \times 10^{-3} \cdot (FWSOC)^{0.5} \cdot P_f \text{ , watts} \qquad (20)$$

$$\text{Eddy current Loss} = 1.537 \times 10^{-3} \cdot (FWSOC) \cdot P_f \text{ , watts} \qquad (21)$$

$$\text{Motor Bearing Loss} = 6.6 \times 10^{-3} \cdot (FWSOC)^{0.5} \cdot P_f \text{ , watts} \qquad (22)$$

$$\text{Flywheel Bearing Loss} = 3.0 \times 10^{-5} \cdot (FWSOC)^{0.5} \cdot E_f + 7.0 \times 10^{-5} \cdot (FWSOC) \cdot E_f \text{ , watts} \qquad (23)$$

$$\text{Aerodynamic Drag} = 1.0 \times 10^{-4} \cdot (FWSOC) \cdot E_f \text{ , watts} \qquad (24)$$

The maximum heat dissipation rate of the flywheel motor is given by:

$$\text{Maximum Heat Dissipation} = 2.0 \times 10^{-2} \cdot P_f \text{ , watts} \quad (25)$$

and the maximum permissible flywheel motor armature current is:

$$\text{Maximum Current} = (P_f/17.8) \cdot (2.0 \times 10^{-2} - 1.176 \times 10^{-2} \cdot (\text{FWSOC})^{0.5} - 1.537 \times 10^{-3} \cdot (\text{FWSOC}))^{0.5}, \text{ Amperes} \quad (26)$$

The mass of the flywheel motor is given by:

$$\text{Flywheel Motor Mass} = 1.896 \times 10^{-4} \cdot P_f \text{ , kg} \quad (27)$$

and the mass of the flywheel:

$$\text{Flywheel Mass} = 8.3 \times 10^{-6} \cdot E_f \text{ , kg} \quad (28)$$

The power loss in the flywheel motor controller (P_{cf}) is expressed as:

$$P_{cf} = 0.06 \cdot I_f^2 + 1.296 \cdot I_f \text{ , watts} \quad (29)$$

The sum of aerodynamic drag and flywheel bearing losses is presented in Figure 4-5 as a function of flywheel angular velocity for a 2100 kJ (0.58 kW·h) rated flywheel. An efficiency map which takes into account the losses in both flywheel motor and controller is shown in Figure 4-6 for a 30 kW rated flywheel motor.

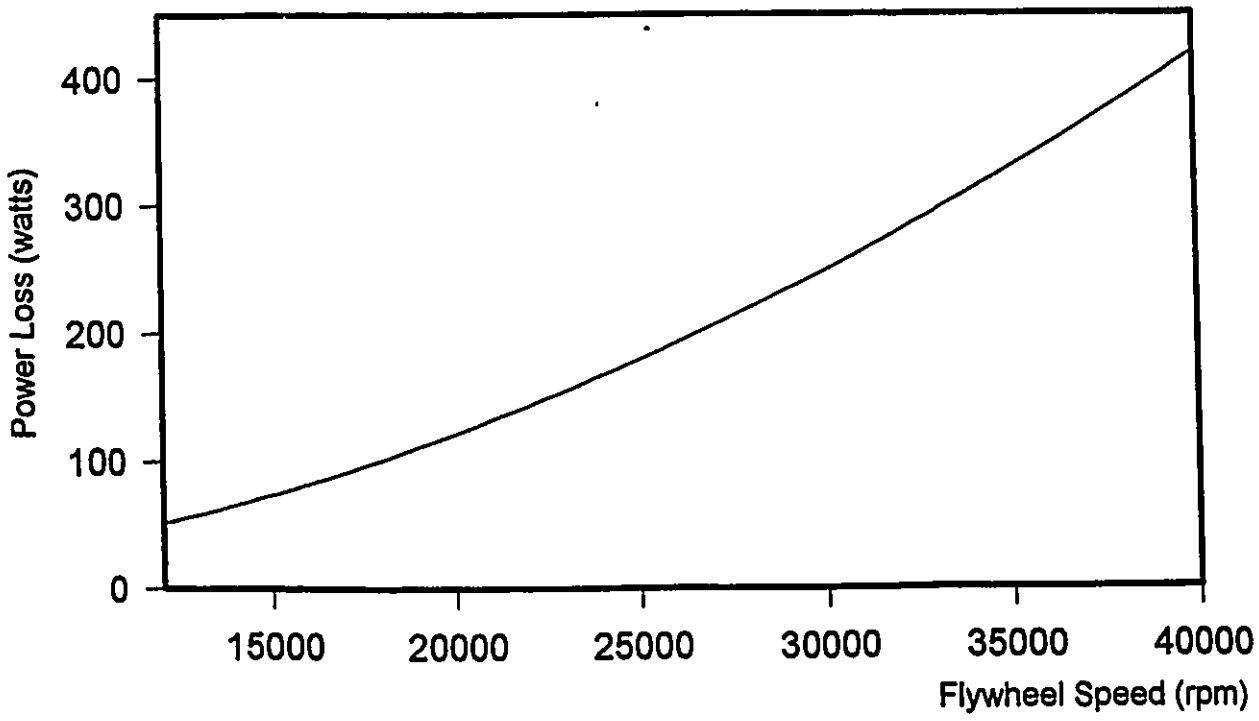

Figure 4-5: Flywheel Drag (bearing and aerodynamic) vs. Speed for a 2100 kJ (0.58 kW·h) Rated Flywheel.

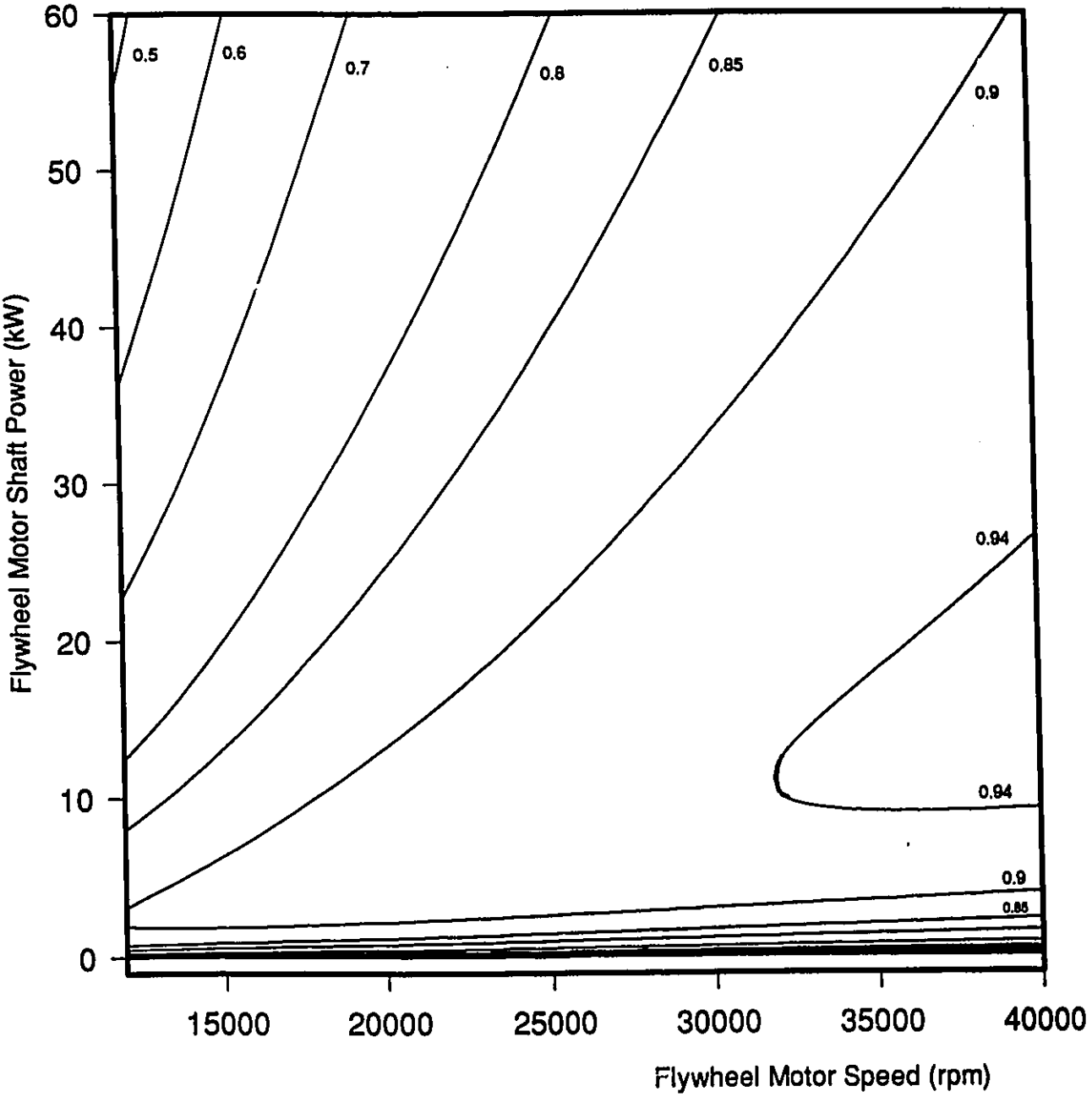

Figure 4-6 : Efficiency Map for 30 kW Rated Flywheel Motor.

CHAPTER 5: OPTIMIZATION RESULTS AND ANALYSIS

5.1 Optimization Results

5.1.1 The Objective Function: BSOC @ FUDS END

The main objective of this study is to size the components of the hybrid electric drivetrain so that the driving range of the vehicle is maximized. Based on the performance of a mini-van operating over the FUDS, the optimal configuration of the hybrid electric drivetrain will be one which uses the minimum amount of charge from the battery in order to complete the FUDS. In other words, the amount of amp-hours (A·h) consumed per kilometre travelled must be minimized.

The minimization of amp-hours consumed was chosen over the minimization of energy consumption because, for the battery, the rate (power) at which energy is delivered determines the amount of amp-hours required to do a certain amount of work (energy). Also, an increase in the power output means a decrease in the total useable capacity (A·h) of the battery. Thus, it is clear that, as an indicator, energy consumption alone is not sufficient to determine if the battery is operating optimally such that vehicle range is maximized. Therefore, the optimization routine used in this study finds the hybrid electric drivetrain configuration which results in the right combination of power and energy draw from the battery such that battery charge or amp-hour consumption is minimized.

However, on its own, the quantity to be minimized (A·h/km) is not sufficient to determine if the drivetrain is yielding the greatest range. Indeed, a hybrid electric vehicle equipped with a very small battery pack is light and therefore will require only a small quantity of amp-hours in order to complete the FUDS. The battery pack is so small however, that it is completely discharged by the time the vehicle reaches the end of the FUDS. Thus, despite the fact that the number of amp-hours consumed to complete the FUDS is minimal, the vehicle range remains ridiculously low. The number of amp-hours consumed to complete the FUDS must therefore be compared to the full charge capacity of the battery pack. Thus, the optimal configuration of the hybrid electric drivetrain is one which uses the smallest percentage of the battery pack's rated amp-hour capacity. Put another way, the optimal hybrid electric drivetrain is one which, after completing the FUDS, leaves the battery pack with the highest percentage or fraction of its initial amp-hour capacity. This quantity to be maximized is called the battery state of charge at the end of the Federal Urban Drive Schedule (BSOC @ FUDS END) and is the only true indicator of expected vehicle range. Hence, optimization will define the hybrid electric drivetrain configuration which yields the highest value of the objective function (BSOC @ FUDS END).

5.1.2 The Optimal Battery Pack Mass

Now, if the same hybrid electric vehicle is equipped with a

very large battery pack, the amount of charge initially available to propel the vehicle is very large. Thus, one would expect the large battery pack to propel the vehicle along a much greater distance than the small battery pack could. However, the increased capacity of a large battery pack also means an increase in the total vehicle mass. In order to move this heavier vehicle along the FUDS, more energy and thus, more charge has to be supplied by the battery. It is obvious that the advantage of increasing the battery pack mass (increased amp-hour capacity) is attenuated by an increase in the amp-hours required to complete the FUDS. Thus, if this trade-off is sufficiently appreciable, a further increase in the size of the battery pack could perhaps lead to a decrease in vehicle range. For this reason, the size of the battery pack (battery pack mass, BPM) was included as one of the variables in the design variable space presented in Table 5-1.

Table 5-1: Design Variable Space

Lower boundary	Design variables	Upper boundary
250 kg	Battery pack mass (BPM)	6000 kg
500 kJ	Flywheel size (FWS)	6500 kJ
10 kW	Flywheel motor size (FWMS)	300 kW
10 kW	Drive motor size (DMS)	300 kW
0.5	FWSOC @ FUDS START & END	1.0

However, in order to appreciate the extent to which battery size influences vehicle range, the BSOC @ FUDS END (which, as

defined earlier, is the indicator of vehicle range) was evaluated for the mini-van equipped with several different battery sizes from 250 kg to 6000 kg. The other components (EMB and drive motor) of the hybrid electric drivetrain were appropriately sized to handle the increasing power levels resulting from an increase in the vehicle's test mass. Indeed, in order to keep the hybrid electric drivetrain efficiency at its maximum (or near maximum) for all battery sizes, and thus, keep BPM as the main variable in the analysis, the optimization routine was carried out on the mini-van operating over the FUDS equipped with four different battery sizes. The legend of Figure 5-1 lists the component sizes resulting from the optimization at four different BPMs.

Again, in order to have BPM as the main variable in the analysis, the aerodynamic characteristics and glider mass of the vehicle remain the same for all sizes of the battery pack. This, of course, is not possible in a real system since the vehicle shape and chassis would require modifications in order to accommodate up to 6000 kg of batteries. In fact, the only characteristics of the hybrid electric vehicle which change during the analysis, apart from the BPM, are the size and mass of the EMB and drive motor. Indeed, there is a 61 kg increase in the EMB/drive motor combined mass as the BPM increases from 250 kg to 6000 kg.

As expected, Figure 5-1 shows that an appreciable increase in range resulting from an increase in battery size cannot be

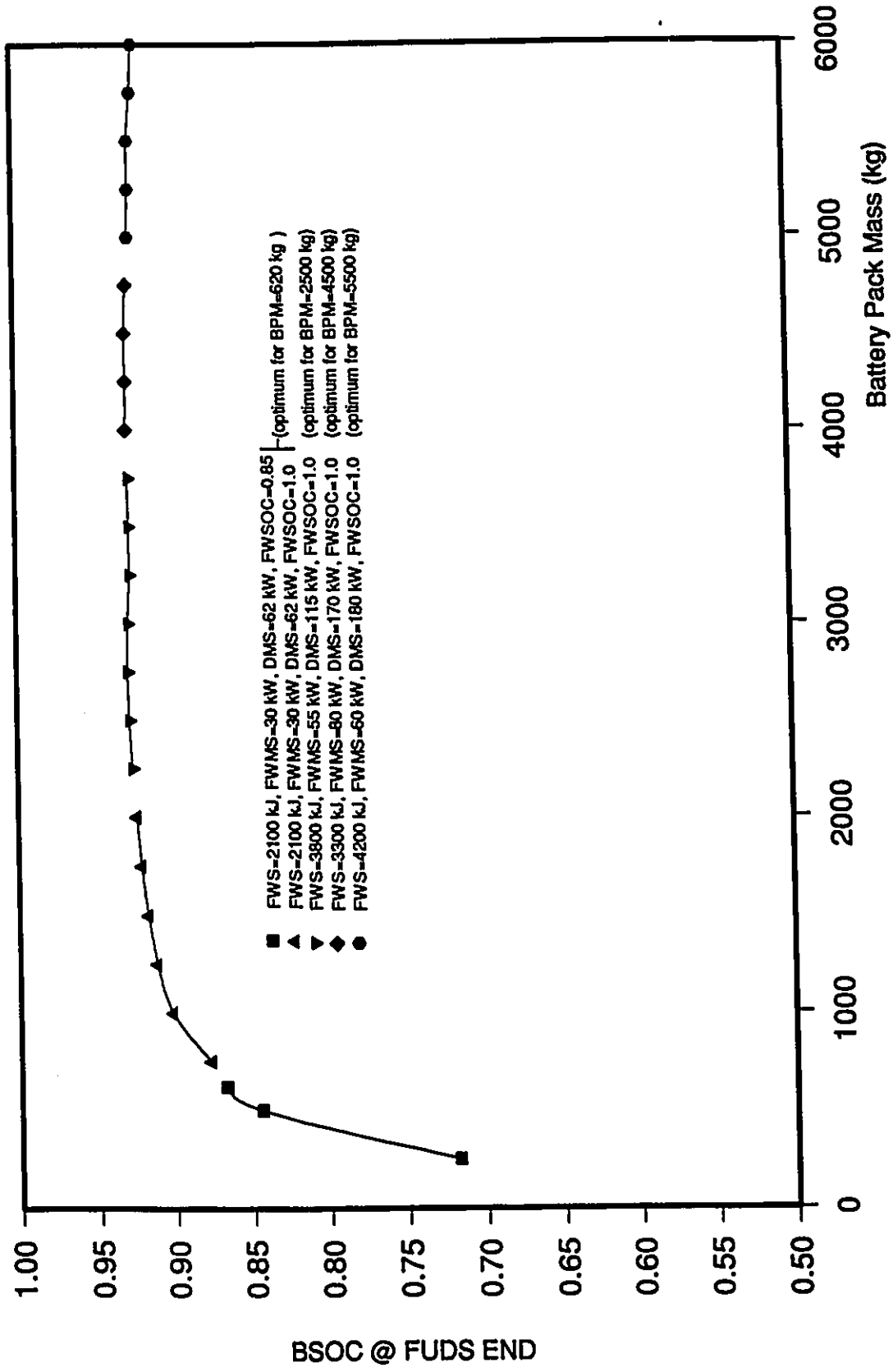

Figure 5-1 : BSOC @ FUDS END vs. Battery Pack Mass.

anticipated for BPMs above 1500 kg. In fact, above 3000 kg, a slight decrease in vehicle range becomes apparent. The analysis using any other type of battery pack would result in a curve similar to that of Figure 5-1 and its behaviour can be explained as follows.

Because of inefficiencies in the drivetrain, regenerative braking cannot recuperate all of the energy delivered by the battery to accelerate the vehicle. Thus, with aerodynamic drag remaining constant, the vehicle's energy consumption increases as the mass of the vehicle increases. It is also obvious that a minimum battery pack size is necessary in order to complete the FUDS. This battery pack is therefore completely discharged at the end of the FUDS (BSOC @ FUDS END = 0) and the vehicle can drive no further. However, if, at the start of the FUDS, an extra kilogram of battery is added to the vehicle, then part of the energy contained in this kilogram is used to supply the extra energy required to propel (over the FUDS) the added kilogram. The rest of the energy or charge remaining in the kilogram at the end of the FUDS contributes to increasing the BSOC @ FUDS END from its initial value of zero. Each subsequent kilogram of battery contributes the same fraction of its charge (approximately 0.93) to progressively increase the battery pack's state of charge at the end of the FUDS (BSOC @ FUDS END). Of course, each kilogram that is added increases the total size of the battery pack. Thus, the amount of charge contributed by each extra kilogram has to be spread out over a larger battery pack and, therefore, the rate

of increase in the BSOC @ FUDS END becomes smaller as each kilogram of battery is added. When the BPM reaches 3000 kg, the amount of charge in the battery pack has increased sufficiently such that the BSOC @ FUDS END approaches the value of 0.93 . Above 3000 kg, no significant increase in the battery pack's state of charge can be expected because each kilogram that is added has a state of charge which is only insignificantly greater than the battery pack's state of charge. Theoretically, BSOC @ FUDS END or vehicle range should increase asymptotically as the battery pack mass is increased to infinity. In this analysis, however, the BSOC @ FUDS END decreases slightly for BPMs above 3000 kg. This can be explained by the fact that the mass of the drive motor and EMB have increased as the battery pack was made progressively larger. This increase in EMB/drive motor mass augments the energy consumption of the vehicle, but, unlike the battery pack mass increase, it does not contribute any energy which can be used to propel the extra EMB/drive motor mass. Thus, the energy has to be supplied by the battery pack and the BSOC @ FUDS END therefore decreases.

Based solely on the maximization of vehicle range, the optimal battery pack mass could be set at 3000 kg. However, in this analysis, the vehicle glider mass remains constant for all battery pack sizes. This is of course impossible if the vehicle chassis is modified to accommodate the increasing mass of batteries. Thus, the increased vehicle mass brought about by an increase in the chassis rigidity could result in an optimal

battery pack mass which is perhaps smaller than 3000 kg. Indeed, increasing the mass of the chassis to accommodate a larger battery pack can be interpreted as a decrease in the battery's energy density (J/kg). This results in a definite decrease of the vehicle range for any battery pack size requiring an increase of the glider mass specified in Table 3-1. And, depending on how the chassis modifications are made, the battery pack mass yielding the greatest range could change substantially (increase or decrease) from its present value of 3000 kg.

Furthermore, other criteria such as equipment costs, maintenance costs and vehicle dynamics could override the objective of range maximization with the result being a redefinition of the optimal battery pack size.

Also, a maximum battery pack mass could be imposed if the objective becomes that of designing an electric vehicle whose overall impact on the environment, in terms of energy consumption, is no greater than that of a fossil fuelled car [69, 70]. Indeed, when other factors are considered (such as: the electric generating station's energy efficiency, power line losses, charger losses and battery turnaround efficiency), the size of the battery pack could be limited so that the net energy consumption of the electric vehicle is no greater than the net energy consumption of a fossil fuelled car (based on heating value of the fuel).

Finally, it should be noted that the asymptotic increase of vehicle range with increasing BPM is characteristic to all electric vehicles using batteries as an energy source (in fact, any energy source whose mass does not decrease as it is being depleted). In particular, the use of a battery pack or fuel cell having a higher energy density than the lead-acid battery would result in an increase of vehicle range (or BSOC @ FUDS END) for all battery sizes. Thus, the curve of Figure 5-1 would be shifted upwards and the horizontal asymptote would lie at a BSOC @ FUDS END greater than 0.93 . Furthermore, the maximum vehicle range would be reached at a BPM which is greater than 3000 kg. Hence, for a high energy density battery, an increase in the size of the battery pack (which has a negative impact on energy consumption) is perhaps more justifiable than with the lead-acid battery since the pay-off in vehicle range is more substantial.

All things considered, prescribing an adequate battery pack mass is obviously not a simple task. The decision depends on many factors which, because of their complexity and interaction, cannot be thoroughly analyzed in this study. Suffice it to say however, that, doubling the battery pack mass does not necessarily double the vehicle range, and the diminishing returns of increasing the battery size become apparent at BPMs which are perhaps much lower than one would anticipate.

5.1.3 The Optimized Hybrid Electric Drivetrain

Because the main objective of this exercise is to maximize the driving range of the hybrid electric vehicle, the battery pack mass has been chosen such that it is the largest battery pack which can meet the payload carrying capability of the mini-van. Based on other electric vehicle designs, the vehicle type used in this study (mini-van) could have a maximum gross vehicle weight rating (GVWR) of approximately 2700 kg [44, 45, 71]. Subtracting from this amount the glider mass (1212 kg), the drivetrain mass (229 kg which includes a 3800 kJ flywheel, a 55 kW flywheel motor, flywheel containment, a 115 kW drive motor, motor controllers and ancillaries), the battery box (45 kg) and a maximum payload of 600 kg, the vehicle could safely carry a maximum battery pack mass of 620 kg. With the battery pack mass fixed at 620 kg, a search for the optimum was conducted within the rest of the design variable space shown in Table 5-1. After five refinements of the search, an optimum was found with the results listed in Table 5-2.

The tolerances listed give an indication of how fine the design variable space was divided during the final optimization search. Thus, a flywheel size (FWS) of 2100 kJ ± 100 kJ means that the objective function (BSOC @ FUDS END) was evaluated for FWSs of 1900 kJ, 2000 kJ, 2100 kJ, 2200 kJ and 2300 kJ with the FWS of 2100 kJ yielding the highest BSOC @ FUDS END. The tolerance given for BSOC @ FUDS END means that the value of the

objective function did not increase by more than 0.05% as the search grid was refined from { 1800 kJ, 2000 kJ, 2200 kJ, 2400 kJ, 2600 kJ } (which yielded a maximum BSOC @ FUDS END for a FWS of 2200 kJ) to { 1900 kJ, 2000 kJ, 2100 kJ, 2200 kJ, 2300 kJ }. Tolerances of ± 0 indicate that the component sizes were fixed because of constraints. Thus, the battery pack mass was constrained to 620 kg, as explained earlier, and the flywheel motor size (FWMS) was constrained to a minimum of 30 kW because anything smaller would overheat and anything larger would reduce the efficiency of the drivetrain, hence, a reduction in the value of the objective function.

Table 5-2: The Optimized Hybrid Electric Drivetrain for GVWR of 2700 kg. (2170 kg test mass)

Design variables	BPM	620 kg ± 0 kg
	FWS	2100 kJ ± 100 kJ
	FWMS	30 kW ± 0 kW
	DMS	62 kW ± 1 kW
	FWSOC @ FUDS START & END	0.85 ± .05
Objective function	BSOC @ FUDS END	0.8674 ± 0.0005
Calculated constants	Battery pack constant power level	7.72 kW
	Flywheel mass	17.4 kg
	Flywheel motor mass	5.7 kg
	Drive motor mass	19.9 kg
	Vehicle test mass	2170 kg

Finally, Table 5-2 shows that the choice of the design variable space is adequate because, for all variables, the optimum is located well within the space and not at the boundary.

5.2 Sensitivity Analysis

5.2.1 Sensitivity to Battery Type

With the hybrid electric drivetrain components being optimally sized, the range of the vehicle could be estimated by repeating the FUDS until the batteries are completely discharged. This would however not be an accurate representation because the range is strictly dependent on the battery model being used. In this study, the battery model is derived using a lead-acid battery designed for short duration, high power pulses (aircraft starting battery). The hybrid electric drivetrain, on the other hand, load levels the battery output and discharges it at a low rate. Because of this continuous discharge at a low rate, a battery pack having a higher energy density would be better suited to the hybrid electric drivetrain. Unfortunately, no accurate data can be found to characterize this type of battery. Indeed, the way in which a low power battery is tested should be different than a high power battery because the requirements of each type are different. The choice for cut-off voltage and constant rate discharge would be different bringing about a change in the definition of the battery's zero state of charge and its rated capacity. The lead-acid battery model used in this study is therefore not an adequate description of an energy

source for the hybrid electric drivetrain. Nevertheless, the optimal hybrid electric drivetrain was found using the lead-acid power battery; and a change in the battery type could modify the result of this optimization.

Generally, all battery types have a terminal voltage which decreases with increasing output current. The battery internal resistance is representative of this phenomenon. Furthermore, a battery having a high power density would be characterized by a low internal resistance and a battery designed for high energy density would be characterized by a high internal resistance [48]. When compared to power batteries, batteries designed for low-rate applications contain a larger amount of acid in proportion to plate-active material. Thus, a reduction in battery mass. This also means that the surface area over which the chemical reaction takes place is reduced. Hence, the rate at which electrons are made available at the negative terminal is reduced and a decrease in the terminal voltage is sensed. The battery internal resistance is therefore increased to explain this drop in terminal voltage. The reason for increasing the amount of acid in a low rate battery is that the acid which has reacted at the surface of the plate can diffuse more rapidly. Thus, the plate is continuously re-flooded with fresh acid so that the constant flow of electrons to the terminals is not interrupted.

A power battery, on the other hand, is designed such that there is a large amount of surface area over which the chemical

reaction can take place in order to provide high current discharges. The short duration power pulses required from a power battery means that renewal of acid does not need to be instantaneous. Indeed, the power battery depends on the availability of "strong" acid at the surface of the plates in order to provide short duration power pulses. Once this acid has been depleted, the power drops off sharply and some time is required for the battery to recuperate before another power pulse can be successfully delivered.

Because of this difference between both battery types (power and low-rate), the search for an optimal hybrid electric drivetrain was repeated for three different battery internal resistances using a battery pack mass of 620 kg and the design variable space of Table 5-1. The battery internal resistance was decreased by a factor of 8.5 to $R_b = \mathbf{0.002} + 0.01 \cdot (1 - BSOC)$ and increased by a factor of 24 to $R_b = \mathbf{0.400} + 0.01 \cdot (1 - BSOC)$. In both cases, the optimized hybrid electric drivetrain configuration is the same as that obtained using a resistance of $R_b = \mathbf{0.017} + 0.01 \cdot (1 - BSOC)$, that is, identical to the configuration presented in Table 5-2. This means that, irrespective of battery type, the maximization of range and the terminal voltage versus current relationship of the battery dictate the choice of a hybrid electric drivetrain so as to minimize both energy and power extracted from the battery pack. Also, it can be deduced from this study that the optimized hybrid electric drivetrain remains optimal as the battery's efficiency

drops during discharge. In fact, because a change in battery pack mass changes the vehicle test mass, the battery pack mass is the only characteristic of the battery pack which influences the choice for an optimal hybrid electric drivetrain. Hence, the vehicle test mass is the true variable which influences the choice for an optimal hybrid electric drivetrain. Therefore, irrespective of the vehicle's mass fraction allotted to the battery pack and irrespective of battery type, the hybrid electric drivetrain described in Table 5-2 is the most efficient EMB/battery hybrid electric drivetrain which could propel over the FUDS a mini-van having a curb weight of 2070 kg (2170 kg including driver).

5.2.2 Sensitivity to Component Sizing

The efficiency of the hybrid electric drivetrain would be reduced if the components were not sized exactly as shown in Table 5-2. A reduction in the drivetrain efficiency means an increase in the amount of charge delivered by the battery, hence, a reduction in range. Figure 5-2 shows how the BSOC @ FUDS END is reduced as each component is independently sized away from its optimum.

It is clear that none of these rated sizes is sensitive. This result is very promising in that a drivetrain design can readily accept different battery masses or different energy sources (e.g., small IC engine, fuel cell) and further, can be

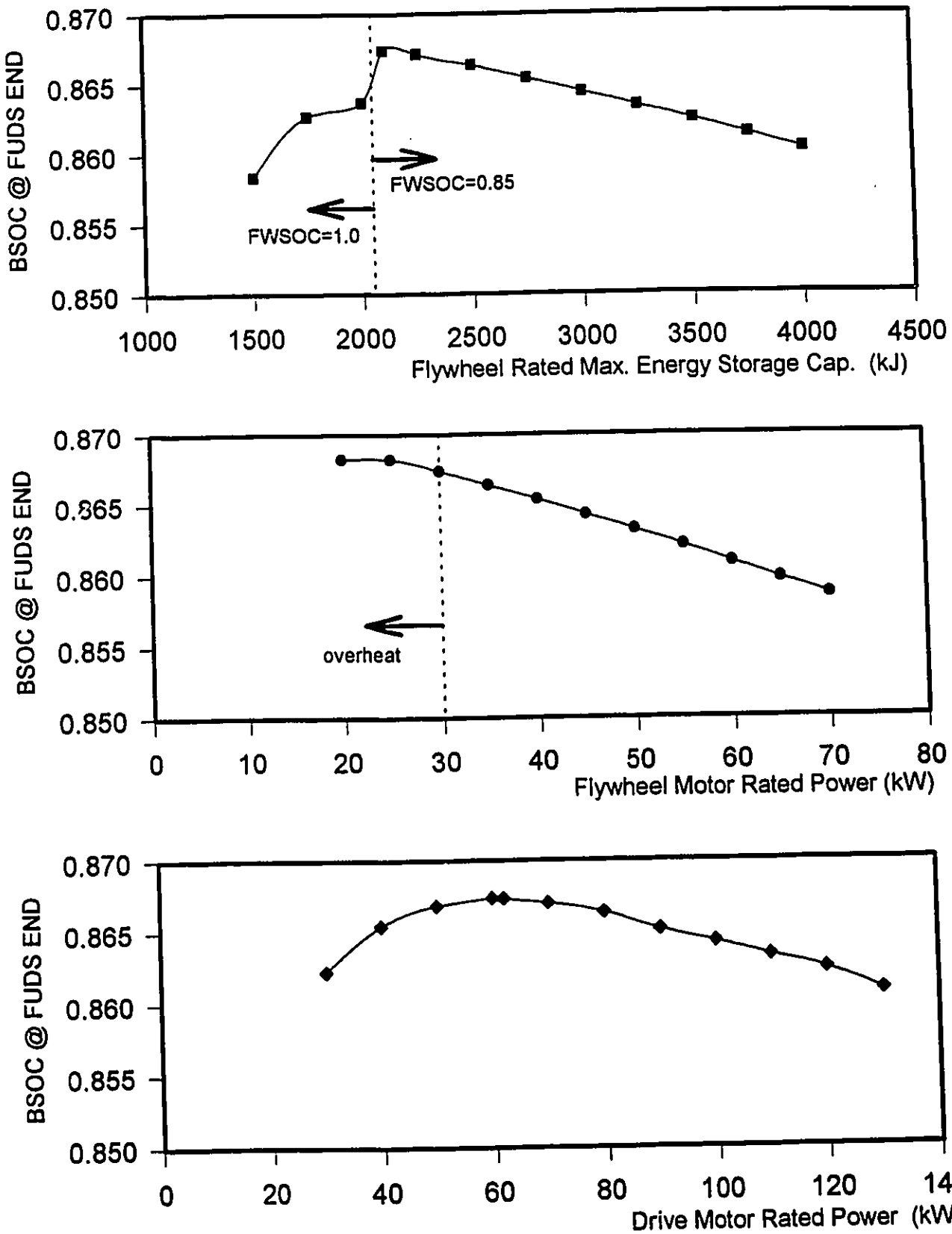

Figure 5-2: BSOC @ FUDS END vs. Component Size.

used in other vehicle types such as sedans or sports models. Most importantly, however, is the fact that the EMB/battery hybrid electric drivetrain can readily accept component design modifications as a result of packaging or cost factors, without any serious degradation in overall drivetrain efficiency or performance.

5.3 Performance Study

5.3.1 Federal Urban Drive Schedule

Using the components recommended in Table 5-2, the vehicle was operated over the FUDS. Figure 5-3 gives the general characteristics and behaviour of all components including: (i) road power requirements; (ii) power requirements at the drive motor controller terminals; (iii) drive motor actual and rated current: (iv) battery power; (v) battery current, voltage and state of charge; (vi) flywheel motor actual and rated current; (vii) flywheel state of charge and (viii) power requirements at the flywheel motor controller terminals.

It is clear that battery load levelling is easily attained. Indeed, the flywheel is used to its fullest potential as it is required to operate over its full speed range. Furthermore, considerable reserve power is almost always available from the flywheel motor/generator. Likewise, drive motor reserve power is quite extensive and thus, this vehicle can be expected to provide an acceleration capability or driveability well in excess of that required for the FUDS.

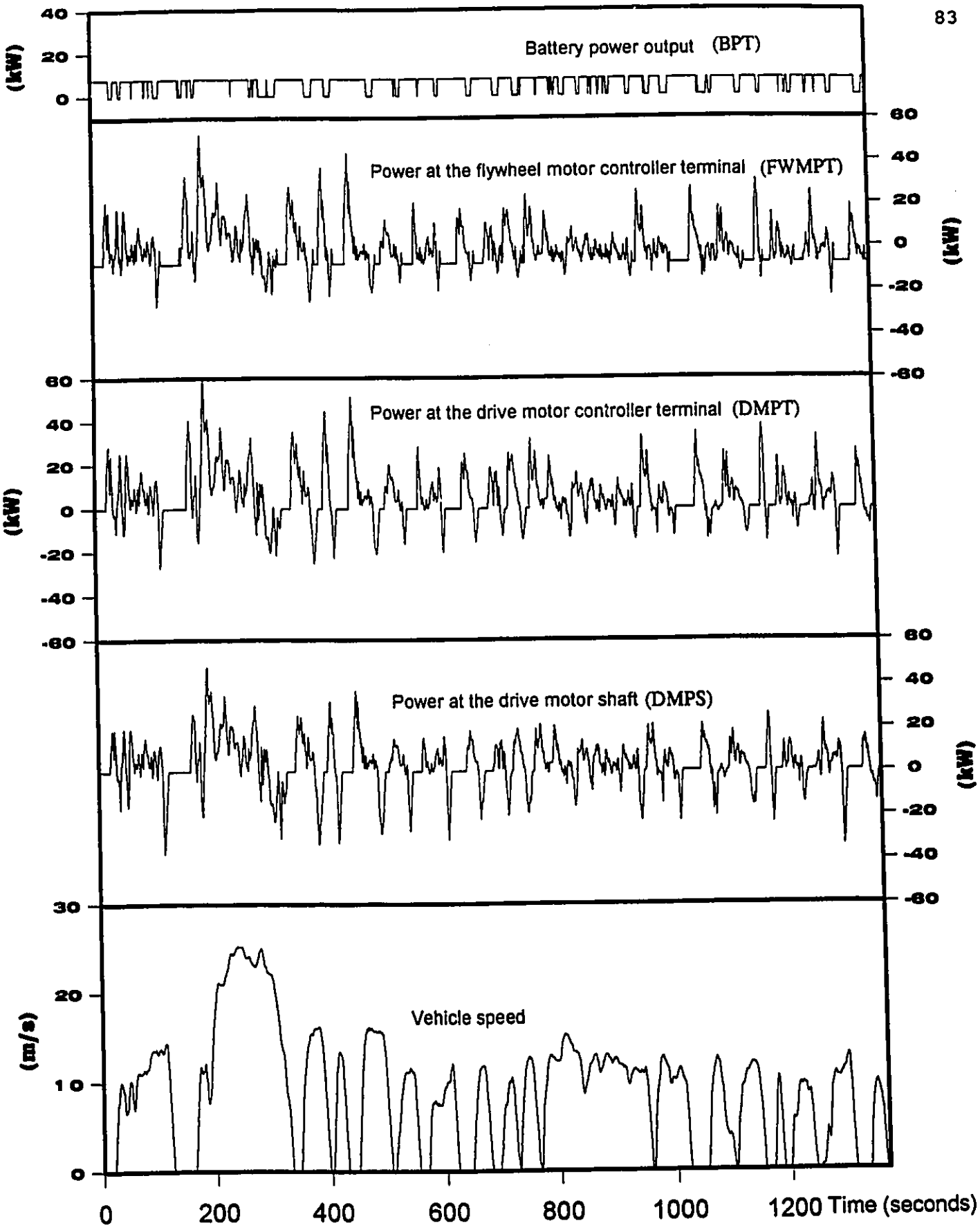

Figure 5-3A: Hybrid Electric Drivetrain Component Performance on the FUDS (Mini-van with Test Mass of 2170 kg)

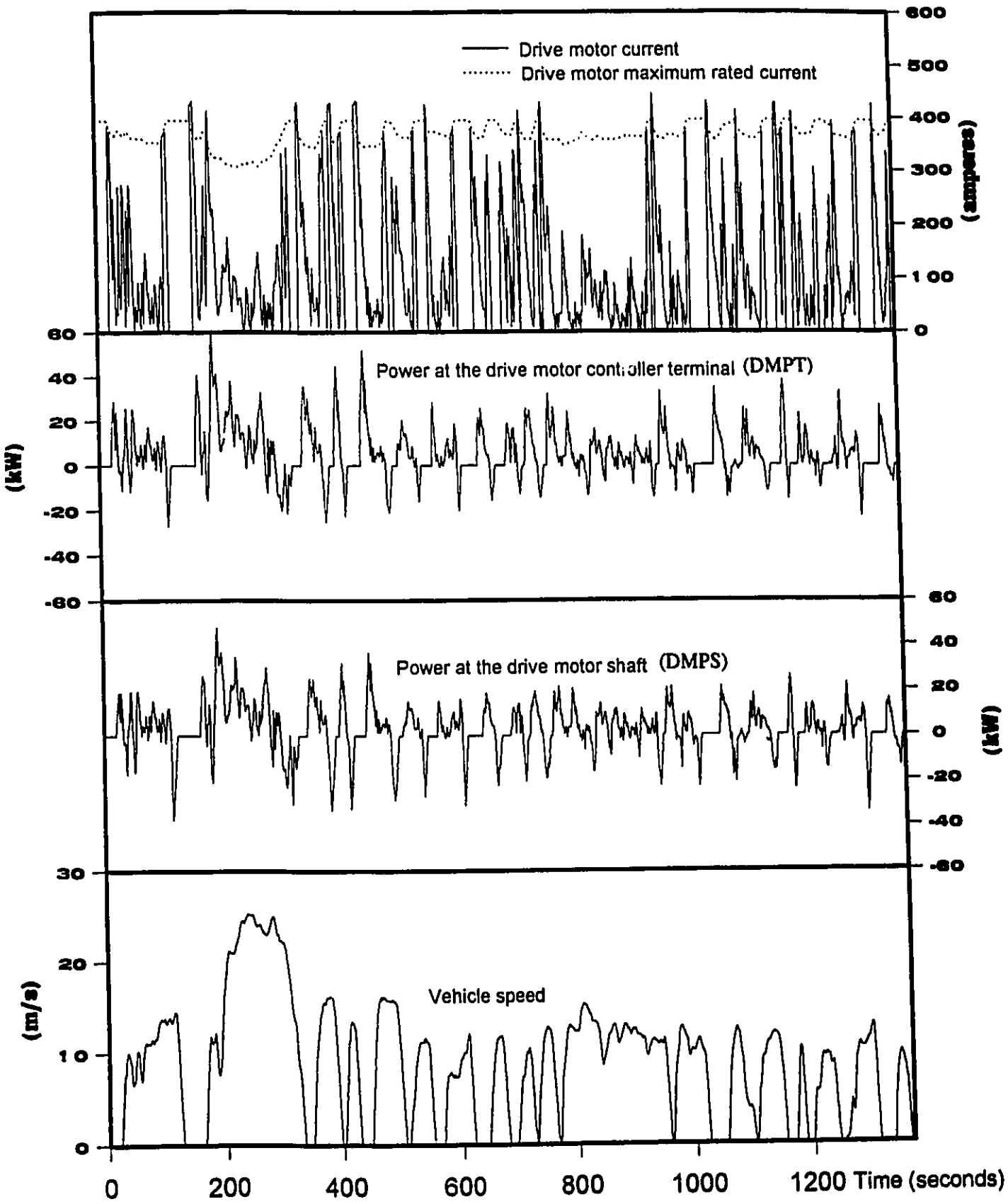

Figure 5-3B: Hybrid Electric Drivetrain Component Performance on the FUDS (Mini-van with Test Mass of 2170 kg)

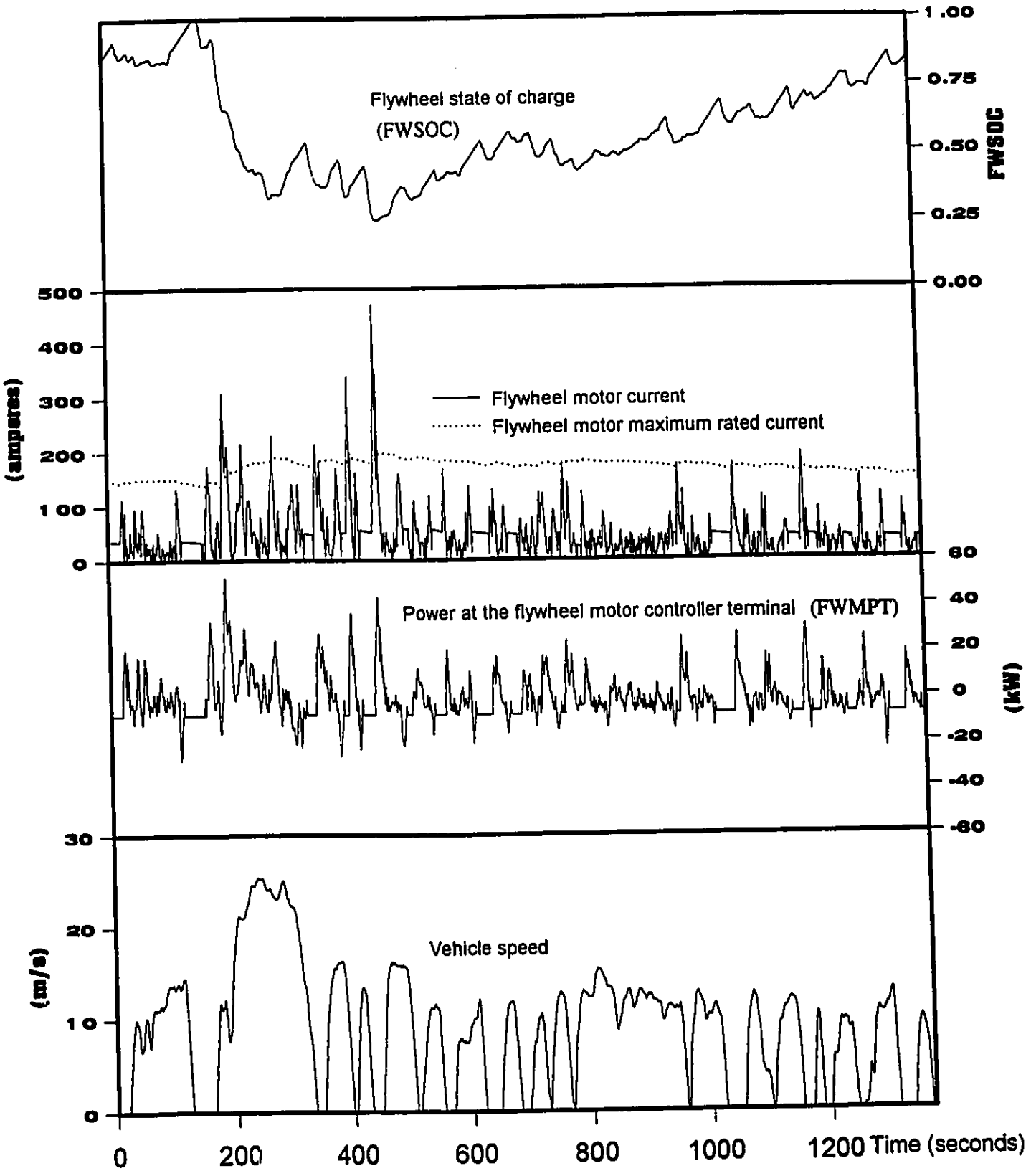

Figure 5-3C: Hybrid Electric Drivetrain Component Performance on the FUDS (Mini-van with Test Mass of 2170 kg)

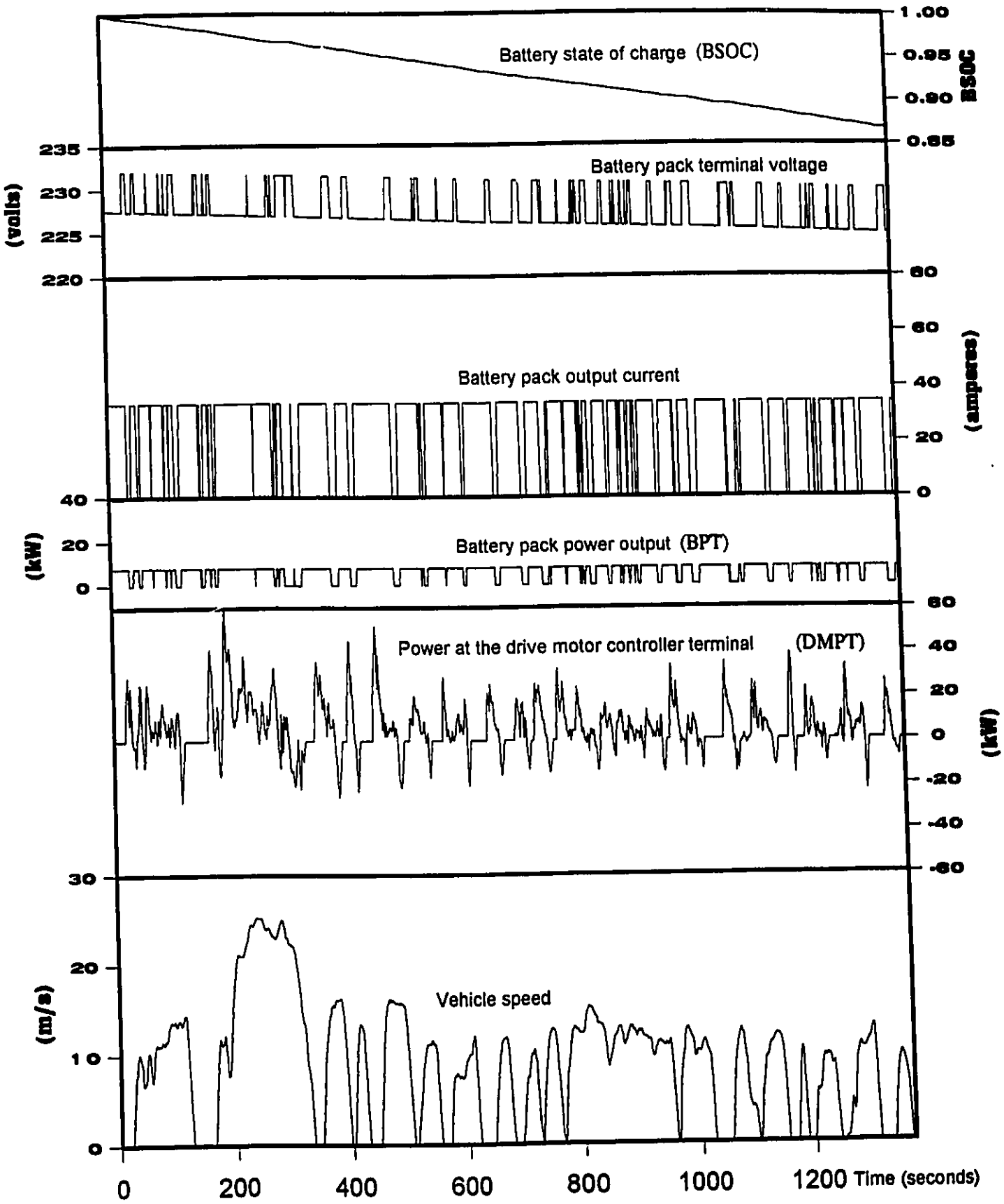

Figure 5-3D: Hybrid Electric Drivetrain Component Performance on the FUDS (Mini-van with Test Mass of 2170 kg)

5.3.2 High Performance Cycle

Although the FUDS is a close representation of reality, most fossil fuelled vehicles have acceleration capabilities greater than those required by the FUDS. It would therefore be advantageous from a marketing point of view for the hybrid electric drivetrain equipped vehicle to equal the maximum performance of a fossil fuelled vehicle. Figure 5-4 shows the maximum acceleration curve of a sub-compact car equipped with a 4 cylinder 1.8 litre displacement diesel engine and manual 5 speed transmission [72]. The deceleration curve was derived from brake

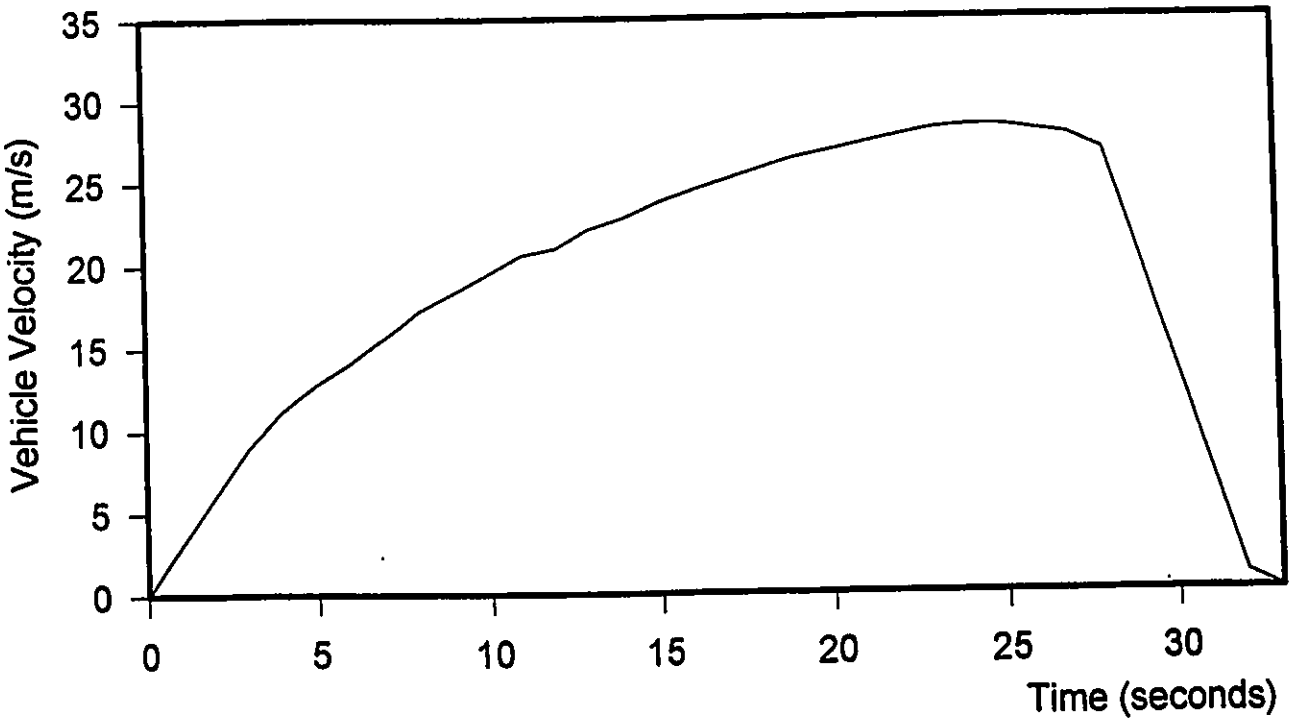

Figure 5-4: Expected Maximum Performance Curve of the Chrysler Mini- Van.

testing done on a factory built 1984 Chrysler mini-van (100 km/hr to 0 km/hr in 55 meters) [73].

As for the FUDS, the mini-van of 2170 kg, equipped with the hybrid electric drivetrain of Table 5-2 was operated over this high performance duty cycle. Figure 5-5 shows that the components of the hybrid electric drivetrain are overworked, especially during the initial low speed acceleration of the vehicle. This is caused by the low operating efficiency of the drive motor (0% to 60 %) at low speed and high torque. The flywheel motor is therefore required to operate at power levels which greatly exceed the power required at the shaft of the drive motor. This is why, in order to slightly alleviate the stress imposed on the flywheel motor, the battery pack constant power output is boosted to 15 kW for the duration of the high performance cycle (deceleration excluded). It is interesting to note however that the amount of energy contained in the flywheel (FWSOC=1.0 to FWSOC=0.39) is sufficient to cover the high losses in the drivetrain and propel the vehicle along the acceleration curve.

During deceleration, however, it is obvious that the hybrid electric drivetrain cannot accept all of the power produced by regenerative braking. In fact, the drive motor/generator model predicts that in order to provide the necessary retarding moment, the current flowing through the windings of the motor should be in the order of 1500 amperes. This results in very high resistive losses which are comparable to the input power at the shaft of

the drive motor. Thus, the drive motor absorbs the brake energy as heat instead of returning it to the drivetrain and the power at the terminals of the drive motor controller is zero. Under these circumstances, the assist of friction brakes would therefore be necessary so as to prevent overheating of the electric motor/generators.

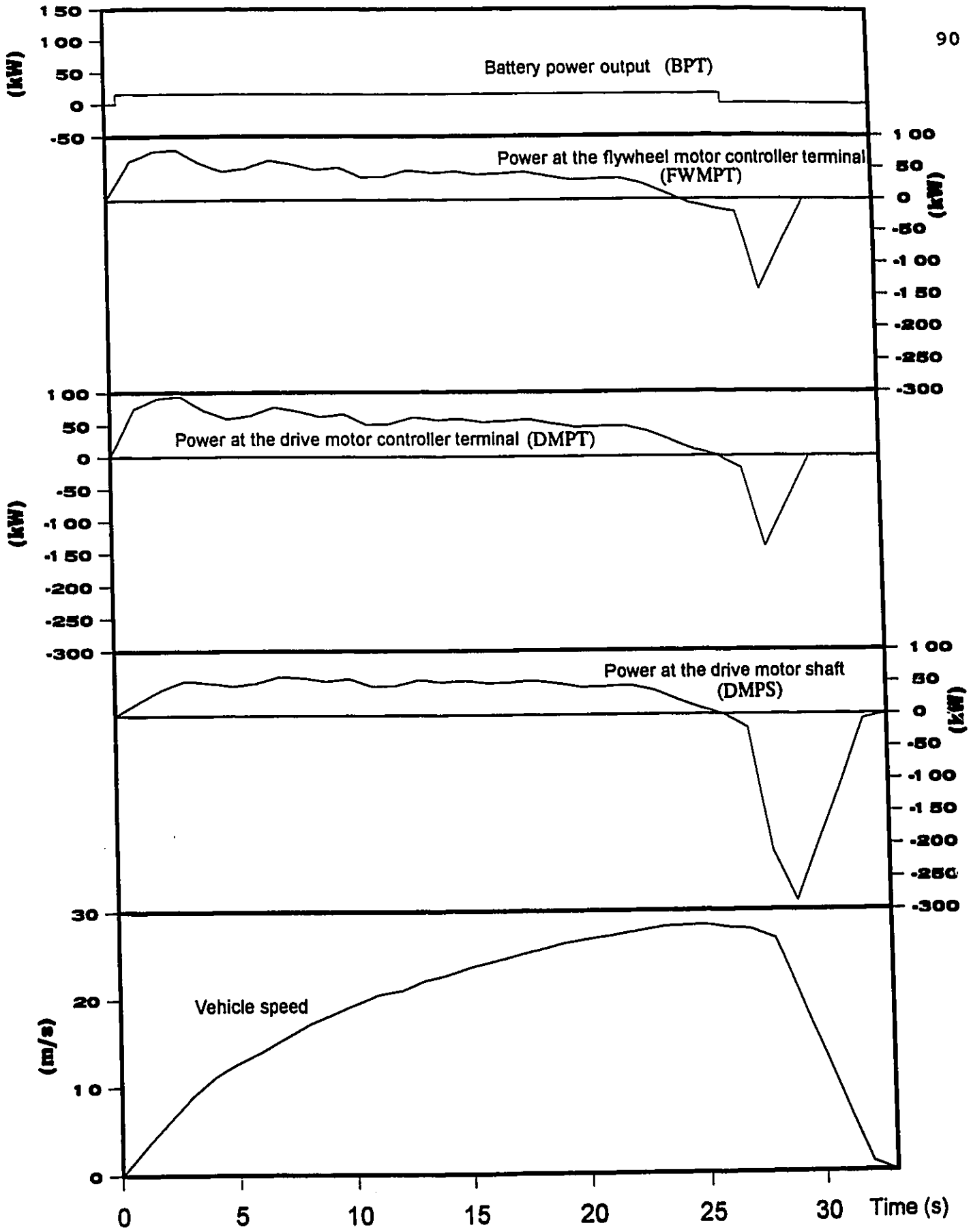

Figure 5-5A: Hybrid Electric Drivetrain Component Performance on the High Performance Duty Cycle (Mini-van with Test Mass of 2170 kg)

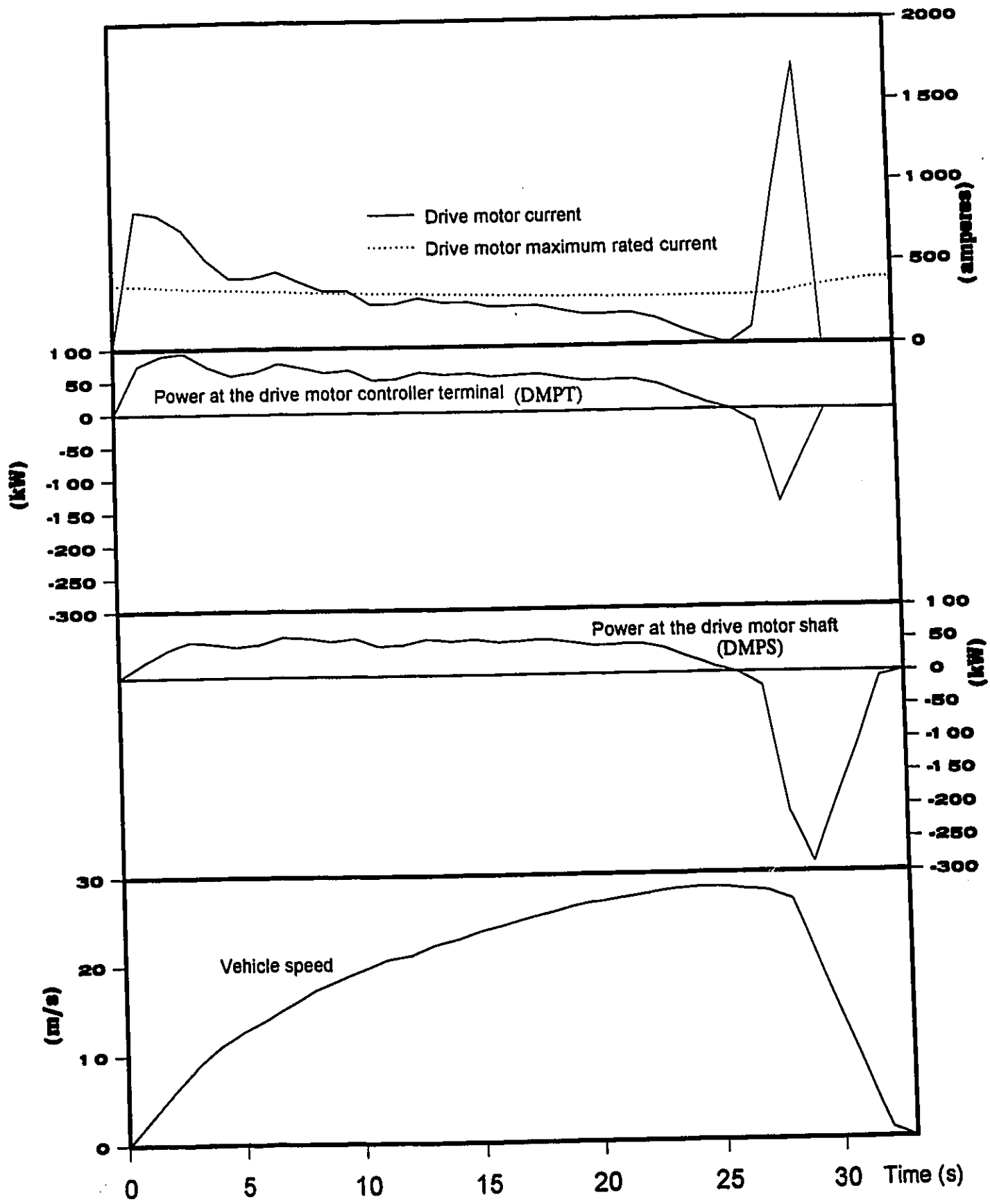

Figure 5-5B: Hybrid Electric Drivetrain Component Performance on the High Performance Duty Cycle (Mini-van with Test Mass of 2170 kg)

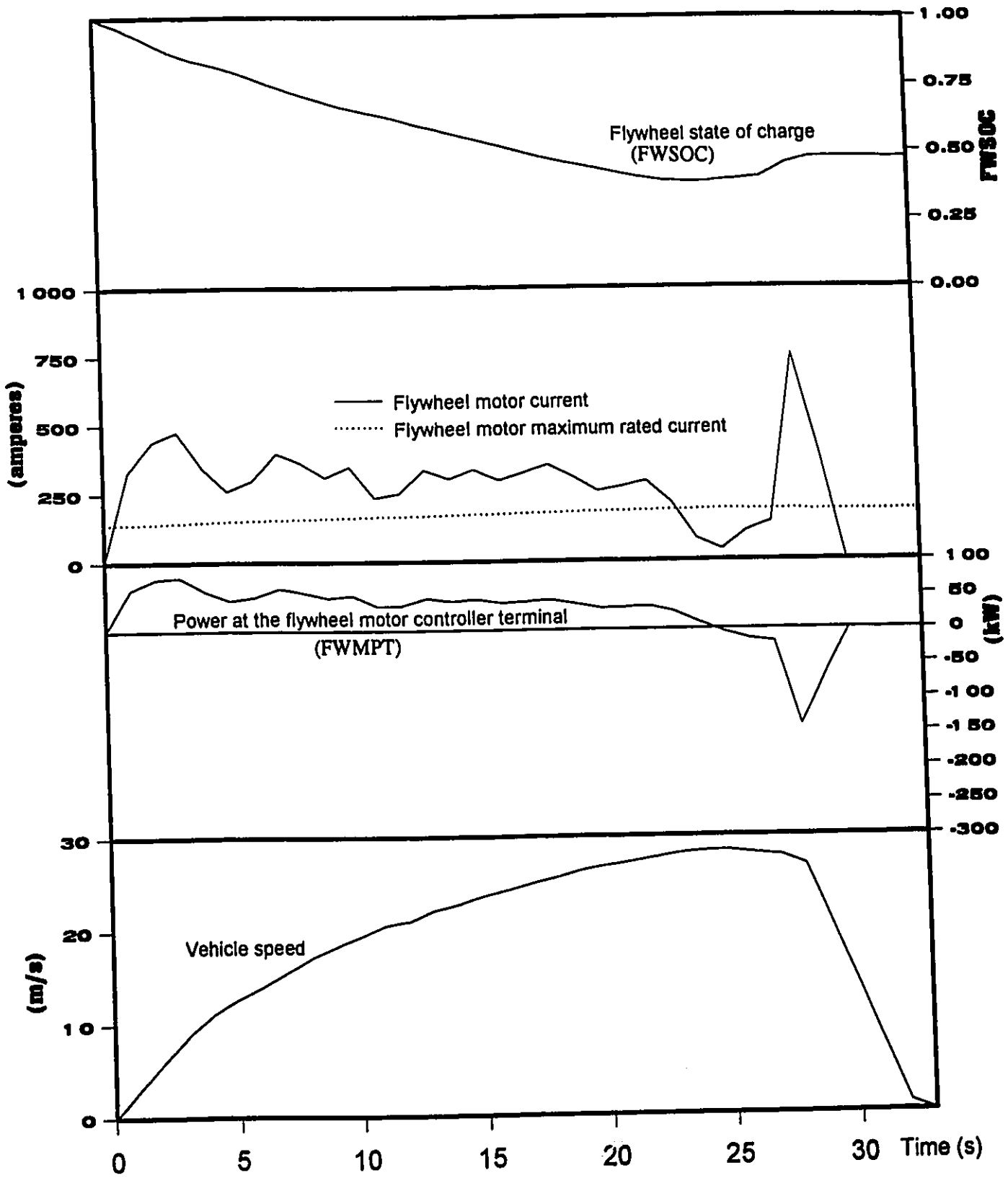

Figure 5-5C: Hybrid Electric Drivetrain Component Performance on the High Performance Duty Cycle (Mini-van with Test Mass of 2170 kg)

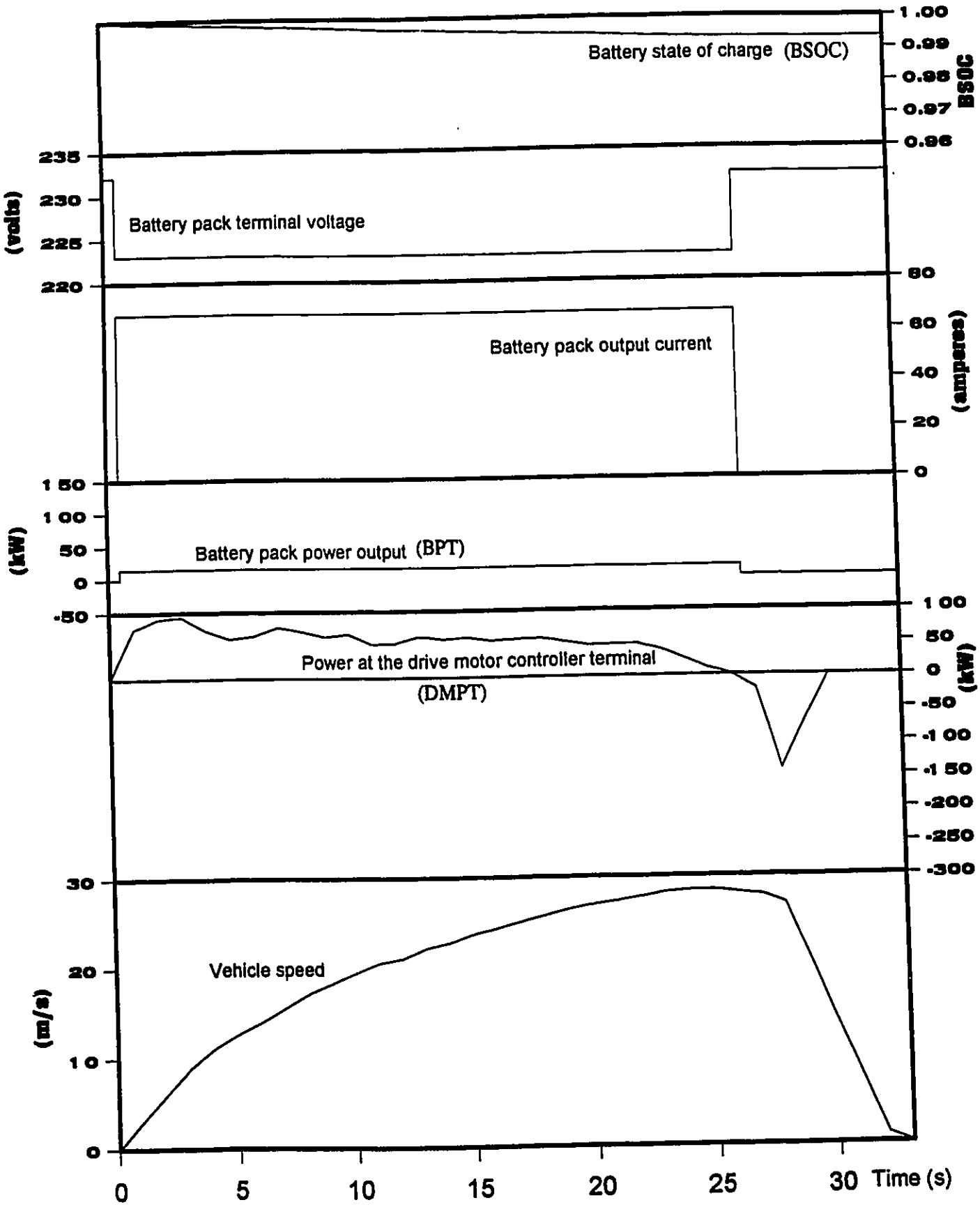

Figure 5-5D: Hybrid Electric Drivetrain Component Performance on the High Performance Duty Cycle (Mini-van with Test Mass of 2170 kg)

5.4 Energy Consumption and Efficiency (Electric Only Drivetrain vs. Hybrid Electric Drivetrain)

Three different drivetrain types were used to perform a comparative analysis of their energy consumption and efficiency. The total amounts of energy being transferred at various points in the drivetrain were summed over the complete FUDS. The quantity and direction of energy flow was recorded at points indicated by ♦ in Figures 5-6, 5-7, 5-8; and Table 5-3 lists the results.

In order to clarify the results of Table 5-3, the following indications should be noted:

(1) The quantities listed in Table 5-3 are those obtained at the end of the FUDS; after the vehicle has completed a single pass through the FUDS.

(2) Unless it is specified, the energies and amounts of charge supplied are not net. Namely, in the electric only drivetrain equipped with regenerative braking, E_d is the sum of energy flowing out of the battery, the net energy removed from the battery (E_n) would be less due to the energy returned to the battery from regenerative braking (E_c).

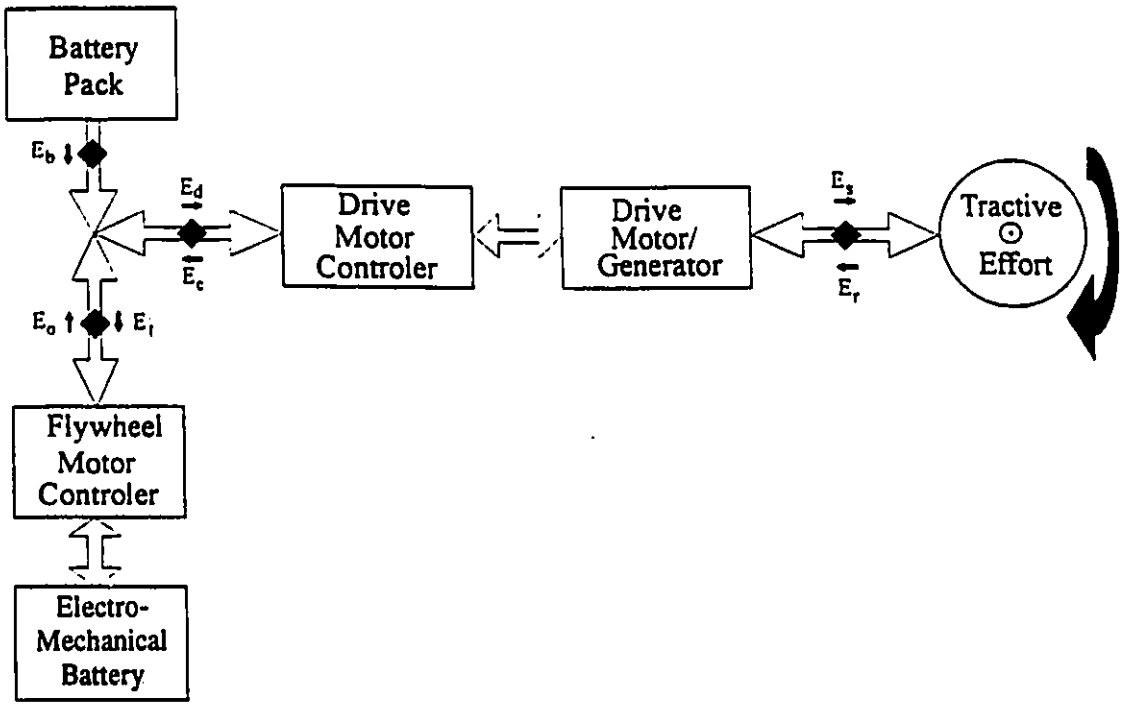

Figure 5-6: Energy Flow through the Hybrid Electric Drivetrain

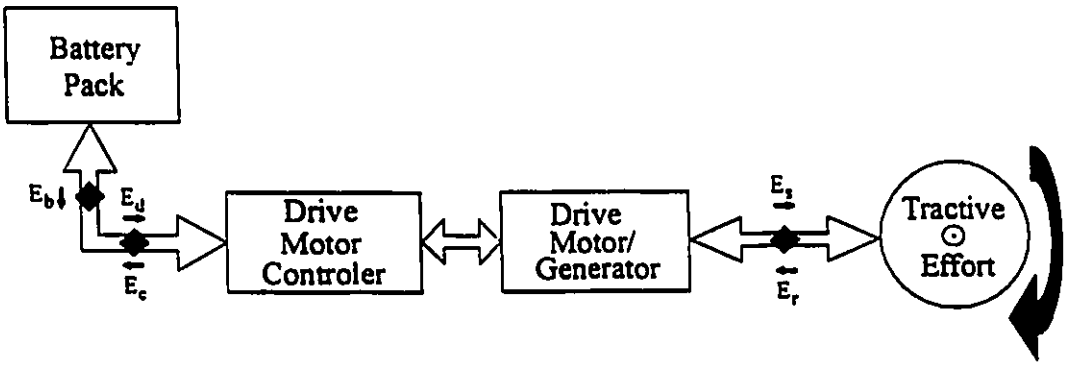

Figure 5-7: Energy Flow through the Electric Only Drivetrain Equipped with Regenerative Braking

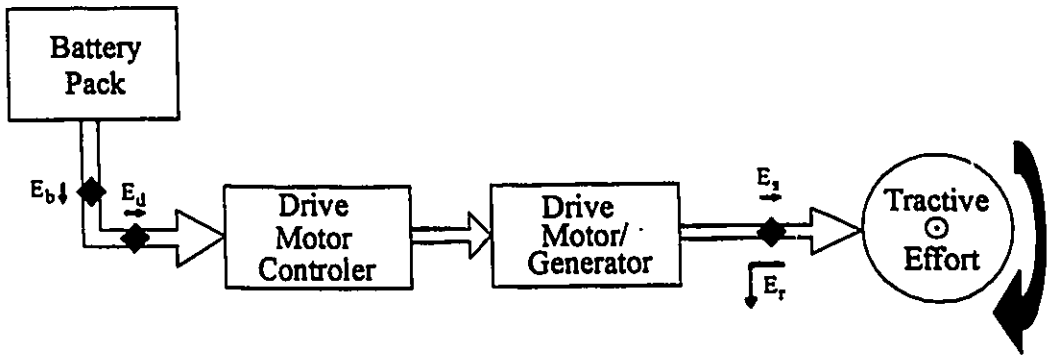

Figure 5-8: Energy Flow through the Electric Only Drivetrain without Regenerative Braking

(3) The hybrid electric drivetrain and electric only drivetrain equipped with regenerative braking have the same E_d and E_c. Therefore, for the hybrid electric drivetrain: $E_d - E_c = E_b + E_o - E_i$ and for both electric drivetrains: $E_b = E_d$.

(4) The amount of energy stored in the flywheel is the same at the beginning and end of the FUDS (FWSOC @ FUDS START & END = 0.85). Therefore, the difference between E_o and E_i is the amount of energy lost in the EMB due to friction and electrical losses.

(5) The efficiencies for the drive motor and EMB include losses in the motor controllers.

Table 5-3: Comparative Analysis of Energy Consumption and Efficiency of Various Drivetrains Operating Over the FUDS (single pass).

	Hybrid Electric Drivetrain	Electric drivetrain equipped with regenera-tive braking	Electric drivetrain without regenera-tive braking
Drive energy required at the drive motor shaft (E_s)	7.11 MJ	7.11 MJ	7.11 MJ
Regenerative braking energy available at the drive motor shaft (E_r)	3.34 MJ	3.34 MJ	3.34 MJ
Energy delivered by battery pack (E_b)	8.32 MJ	9.14 MJ	9.14 MJ
Regenerative braking energy available to recharge battery pack or EMB (E_c)	2.11 MJ	2.11 MJ	0 MJ
Energy delivered by EMB (E_o)	4.49 MJ	-	-
Energy returned to EMB (E_i)	5.78 MJ	-	-
EMB efficiency	77.7 %	-	-
Battery pack mass (BPM)	620 kg	713.1 kg	713.1 kg
Battery pack rated capacity	1387 A·h	1595 A·h	1595 A·h
BSOC @ FUDS END	0.8674	0.8880	0.8694
Amount of charge supplied by battery pack	183.9 A·h	208.1 A·h	208.2 A·h
Net energy delivered by battery pack (E_n)	(A) 8.32 MJ	(B) 7.84 MJ	(C) 9.14 MJ
Drive motor efficiency	73.8 % (1)	73.8 % (1)	77.8 % (2)
Drivetrain net energy efficiency (3)	45.3 %	48.1 %	41.2 %
Reduction in energy consumption with the use of regenerative braking	0.82 MJ (4) or 9%	1.30 MJ (5) or 14.2 %	0 MJ or 0 %
Battery turnaround efficiency	-	61.7% (6)	-
Regenerative braking efficiency	49.1%	38.9 % (7)	0%

(1) $(E_s+E_c)/(E_d+E_r)$, (2) E_s/E_d, (3) $(E_s-E_r)/E_n$, (4) C-A, (5) C-B,

(6) $(C-B)/E_c$, (7) $(C-B)/E_r$

(6) The drive energy (E_s) and regenerative braking energy (E_r) are obtained from the shaft power of the drive motor. The drivetrain efficiency therefore does not include losses due to rolling resistance.

(7) The drive motor efficiency includes losses in both drive and regenerative braking modes. It therefore represents the efficiency with which the motor/generator transfers electrical power into work and vice versa, averaged over the speed and torque range required by the FUDS.

(8) All vehicles have the same test mass of 2170 kg. In addition, for both electric only drivetrains, the EMB and its motor controller were replaced by an equivalent mass of batteries (93 kg).

(9) E_n represents the net amount of energy extracted from the battery pack. For the hybrid electric drivetrain and the electric only drivetrain without regenerative braking, E_n is easy to determine because the batteries are never recharged. For the electric drivetrain equipped with regenerative braking, E_n can be estimated using the battery state of charge. Because both batteries were discharged at the same rate (FUDS), the energy savings resulting from the use of regenerative braking can be approximated with the comparison of BSOC @ FUDS END for both electric only drivetrains. Table 5-4 shows the proportionality between BSOC @ FUDS END and energy consumption.

Table 5-4: BSOC @ FUDS END and the Net Energy Extracted from the Battery Pack

	Electric drivetrain equipped with regenerative braking	Electric drivetrain without regenerative braking
BSOC @ FUDS END	0.8880	0.8694
Fraction of the battery's rated capacity which is used to complete the FUDS (1.0 - BSOC @ FUDS END)	0.1120	0.1306
Net energy extracted from battery pack (E_n)	(B) 7.84 MJ	(C) 9.14 MJ

$$\frac{7.84}{9.14} = \frac{0.1120}{0.1306}$$

(10) The battery packs are fully charged at the beginning of the FUDS. Therefore, the energy consumptions do not include losses related to the initial charging of the battery packs.

(11) The battery internal losses are not considered in this analysis except for those related to the regenerative braking in the electric drivetrain equipped with regenerative braking. Indeed, the analysis accounts for the energy lost as the battery is being partially recharged from regenerative braking and the energy lost as this partial charge is returned to the drivetrain. The battery turnaround efficiency represents these losses which means that 61.7% of E_c is re-used to propel the vehicle, the rest (0.807 MJ) is lost in the battery.

(12) The drivetrain net energy efficiency represents the percentage of energy extracted from the battery which does not get lost in the drivetrain and is effectively used to meet the net energy demands (E_s - E_r) of the vehicle. It therefore includes all losses in the drive motor, motor controllers, EMB and, for the electric drivetrain equipped with regenerative braking, it includes losses in the battery associated with the redistribution of the regenerative braking energy.

5.4.1 Energy Density, Power Density and Range

It is somewhat distressing to note that the hybrid electric drivetrain is not as efficient as the electric drivetrain equipped with regenerative braking (45.3% vs. 48.1% in terms of net energy required at drive motor shaft over net energy supplied by battery; $(E_s-E_r)/E_n$). The higher energy consumption of the hybrid electric drivetrain (8.32 MJ) is attributed directly to the energy losses in the EMB and its controller. Indeed, the hybrid electric drivetrain consumes 6.1% more energy than the electric only drivetrain equipped with regenerative braking (8.32 MJ vs. 7.84 MJ). It is however important to note that the amount of charge required to propel the hybrid electric vehicle is reduced when compared to the conventional electric vehicle (183.9 A·h vs. 208.1 A·h). This means that the battery pack of the hybrid electric drivetrain would require less time to recharge. Hence, an energy savings is gained which could offset the energy lost in the EMB.

For the hybrid electric drivetrain, the reduction in amp-hours or charge consumed to complete the FUDS stems primarily from battery load levelling and the resultant low power (7.72 kW) draw from the battery which allows more energy to be supplied by each charge extracted from the battery. In other words, battery load levelling increases the energy density of the battery. Another way of understanding how the energy density of the battery would be increased is to discharge the batteries further by repeating the FUDS several times and monitoring the terminal voltage of the battery pack. In order to avoid damaging the battery, the terminal voltage of the battery pack under load should never be allowed to fall below a certain specified cut-off voltage.

Table 5-5 gives the total amounts of energy and charge supplied by the battery pack when the vehicle operates over the FUDS and repeats the cycle until the terminal voltage of the gauge battery drops to 10.5 volts. It is important to note however that the hybrid electric drivetrain reaches a battery state of charge of 0.2 before the terminal voltage has a chance to reach 10.5 volts. Indeed, at a discharge rate of 7.72 kW, the terminal voltage of the gauge battery is still very high at 11.7 volts despite the fact that 80% of the battery's rated capacity has been supplied.

Unfortunately, the battery model used in this study cannot predict the performance of the battery pack as its state of

Table 5-5A: Comparative Analysis of Energy and Power Density of Various Drivetrains and their Components for the Vehicle Repeating the FUDS to a Cut-off Voltage of 10.5 Volts or BSOC = 0.2 .

	Hybrid Electric Drivetrain	Electric drivetrain equipped with regenera-tive braking	Electric drivetrain without regenera-tive braking
BSOC @ 10.5 volts cut-off voltage	0.2 @ 11.7 V	0.7648	0.7184
Amount of charge supplied to reach 10.5 volts cut-off voltage	1110 A·h @ 11.7 V	448 A·h	449 A·h
Amount of energy supplied by battery pack to reach 10.5 volts cut-off voltage (1)	48.6 MJ @ 11.7 V	19.6 MJ	19.6 MJ
Peak power output from battery pack	7.72 kW	60.0 kW	60.0 kW
Battery pack mass (including battery box)	665 kg	758 kg	758 kg
Battery pack energy density	20.3 W·h/kg	7.18 W·h/kg	7.18 W·h/kg
Battery pack power density	11.6 W/kg	79.2 W/kg	79.2 W/kg
Distance travelled (range) to reach 10.5 volts cut-off voltage or BSOC = 0.2 (1)	68 km @ 11.7 V	25 km	25 km
Useable energy from EMB (1.0 → 0.25 FWSOC)	1.58 MJ	-	-
Peak power output from EMB	52.3 kW	-	-
EMB mass (flywheel, motor, controller and containment)	93.1 kg	-	-
EMB energy density	4.70 W·h/kg	-	-
EMB power density	562 W/kg	-	-

(1) Refer to Chapter 4.1 for criteria used in defining full discharge of the battery pack.

Table 5-5B: Comparative Analysis of Energy and Power Density of Various Drivetrains and their Components for the Vehicle Repeating the FUDS to a Cut-off Voltage of 10.5 Volts or BSOC = 0.2 .

	Hybrid Electric Drivetrain	Electric drivetrain equipped with regenera-tive braking	Electric drivetrain without regenera-tive braking
Useable energy from energy/power source (battery pack and EMB combined) (1)	50.2 MJ	19.6 MJ	19.6 MJ
Peak power output from energy/power source (battery pack and EMB combined)	60.0 kW	60.0 kW	60.0 kW
Mass of energy/power source (battery pack and EMB combined)	758 kg	758 kg	758 kg
Energy density of energy/power source (battery pack and EMB combined)	18.4 W•h/kg	7.18 W•h/kg	7.18 W•h/kg
Power density of energy/power source (battery pack and EMB combined)	79.2 W/kg	79.2 W/kg	79.2 W/kg
Total energy supplied to the wheels of the vehicle by the drive motor shaft (1)	41.9 MJ	15.2 MJ	15.2 MJ
Peak power output from drive motor shaft	47.6 kW	47.6 kW	47.6 kW
Drivetrain mass (EMB, battery, drive motor, controller, ancillaries)	858 kg	858 kg	858 kg
Drivetrain energy density	13.6 W•h/kg	4.93 W•h/kg	4.93 W•h/kg
Drivetrain power density	55.5 W/kg	55.5 W/kg	55.5 W/kg

(1) Refer to Chapter 4.1 for criteria used in defining full discharge of the battery pack.

charge falls below 0.2 (refer to Chapter 4.1 for limitations of the battery model). Nevertheless, it is reasonable to assume that the battery pack in the hybrid electric drivetrain could continue to supply a substantial amount of energy while operating in the range of very low BSOC (0.2 and lower). For this reason, the energy densities of the hybrid electric drivetrain and its components would in actual fact be greater than those listed in Table 5-5. Despite the limitations imposed by the battery model, the hybrid electric drivetrain has an energy density which is almost three times larger than that of the electric only drivetrain (13.6 W·h/kg vs. 4.93 W·h/kg).

Indeed, for the electric drivetrain equipped with regenerative braking, a 10.5 volt cut-off voltage (refer to Chapter 4.1 for comments concerning the choice of cut-off voltage) is reached after only 448 A·h and 19.6 MJ have been supplied by the battery pack. The 60 kW peak load required of the battery (47.6 kW at the drive motor shaft) is of course responsible for this sudden drop in terminal voltage. The battery should at this point be recharged or the demand on the battery should be reduced; hence, the electric drivetrain equipped with regenerative braking is unable to meet the FUDS. The hybrid electric drivetrain on the other hand does not reach this cut-off voltage even after more than twice the amount of charge and energy (1110 A·h and 48.6 MJ) have been removed. It is therefore obvious that, for the same vehicle mass, the hybrid electric drivetrain would give the vehicle a greater range (68 km

compared to 25 km).

Because of this difference in expected range, comparisons between the hybrid electric drivetrain and the electric only drivetrain equipped with regenerative braking must be interpreted with caution. Thus, in order to fully appreciate the advantages of the hybrid electric drivetrain, a comparison should be made on the basis of equal range and not equal vehicle mass. However, this objective of equal range may not be possible to achieve if the range that is specified is too high. As was shown in Figure 5-1, for any electric vehicle, an increase in the size of the battery does not necessarily result in an increase of vehicle range. Indeed, a maximum vehicle range exists for all battery types and the only way to increase this maximum range is to use a battery with a higher energy density. The hybrid electric vehicle lends itself well to the use of a high energy density battery. The electric only vehicle, on the other hand, requires a battery pack having a high power density which means a lowering of the energy density. Thus, the range used to compare both vehicle types would be dictated by the electric only vehicle and would be equal to the maximum range that the electric only vehicle can provide using its low energy density battery. The hybrid electric drivetrain, equipped with its high energy density battery could therefore meet the specified range with a smaller battery pack. The advantage here is obvious; based on equal range, the lighter hybrid electric vehicle consumes less energy than the electric only vehicle.

Hence, the EMB/battery hybrid electric drivetrain provides advantages beyond high performance driveability which unfortunately cannot be accurately accounted for with the current state of battery modelling. Battery load levelling will influence both battery life and battery design. That is to say, a battery used in a conventional electric only drivetrain must be designed as a "power" unit while a battery used in the EMB/battery hybrid electric drivetrain must be designed as an "energy" unit if full advantage of the hybrid drivetrain is to be realized. The author believes that this could significantly reduce the battery cost and increase the energy available per unit mass of battery.

Ideally, two different battery models would be necessary in order to accurately evaluate and compare the driving range of both vehicles. Battery modelling was not the objective of this study; the battery model used in this study provided the means to establish how the hybrid electric drivetrain should be designed in order to maximize the energy density of the battery pack.

5.4.2 The EMB Efficiency

It is tempting to compare the battery turnaround efficiency (61.7%) with the EMB overall efficiency (77.7%). However, these efficiencies are not representative of the same concept because both units do not have an equal role in the operation of the drivetrain. Indeed, the amount of energy being handled by the battery is only that amount related to regenerative braking (2.11

MJ). The EMB on the other hand is being summoned continuously which means it must transfer almost three times more energy than the battery. Obviously, both units do not perform the same task. It would therefore be more appropriate to compare the EMB/battery hybrid electric drivetrain against a battery/battery hybrid electric drivetrain; a vehicle equipped with an "energy" battery and a smaller "power" battery which would be used like the EMB to load level the "energy" battery. Using the sodium-sulphur high temperature battery with a maximum possible power density of 175 W/kg [71, 74], a power battery of 300 kg would be necessary to handle the 52.3 kW peaks. The size of the energy battery would therefore be reduced to 413 kg compared to 620 kg for the EMB/battery hybrid electric drivetrain.

Furthermore, the performance of the lead-acid battery pack used in the electric drivetrain equipped with regenerative braking is questionable in so far as its capability to accept charge at the high rates associated with regenerative braking. Indeed, no maximum voltage has been imposed to limit any damage that may be caused to the battery during high rate charging. Fortunately, for the electric drivetrain equipped with regenerative braking, the terminal voltage only peaks to 16 Volts during the hardest deceleration in the FUDS. Indeed, a peak regenerative braking power of 37.3 kW forces each gauge battery to be recharged at a rate of 36.3 amperes. However, under more demanding cycles, the electric drivetrain equipped with regenerative braking would have to dump some of the regenerative

braking energy in order to prevent damage to the battery and limit the dangerous out-gassing of hydrogen. This "dumping" of regenerative braking energy would therefore result in a decrease of the electric drivetrain's overall energy efficiency.

One must also consider that the battery turnaround efficiency varies with BSOC and battery age. On the other hand, the "low power" demands on the battery in a hybrid electric drivetrain are virtually independent of the severity of the duty cycle and the expected performance and efficiency of the hybrid electric drivetrain remain constant and predictable, irrespective of the BSOC.

5.4.3 Regenerative Braking

The use of regenerative braking in the hybrid electric drivetrain provides an energy savings of only 9% when compared to the conventional electric drivetrain without regenerative braking. Indeed the operation of the hybrid electric drivetrain is such that the energy recovered from regenerative braking (2.11 MJ) is barely enough to compensate for the losses in the EMB (1.29 MJ). Nevertheless, the use of regenerative braking in the hybrid electric drivetrain is necessary; without this type of operation, the energy consumption of the hybrid electric vehicle would increase because the losses in the EMB (1.29 MJ) would have to be covered by the battery pack. Furthermore, the use of regenerative braking reduces the wear rate on the conventional

friction brakes. This is especially true considering the relatively large mass of a battery powered electric vehicle which imposes more stress on the braking system.

When energy consumption alone is considered, it appears that the use of the hybrid electric drivetrain is somewhat unjustified. However, thanks to battery load levelling, the hybrid electric drivetrain provides an increase in the vehicle's range due to an increase in the battery's energy density. Also, unlike the conventional electric vehicle, the maximum performance (acceleration) of the hybrid electric vehicle does not decrease as the battery is being discharged. These two very important benefits more than compensate for the hybrid electric drivetrain's increased energy consumption (6.1% more than the electric drivetrain equipped with regenerative braking). Again, in all fairness, comparisons should be made on vehicles of equal range. This would undoubtedly make the electric only drivetrain more energy consuming than the hybrid electric drivetrain because the battery pack size required for the electric only drivetrain would be greater than that required for the hybrid electric drivetrain.

On more aerodynamic vehicles (e.g., sedans), the use of regenerative braking becomes more worthwhile because less of the force required for deceleration is provided by aerodynamic drag. This situation puts the hybrid electric drivetrain at an advantage because, irrespective of the BSOC, the EMB capability

to accept charge is higher than that of the battery pack. Indeed, the EMB can absorb energy at peak rates of 41.5 kW @ 20 000 rpm and 58 kW @ 40 000 rpm.

For the electric drivetrain equipped with regenerative braking, the regenerative braking efficiency represents the fraction of available regenerative energy (3.34 MJ) which is reused to propel the vehicle (1.30 MJ). Therefore, 61.1% of the regenerative braking energy is lost as it goes through the drive motor, is stored in the battery and is re-routed to the drive motor controller terminals. A "true" regenerative braking efficiency cannot be calculated for the hybrid electric drivetrain because the EMB is not dedicated solely to the management of regenerative braking energy. Indeed, the regenerative braking energy gets confounded with other energies that the EMB is required to handle. The contribution of regenerative braking on the EMB efficiency is therefore unknown. However, by using the EMB's turnaround efficiency of 77.7% and the drive motor's average efficiency of 63.2% in braking mode, a regenerative braking efficiency of 49.1% can be approximated for the hybrid electric drivetrain.

CHAPTER 6: RECOMMENDATIONS FOR FURTHER STUDIES AND DEVELOPMENT OF THE HYBRID ELECTRIC VEHICLE

6.1 Performance and Energy Management of the Hybrid Electric Drivetrain Operating on Actual Duty Cycles

The sizing of the hybrid electric drivetrain components and its mode of operation are a result of an optimization which is based on the minimization of charge drawn from the battery pack while the vehicle completes a somewhat "ideal" cycle (FUDS). In reality, however, the drivetrain would be subjected to a duty cycle which in most instances is different than the FUDS, varies continuously and is unpredictable. The management of energy or power flow between components in the hybrid electric drivetrain is therefore more complicated as the control strategy is required to adjust itself to a more dynamic system.

Unlike the objective of the optimization which was to minimize the amount of charge drawn from the battery, the first objective of the hybrid electric drivetrain now becomes that of providing the vehicle with a constant and predictable performance (acceleration). The hybrid electric vehicle must therefore have a driveability which is akin to that of fossil fuelled vehicles. Thus, irrespective of the battery state of charge, the operator of the vehicle can expect the hybrid electric drivetrain to deliver its maximum performance if and when it is required. In other words, the drive wheels of the vehicle must have available

at all times a preset maximum amount of power which could vary only with vehicle speed. In order to meet this criterion, the FWSOC must be monitored continuously so that the amount of energy in the flywheel is always sufficient to provide the drive wheels with a continuous maximum power as the vehicle accelerates from a given speed to its top speed. This, of course, requires a more flexible management of energy flow than was allowed during the optimization. This flexibility can be achieved by allowing the battery pack power output to vary continuously between zero and its maximum rated power output.

For the vehicle operating on a level surface at moderate speeds, the FWSOC can easily be controlled so that it is always sufficient and never leaves the driver with a shortfall of power. However, under continuous high speed cruising or continuous hill climbing, it is reasonable to expect that the energy of the EMB would at some point be depleted. Under these circumstances, the battery pack becomes the only source of energy available but, unfortunately, its maximum power output is dependent on its design and its state of charge. Thus, it is unlikely that the operator of such a vehicle would tolerate a sudden drop in vehicle performance in the middle of a long climb caused by the battery state of charge which is too low for the battery to provide the necessary power.

An obvious solution to this shortfall is to equip the hybrid electric drivetrain with a battery pack designed to provide high

power discharges even at low BSOC. If this type of battery pack design is chosen, it appears that the use of an EMB is somewhat redundant. Nevertheless, a substantial increase in the useable life of the battery pack could be expected if maximum use is made of the EMB. This would be possible in the majority of displacements effected by passenger cars in urban areas where most of the power peaks required for acceleration could be taken up by the EMB in order to keep to a minimum the high rate discharging of the battery pack. There are other solutions which could be considered in order to make the hybrid electric vehicle acceptable under all driving conditions. Increasing the size of the EMB is one, electrifying certain portions of road (such as long hills, multiple lane highways) is another [75, 76]. And, finally, giving the operator an advance warning of the limited capability of his vehicle to provide continuous high power (i.e.: a slow decrease in the power available at the drive wheels when the EMB approaches full discharge).

Obviously, the management of energy between the hybrid electric drivetrain components and how this would be effected on duty cycles which are unpredictable is an area which requires more analysis and study.

6.2 Other EMB Based Hybrid Electric Drivetrain Configurations

The EMB is quite versatile as a "power unit" and as such could be used in conjunction with other "energy sources". The

I.C. engine coupled to an electric generator becomes very attractive as an energy source if it is sized and optimized to provide a constant low power [44]. Indeed, the role of the I.C. engine generator in the hybrid electric drivetrain is the same as that of the lead-acid battery pack used in the optimization. However, the study of such a drivetrain (EMB/I.C. engine) is different than the EMB/battery drivetrain. The reduced mass of the I.C. engine, generator and fuel tank is a definite advantage when compared to the lead-acid battery. Also, the objective function now becomes the minimization of fuel consumption of the I.C. engine as the vehicle completes the FUDS. The outcome of the optimization would be the correct sizing of the I.C. engine so that it operates at its point of minimum specific fuel consumption (kg/s/W).

Another energy source which is an ideal complement to the EMB is the fuel cell. Indeed, the fuel cell is a low power device which, on its own, is unable to propel the vehicle. The evaluation of the EMB/fuel cell hybrid electric drivetrain could be exactly the same as the EMB/battery hybrid electric drivetrain. Of course, the battery model needs to be replaced by a model describing the performance of the fuel cell and, because the fuel cell has a relatively high energy density compared to the lead-acid battery, a decrease in vehicle mass and/or an increase in vehicle range can be expected. Unfortunately, the fuel cell has a low power density and for this reason, it cannot be used as a backup to the EMB unless it is grossly oversized.

Thus, the use of fuel cells as an energy source in the hybrid electric drivetrain is an area which could be studied considerably, especially if this leads to a redefinition of constraints and performance objectives.

6.3 Battery Modelling and Range Evaluation

In order to optimize and accurately evaluate the useable range of a hybrid electric vehicle utilizing fuel cells or batteries as an energy source, more information about fuel cell/battery performance is required. Indeed, the electric vehicles of tomorrow will most likely have useable range included in their list of specifications and, unlike the fuel consumption ratings (EPA) of fossil fuelled vehicles, evaluations of useable range for electric vehicles have not been standardized [77].

For the purposes of optimization and range estimation, testing of fuel cells and batteries needs to be done in order to obtain a terminal voltage vs. current relationship for several battery/fuel cell sizes (mass). Alternatively, the test could be conducted on a single cell of specified mass. This single cell could be used as a gauge cell and a fuel cell pack or battery pack could be modeled as a stacking (in parallel and/or series connection) of several gauge cells.

A simple method of testing batteries is to discharge a battery, which is initially fully charged, into a resistive load.

By simply recording the time, terminal voltage and current, for several different resistive loads, a performance map similar to the one shown in Figure 4-2 could be established. The integration of the current vs. time curve would give the amount of charge supplied by the battery from the onset of discharge to any point thereafter. The battery's depth of discharge (DOD) at any point can be expressed as the ratio of charge supplied up to this point over a fixed amount of charge which can be chosen arbitrarily. Ideally, the fixed amount of charge should be chosen to be sufficiently large so as to eliminate the possibility of obtaining DOD ratios greater than unity. The discharge test would terminate, hence, the battery would be considered to be fully discharged when the terminal voltage rate of decrease changes dramatically (sharp decrease). The terminal voltage rate of decrease (V/s) should therefore be continuously recorded and compared to the rate of decrease obtained at the onset of discharge. For example; a rate of decrease which becomes ten times greater than that obtained at the onset of discharge indicates that the battery is fully discharged. The use of a simple cut-off voltage as an indication of a battery's full discharge introduces some bias because it is a prescribed value which changes depending on the rate at which a battery is being discharged (lower cut-off voltages are prescribed for high rate discharge).

The test method described above, especially if it is done at very low discharge rates, is certainly appropriate to evaluate

and compare the performance of a battery or fuel cell pack in a hybrid electric drivetrain. Furthermore, by using the change in terminal voltage rate of decrease as a standard in identifying a fully discharged battery, an accurate estimation of range and trustworthy comparisons between competitors become possible.

6.4 Other Electric Vehicle Design Objectives

6.4.1 Accessory Load

In this study of electric vehicles, the energy consumption of accessories such as lighting, ventilation, defrosting, air conditioning, etc. has not been considered. Indeed, the power to operate these accessories is not negligible and if it comes from the main battery pack through a DC to DC convertor, the added load means a decrease in the vehicle's useable range [69, 78]. This is especially true for the conventional electric drivetrain because the peak loads required from the battery pack to propel the vehicle are made more intense by the addition of the accessory load. The accessory load is perhaps insignificant when compared to the peak load but the drop in terminal voltage becomes disproportionately noticeable because the battery is required to operate in a range of high internal resistance caused by the high current draw.

For the hybrid electric drivetrain, the accessory load could perhaps be comparable to the constant power output of the battery pack (7.72 kW). However, even if, for example, the use of

accessories were to double the constant power output from the battery pack, the total power output remains relatively low. The added stress imposed on the battery pack is therefore greatly reduced when compared to the electric drivetrain, hence, an increase in the battery's service life can be expected. Furthermore, the use of accessories and its effect on vehicle range can more easily be accounted for in the design of a battery pack intended for hybrid electric drivetrains.

6.4.2 Drive Motor Efficiency

This study has effectively demonstrated that the hybrid electric drivetrain excels in meeting the performance requirements of an urban duty cycle. Unfortunately, electric motors are generally inefficient at low speed when high torque is required. This is clearly shown in Figure 5-5B where the first 4 seconds of acceleration indicate that the input power to the drive motor is almost twice that of the output power at the shaft. It is therefore probable that the hybrid electric drivetrain would benefit from the use of a transmission, especially if the vehicle is repeatedly required to accelerate from a standstill and decelerate to a full stop. Incorporating a simple two speed automatic transmission into the design of the hybrid electric drivetrain could be studied in order to compare its benefits (increased drive motor efficiency) and its drawbacks (increased mass and friction).

CHAPTER 7: CONCLUSION

This study has presented the design and expected performance of a hybrid electric drivetrain which could potentially be used to propel (and decelerate) a light duty passenger vehicle. The drivetrain consists of an energy source, a power source, electric motor controllers and a drive motor. The energy source is a 620 kg lead-acid battery pack contained in a 45 kg battery box. The power source is a 93 kg electro-mechanical battery consisting of a high energy density fibre composite rotor (2100 kJ @ 40 000 rpm, 17 kg) directly coupled to a permanent magnet D.C. motor/generator (shaft power: 30 kW continuous @ 40 000 rpm, 58 kW peak @ 40 000 rpm, 6 kg). The unit, which can be recharged as well as discharged, operates within a speed range of 20 000 to 40 000 rpm and is enclosed in a sealed vacuum containment of 50 kg. The drive motor which is used to decelerate as well as propel the vehicle is a 20 kg permanent magnet D.C. motor/generator rated at 62 kW @ 7500 rpm continuous, 145 kW @ 7500 rpm peak. The drivetrain uses two variable frequency, variable time pulse electronic power controllers of 20 kg each to interface the EMB and drive motor with the lead-acid battery pack.

The operation of the EMB/Battery hybrid electric drivetrain is such that the EMB is used to handle the power peaks required to accelerate and provided by deceleration of the vehicle. The battery pack can therefore be discharged at a continuous low power level of 7.72 kW. The power output from the battery pack

is used to assist the EMB during peak power requirements and to recharge the EMB during low or nil power demands. Indeed, the main objective of the hybrid electric drivetrain is to load level the battery pack which results in two major benefits. The first is an increase in the battery pack's service life through the elimination or reduction in the number of high current peaks flowing through the battery. This mode of operation imposes considerable stress on a battery, especially when it approaches full discharge. The second benefit of battery load levelling is an increase in the useable driving range of the vehicle. Because batteries are generally characterized by a terminal voltage under load which decreases with increasing output current, battery capacity (amp-hours) and energy density (J/kg) are increased as the output power is reduced.

Thus, the main objective of this study was to present a control strategy for the management of energy flowing between the components of the hybrid electric drivetrain and to size these components so as to minimize the amount of charge (amp-hours) supplied by the battery pack per kilometre travelled by the vehicle. The performance objectives were such that a hybrid electric drivetrain equipped mini-van having a GVWR of 2700 kg (2170 kg test mass) should complete the 12 km Federal Urban Drive Schedule without overheating the electric motors and without overcharging or completely discharging the EMB.

Models were developed for the components in the hybrid

electric drivetrain so as to represent the performance and losses of each component as a function of their size and operating conditions (speed, power, state of charge). With the objective function being the maximization of charge remaining in the battery at the end of the FUDS, the use of an exhaustive search optimization technique resulted in the optimal sizing of both electric motors and the flywheel. Sensitivity analysis has shown however that the objective function is not very sensitive to changes in the electric motor or flywheel sizes. Indeed, a variation of component size in the range of -50% to +100% results in a 1% decrease of the objective function.

On the other hand, for the battery pack, sizing greatly influences the driving range of the vehicle. Indeed, the value of the objective function increases as the battery pack size increases up to 1500 kg. Above this mass, however, no appreciable gain in vehicle range can be expected. With the main objective of this study being the maximization of the vehicle's range, the size of the battery pack was maximized and, hence, solely limited by the payload carrying capability of the mini-van. Indeed, the mini-van is expected to carry a payload of 600 kg which leaves enough room for 620 kg of batteries. However, knowing that vehicle range is not proportional to battery pack size, a further reduction in battery pack mass is possible when other factors such as; equipment costs, maintenance/operating costs and energy consumption are considered.

The optimized EMB/battery hybrid electric drivetrain was compared to a battery only electric drivetrain in terms of energy consumption, power density, energy density and expected range. For the mini-van of 2170 kg operating over the FUDS, the hybrid electric drivetrain consumes 6% more energy than the electric only drivetrain. The EMB with its turnaround efficiency of 78% is responsible for this slight increase in energy consumption but the 12% reduction in the amount of amp-hours consumed by the hybrid electric drivetrain has the effect of decreasing the energy required for recharging and increasing the battery pack's energy density. Indeed, based on a cut-off voltage of 10.5 volts for the electric drivetrain and 11.7 volts for the hybrid electric drivetrain, the battery pack of the hybrid electric drivetrain has an energy density which is 2.8 times greater than the electric only drivetrain. In terms of range, this translates into 68 km for the hybrid electric drivetrain compared to 25 km for the electric drivetrain when the FUDS is repeated until full discharge of the battery pack.

Defining the full discharge of the batteries has, of course, a great influence on the estimation of range. Using cut-off voltage or end-point voltage is the most widely accepted method of assessing a battery's full discharge and cut-off voltages can be specified to be as low as 7 volts for very high rate discharge or as high as 11.5 volts for very low rate discharge. Unfortunately, the battery model used in this study does not predict the performance of the battery all the way down to deep

discharge. Consequently, for this study, the choice of cut-off voltages was limited by the operating points within which dependable results could be obtained from the battery model. The values of driving range and energy density given in this study should therefore be interpreted with caution. These are strictly estimates which serve as a guide in comparing different drivetrain types equipped with the same battery pack. In order to obtain an accurate estimate of range for the hybrid electric drivetrain, battery testing must be conducted at very low discharge rates using the appropriate cut-off voltage.

Unlike the energy density, it appears that the drivetrain power density remains the same for both drivetrain types (electric or hybrid electric). Indeed, it seems appropriate that the power density be governed solely by the capacity of the drive motor. Hence, the calculation of power density is based on the peak power requirement in the FUDS which is in the order of 48 kW while the vehicle is travelling at a velocity of 60 km/hr. This results in a drivetrain power density of 56 W/kg if the drivetrain is considered as a complete unit including batteries, EMB, motors, controllers and ancillaries. Furthermore, based on the peak power output of the drive motor which is 145 kW @ 120 km/hr , the power density of the drivetrain can be as high as 170 W/kg. Unfortunately, the conventional electric vehicle will profit from this high power density only if the battery pack is fully charged. Hence, the power density of the electric only drivetrain falls as the batteries are discharged and it could now

be stated that power density will differ depending on the type of drivetrain. Indeed, irrespective of the battery state of charge, the hybrid electric drivetrain can maintain a constant drivetrain power density if the management of energy is done judiciously so as to prevent the complete discharging of the EMB.

The proper management of energy or power flow between the components of a hybrid drivetrain is essential to its operation and it must be done so as to take full advantage of the hybrid drivetrain concept. It is perhaps the characteristic of the hybrid drivetrain which requires the most investigation for the successful implementation of a practical hybrid drivetrain equipped vehicle. Indeed, the maximum performance of the hybrid electric vehicle must remain constant, predictable and available at all times. Long duration hill climbing and constant high speed cruising present the greatest challenge for the design of any electric vehicle.

It is hoped that this study has succeeded in providing some basis and has defined certain objectives for the design of a practical hybrid electric vehicle and in particular, the design of a suitable energy source (e.g.: battery pack, fuel cell, I.C. engine).

LIST OF REFERENCES

1. Gelb, G.H., Richardson, N.A., Wang, T.C. and DeWolf, R.S.; "Design and Performance Characteristics of a Hybrid Vehicle Powertrain", SAE 690169, 1969.

2. Frank, A.A., Winkelman, J.R.; "Computer Simulation of the University of Wisconsin Hybrid-Electric Vehicle Concept", SAE 730511, 1973.

3. Frank, A.A. and Beachley, N.H.; "Evaluation of the Flywheel Drive Concept for Passenger Vehicles", SAE 790049, 1979.

4. Frank, A.A. and Jamzadeh, F.S.; "Optimal Control for Maximum Mileage of a Flywheel Energy-Storage Vehicle", SAE 820747, 1982.

5. Schilke, N.A. and Rohde, S.M.; "The Fuel Economy Potential of Heat Engine/Flywheel Hybrid Vehicles", SAE 810264, 1981.

6. Schilke, N.A., DeHart, A.O., Hewko, L.O., Matthews, C.C., Pozniak, D.J. and Rohde, S.M.; "The Design of an Engine-Flywheel Hybrid Drive System for a Passenger Car", SAE 841306, 1984.

7. Liddle, S.G.; "An Analytical Study of the Fuel Economy and Emissions of a Gas Turbine-Electric Hybrid Vehicle", SAE 760122, 1976.

8. "Phase I of the Near Term Hybrid Passenger Vehicle Development Program", Final Report, Sponsored by the United States Department of Energy, DOE/JPL/955190-01, October 1980.

9. Levin, R., Liddle, S.G., Deshpande, G., Trummel, M. and Vivian, H.; "Hybrid Vehicle Assessment, phase 1, Petroleum Savings Analysis", Jet Propulsion Laboratory, Passadena, CA. JPL/5030-569, March 1984.

10. Liddle, S.G.; "Hybrid Vehicle Petroleum Study", IECEC 1990, Vol. 4, pp. 126-131.

11. Burke, A.F., Hardin, J.E. and Dowgiallo, E.J.; "Application of Ultracapacitors in Electric Vehicle Propulsion Systems", 34th International Power Sources Symposium, Cherry Hill, New Jersey, June 1990, pp. 328-333.

12. Burke, A.F.; "Hybrid/Electric Vehicle Design Options and Evaluations", SAE 920447, 1992.

13. Burke, A.F.; "On-Off Engine Operation for Hybrid/Electric Vehicles", SAE 930042, 1993.

14. Adams, W.A., Oliveira, J.C.T. and Song, G.; "Development of Hybrid/Electric Propulsion Systems", Transport Canada Report prepared by Electrochemical Science and Technology Centre, Ottawa, September 1993.

15. Murray, H.S. and Huff, J.R.; "Fuel Cell/Battery Hybrid Vehicle Assessment", Los Alamos National Laboratory Report, LA-10948-MS, October 1987.

16. Buchwald, P., Christensen, G., Larsen, H. and Sunn Pedersen, P.; "Improvement of Citybus Fuel Economy Using a Hydraulic Hybrid Propulsion System; A Theoretical and Experimental Study", SAE 790305, 1979.

17. Schreiber, J.G., Shaltens, R.K. and Beremand, D.G.; "Electric and Hybrid Electric Vehicle Study Utilizing a Time-Stepping Simulation", IECEC 1992, Vol. 3, pp. 3.159-3.165, IECEC 929136.

18. Marr, W.W. and Sekar, R.R.; "Analysis of a Diesel-Electric Hybrid Urban Bus System", SAE 931796, 1993.

19. Lines, S.; "Hybrid Electric Vehicles : Final Report", Natural Resources Canada Report Prepared by ORTECH International, November 1993.

20. Triger, L., Paterson, J. and Drozdz, P.; "Hybrid Vehicle Engine Size Optimization", SAE 931793, 1993.

21. Flanagan, R.C.; "Program Overview and Diesel/Flywheel Hybrid Powertrain Design", Proceedings 18th IECEC 1982, pp. 1955-1960, IEEE No. 829325.

22. Brusaglino, G. "Development of Two Hybrid Bus Versions: With Batteries or Flywheel", 5th International Electric Vehicle Symposium, Philadelphia, October 1978; No. 782402(E).

23. Brusaglino, G.; "The Fiat Hybrid Bus Program", SAE 820268, 1982.

24. "Emissions and Fuel Economy Tests of the University of Florida Hybrid Bus", EPA Report, December 1977.

25. Roan, V.P.; "A Diesel Electric Hybrid Bus", SAE 780294, 1978.

26. Bumby, J.R. and Forster, I.; "Optimisation and Control of a Hybrid Electric Car", Proceedings of the Institution of Electrical Engineers, Vol. 134, Part D., No. 6, November 1987, pp. 373-387.

27. Bumby, J.R. and Forster, I.; "A Hybrid Internal Combustion Engine/Battery Electric Passenger Car for Petroleum Displacement"; Proceedings of the Institution of Mechanical Engineers, Vol. 202, No. D1, pp. 51-64, 1988.

28. Donaghue, J.F., Burghart, J.H.; "Optimization Methods Applied to Hybrid Vehicle Design", United States Department of Energy Report, June 1983, DOE/NASA/0084-1.

29. Kramer, W.E. and Winn, C.B.; "Optimized Control of a Solar Powered Vehicle with Control Constraints", IECEC 1992, Vol. 1, pp. 1.395-1.400, IECEC 929227.

30. Willis, F.G., Kaufman, W.F. and Kern, G.A.; "Mechanical Hybrid Vehicle Simulation", SAE 790015, 1979.

31. Willis, F.G. and Radtke, R.R.; "Hybrid Vehicle Systems Analysis", SAE 850225, 1985.

32. Spiekhout, J., Van der Graaf, R. and Kriens, R.F.C.; "A Universal, Modular Simulation Program for Hybrid Powertrains", 26th International Symposium on Automotive Technology and Automation (ISATA), September 1993, pp. 647-654, #93EL0049.

33. Lustenader, E.L., Chang, Dr. G., Richter, Dr. E., Turnbull, F.G. and Hickey, J.S.; "Flywheel Module for Electric Vehicle Regenerative Braking", 12th Intersociety Energy Conversion Engineering Conference (IECEC), 1977, IECEC No. 779046.

34. Lustenader, E.L., Edelfelt, I.H., Jones, D.W., Plunkett, A.B., Richter, E. and Turnbull, F.G.; "Regenerative Flywheel Energy Storage System", IECEC 1979, Vol.1, pp.343-351, IECEC 799077.

35. "Near-Term Electric Test Vehicle, ETV-2, Phase II", Final Report, DOE/CE/541213-01, AiResearch Contract No. DEAC03-76CS51213-01, April 1981.

36. Chang, M.-C.; "Computer Simulation of an Advanced Hybrid Electric-Powered Vehicle", SAE 780217, 1978.

37. Heidelberg, G., Mertens, K., Reiner, G. and Stickel, H.; "Testing Magnetodynamic Energy Storage Units", IECEC, Vol. 2, pp. 75-80, 1988.

38. Flanagan, R.C., Aleong, C., Anderson, W. and Olberman, J.; "Design of a Flywheel Surge Power Unit for Electric Vehicle Drives", IECEC 1990, Vol. 4, pp. 211-217.

39. Flanagan, R.C. and Keating, M.; "Evaluation of a Flywheel Hybrid Electric Vehicle Drive", IECEC 1990, Vol. 4, pp. 205-210.

40. Rowlette, J.J.; "Influence of Load-Levelling, Regeneration, and Recuperation on Battery Capacity". Jet Propulsion Laboratory, Pasadena, California, 1980.

41. Flanagan, R.C.; "Photovoltaic/Flywheel Lightstation System Design and Prototype Rotor Tests", IECEC No. 879087, 1987.

42. Flanagan, R.C.; "Design, Manufacture and Test Results for Four High Energy Density Fibre Composite Rotors", IECEC No. 869202, 1986.

43. Kirk, J. and Evans, H.E.; "Inertial Energy Storage Magnetically Levitated Ring-Rotor", IECEC 1985, pp. 2.372-2.377.

44. Anderson, W.M.; "An Electric Van with Extended Range", pp. 73-83, SAE 900181, 1990.

45. Heiselmann, H.W.; "Acceptance, Verification and Performance Test Results for the Bedford CF Electric Van", DOE Report No. EGG-SE-7033, January 1986.

46. Rowland, E.A. and Hartman, G.S.; "Evaluation of Battery Performance for an Electric Vehicle With Regenerative Braking", 5th International Electric Vehicle Symposium, Philadelphia, October 1978; No. 783106(E).

47. Unnewehr, L.E. and Nasar, S.A.; "Electric Vehicle Technology", John Wiley, New York, 1982.

48. "Battery Book One, Lead-Acid Traction Batteries", Curtis Instruments, Inc., Mt Kisco, N.Y. 1980.

49. Shepherd, C.M.; "Theoretical Design of Primary and Secondary Cells", U.S. Naval Research Laboratory, No. 6129, 1964.

50. Ragone, D.V.; "Review of Battery Systems for Electrically Powered Vehicles", SAE 680453, 1968.

51. Kruse, R.E. and Huls, T.A.; "Development of the Federal Urban Driving Schedule", SAE 730553, 1973.

52. Fitzpatrick, N.P. and Strong, D.S.; "Aluminium-Air, a Battery/Battery Hybrid for an Off-Road Vehicle", 9th International Electric Vehicle Symposium, Toronto, November 1988.

53. Parish, D.W., Fitzpatrick, N.P., O'Callaghan, W.B. and Anderson, W.M.; "Demonstration of Aluminium-Air Fuel Cells in a Road Vehicle", SAE 891690, 1989.

54. Agruss, B.; "Testing Batteries for Vehicular Applications", Journal of the Electrochemical Society, Vol. 117, No. 9, p. 1204, September 1970 and Vol. 118, No. 2, p. 375, February 1971.

55. Hornstra, F.; "Test Programs at the National Battery Test Laboratory", Journal of Power Sources, Vol. 17, Nos. 1-3, 1986.

56. Nowak, D.K.; "Evaluation of a New Charge Algorithm for a Lead-Acid Battery with Gelled Electrolyte Using a 96V Gel Cell IV as a Test Battery", Final Report, DOE/NV/10672-1, 1989.

57. Taylor, D.F. and Siwek, E.G.; "The Dynamic Characterization of Lead-Acid Batteries for Vehicle Applications", SAE 730252, 1973.

58. Rowlette, J.J.; "Charge Efficiency Tests of ESB EV-106 Lead-Acid Batteries", United States Department of Energy Report, DOE/CS-54209-1, January 1981.

59. Burrows, B.W., Wysor, W.J. and Hartman, R.J.; "Semi-Industrial Batteries for Electric Vehicle Fleet Application", 5th International Electric Vehicle Symposium, Philadelphia, October 1978, No. 783301(E).

60. Moosavi-Rad, H., Ullman, D.G.; "A Band Variable-Inertia Flywheel Integrated-Urban Transit Bus Performance", SAE 902280, 1990.

61. Pourmovahed, A., Beachley, N.H. and Fronczak, F.J.; "Modelling of a Hydraulic Energy Regeneration System", Journal of Dynamic Systems, Measurements and Control", Vol. 114, No. 1, March 1992, pp. 155-165.

62. "Special Electric-Car Report"; Car and Driver Magazine, Ziff-Davis Publishing, New York, Vol. 26, No. 12, June 1981, pp. 41-62.

63. Nelson, R.H., Jacovides, L.J., Schauerte, F.J. and Woods, E.J.; "Electric Vehicle Simulation Program", 5th International Electric Vehicle Symposium, Philadelphia, October 1978, No. 782207(E).

64. Rao, S.S.; "Optimization Theory and Applications", John Wiley, New York, 1984.

65. White, K.E.; "A Digital Computer Program for Simulating Electric Vehicle Performance", SAE 780216, 1978.

66. Baer, M.R.; "Aerodynamic Heating of High-Speed Flywheels in Low Density Environments", Sandia Laboratories, Albuquerque, N.M., No. SAND 78-0957, 1978.

67. Flanagan, R.C. and Suokas, L.A.; "Regenerative Drive for Subway Trains", Journal of Engineering for Industry, Vol. 98. No. 3, August 1976.

68. Loewenthal, S.H., Scibbe, H.W., Parker, R.J. and Zaretsky, E.V.; "Operating Characteristics of a 0.87 kW-hr Flywheel Energy Storage Module", SAE 859018, 1985.

69. Sheridan, D.C., Bush, J.J. and Kuziak, W.R., Jr.; "A Study of the Energy Utilization of Gasoline and Battery-Electric Powered Special Purpose Vehicles", SAE 760119, 1976.

70. Serin, E.I. and Midler, A.S.; "Some Questions Pertaining to the Economic and Fuel Efficiencies of Electric Vehicles", Soviet Electrical Engineering, Vol. 57, No. 4, 1986, pp. 39-41.

71. Hamilton, W.; "Electric Van Performance Projections, Final Report", Electric Power Research Institute, No. RP2882-1, October 1988.

72. "Isuzu I-Mark LSs"; Road Test Published in Road & Track Magazine, CBS Publications, New York, vol. 34, No. 2, October 1982, p. 93.

73. "Plymouth Voyager"; Road Test published in Road & Track Magazine, CBS Publications, New York, Vol. 35, No. 8, April 1984, p. 59.

74. "Battery and Electric Vehicle Update"; Report Published in Automotive Engineering, SAE, Vol. 100, No. 9, September 1992, pp. 17-29.

75. Ross, H.R. and Ducat, G.A.; "Southern California R, D & D Program on Highway Electrification Systems, Research Newsletter Published by South California Edison, January 1990.

76. Ulbrich, E.A., Jr.; "Switched Linear Induction Motor Freeway System Data", SAE 931799, 1993.

77. Von Courbière, R. and Müller, H.G.; "Requirements for EV-Batteries and Consequences for Test Procedures", Journal of Power Sources, Vol. 17, No. 1-3, 1986.

78. Unnewehr, L.E.; "Electric Vehicle systems", Electric Vehicle News, May 1974, pp. 19-24.